TURUN
YLIOPISTO
UNIVERSITY
OF TURKU

Evolving Diagnostics of Myocardial Infarction

Differentiating Acute and Chronic cTnT Elevations with Improved Assay

Rami Aalto

TURUN YLIOPISTON JULKAISUJA – ANNALES UNIVERSITATIS TURKUENSIS
SARJA – SER. F OSA – TOM. 82 | TECHNICA – INFORMATICA | TURKU 2026

TURUN
YLIOPISTO
UNIVERSITY
OF TURKU

EVOLVING DIAGNOSTICS OF MYOCARDIAL INFARCTION

Differentiating Acute and Chronic cTnT Elevations with Improved Assay

Rami Aalto

TURUN YLIOPISTON JULKAISUJA – ANNALES UNIVERSITATIS TURKUENSIS
SARJA – SER. F OSA – TOM. 82 | TECHNICA – INFORMATICA | TURKU 2026

University of Turku

Faculty of Technology
Department of Life Technologies
Molecular Biotechnology and Diagnostics
Doctoral Programme in Technology

Supervised by

Associate Professor, Saara Wittfooth
Biotechnology
Department of Life Technologies
University of Turku
Turku, Finland

PhD, Qi Wang
Biotechnology
Department of Life Technologies
University of Turku
Turku, Finland

Reviewed by

Docent, Päivi Laitinen
University of Oulu
Oulu, Finland

Docent, Kai Eggers
Department of Medical Sciences
Uppsala University
Uppsala, Sweden

Opponent

Professor, Tuija Männistö
Faculty of Health Sciences
University of Eastern Finland
Kuopio, Finland

ISBN 978-952-02-0635-2 (PRINT)
ISBN 978-952-02-0636-9 (PDF)
ISSN 2736-9390 (Painettu/Print)
ISSN 2736-9684 (Sähköinen/Online)
Painosalama, Turku, Finland 2026

Rakkailleni

UNIVERSITY OF TURKU
Faculty of Technology
Department of Life Technologies
Molecular Biotechnology and Diagnostics
RAMI AALTO: Evolving Diagnostics of Myocardial Infarction; Differentiating Acute and Chronic cTnT Elevations with Improved Assay
Doctoral Dissertation, 188 pp.
Doctoral Programme in Technology
May 2026

ABSTRACT

Cardiovascular diseases (CVD) are the most common cause of death and coronary artery disease is the most prevalent CVD. In addition to morbidity and death, atherosclerotic cardiovascular disease produces major economic burden in society which is a combination of treatment costs and productive years lost.

Atherosclerotic cardiovascular disease may lead to myocardial infarction (MI) where occlusion of coronary blood flow leads to myocardial ischemia and necrosis. Electrocardiography (ECG) is commonly utilized to rapidly identify ST-elevation myocardial infarction (STEMI). During non-ST-elevation myocardial infarction (NSTEMI) ECG changes can be inconclusive and further biomarker tests are warranted. Nowadays, cardiac troponins (cTn) are the preferred biomarkers of myocardial damage. Unfortunately, both cardiac troponin I (cTnI) and cardiac troponin T (cTnT) assays currently utilized are unable to differentiate between cTn elevation induced by MI and non-MI conditions, such as end-stage renal disease (ESRD). Intact or almost intact forms of cTnT (long cTnT) show improved specificity for MI when differentiating between chronic and acute cTnT elevation. To measure long cTnT reliably, highly sensitive assay is needed. The assay sensitivity can be enhanced by improving the properties of the labels used in the immunoassay.

In this thesis, the first immunoassay targeting long forms of cTnT was developed, evaluated for its performance and clinically evaluated with MI and ESRD patients treated at the Turku University Hospital. The assay was compared to the 5th gen Roche Elecsys hs-cTnT assay. In addition, the stability of the sample matrix was evaluated in the context of the novel assay. The thesis also includes synthesis and characterization of novel europium chelate labels for time-resolved fluorescence immunoassays.

The long cTnT immunoassay was successfully developed and evaluated. For the first time ever, it was clinically demonstrated that an assay targeting intact or almost intact cardiac troponin T could differentiate between cTnT elevation in MI and ESRD. The novel method clinically outperformed Elecsys hs-cTnT in this regard, especially by utilizing long/total cTnT ratio in the early hours of MI. Additionally, three new europium labels were successfully synthesized and characterized.

KEYWORDS: Atherosclerosis, coronary artery disease, myocardial infarction, cardiac troponin, troponin fragmentation, long forms of cardiac troponin T, immunoassays, europium chelates, time-resolved fluorescence.

TURUN YLIOPISTO
Teknillinen tiedekunta
Bioteknologian laitos
Molekulaarinen biotekniikka ja diaknostiikka
RAMI AALTO: Sydäninfarktin kehittyvä diagnostiikka; kroonisen ja akuutin cTnT-pitoisuuden erottaminen parannetulla mittausmenetelmällä
Väitöskirja, 188 s.
Teknologian tohtoriohjelma
Toukokuu 2026

TIIVISTELMÄ

Sydän- ja verisuonitaudit ovat maailmanlaajuisesti yleisin kuolinsyy ja sepelvaltimotauti niiden yleisin muoto. Ateroskleroottinen sepelvaltimotauti aiheuttaa sairastavuuden ja kuolleisuuden lisäksi huomattavia taloudellisia rasitteita, jotka koostuvat hoitokustannuksista ja menetetyistä työvuosista.

Sepelvaltimotauti voi johtaa sydäninfarktiin, jossa sepelvaltimon tukkeuma aiheuttaa sydänlihaksen iskemiaa ja nekroosia. Elektrokardiografia on keskeinen menetelmä ST-nousuinfarktin tunnistamisessa. Ei-ST-nousuinfarktissa (NSTEMI) EKG-muutokset voivat kuitenkin olla epäselviä ja diagnoosi perustuu tällöin usein sydänperäisten troponiinien (cTn) mittaamiseen. Nykyiset kaupalliset määritykset eivät kykene erottamaan sydäninfarktin aiheuttamaa cTn-pitoisuuden nousua muista ei-infarktiperäisistä tiloista, jotka aiheuttavat kohonneita cTn-pitoisuuksia. Ehjä tai lähes ehjä troponiini (pitkä cTnT) osoittaa parempaa spesifisyyttä sydäninfarktille kyeten erottamaan krooniset ja akuutit cTn nousut. Pitkän cTnT:n mittaaminen edellyttää erittäin herkkää menetelmää, jonka suorituskykyä voidaan tehostaa parantamalla käytettyjen leimamolekyylien ominaisuuksia.

Tässä väitöskirjassa kehitettiin uusi immunomääritys, joka tunnistaa sydänperäisen troponiini T:n pitkät muodot. Menetelmän kliininen toiminta arvioitiin Turun yliopistollisessa keskussairaalassa hoidettujen sydäninfarkti ja ESRD -potilaiden avulla. Määritystä verrattiin 5. sukupolven Roche Elecsys hs-cTnT-määritykseen. Lisäksi tutkittiin näytematriisin säilyvyyttä ja menetelmä arvioitiin CLSI:n ohjeistuksen mukaisesti. Väitöskirjaan sisältyi myös uusien aikaerotteisten fluoresenssi europiumkelaattileimojen synteesi ja karakterisointi.

Tässä väitöskirjatutkimuksessa kehitettiin ja arvioitiin ensimmäinen troponiinin pitkiä muotoja mittaava immunomääritys ja kyettiin kliinisesti osoittamaan ensimmäistä kertaa, että määritys, joka tunnistaa ehjän tai lähes ehjän sydänperäisen troponiini T:n, kykenee erottamaan toisistaan sydäninfarktissa ja munuaistaudissa havaittavan cTn-pitoisuuden. Kehitetty menetelmä suoriutui näiden potilasryhmien erottelusta paremmin kuin Elecsys hs-cTnT, varsinkin kun hyödynnettiin pitkän ja kokonaistroponiinin suhdetta infarktin alussa. Lisäksi kolme uutta europium vasta-aineleimaa onnistuttiin syntetisoimaan ja karakterisoimaan.

ASIASANAT: Ateroskleroosi, sepelvaltimotauti, sydäninfarkti, sydänperäinen troponiini, troponiinin pilkkoontuminen, sydänperäisen troponiini T:n pitkät muodot, vasta-ainetestit, europiumkelaatit, aikaerotteinen fluoresenssi.

Table of Contents

Abbreviations

aar	Amino acid residue
ACC	American College of Cardiology
ACS	Acute coronary syndrome
AHA	American Heart Association
ALK1	Activin receptor-like kinase 1
Apo	Apolipoprotein
ArC	Aromatic carbon
ArH	Aromatic hydrogen
AST	Aspartate aminotransferase
AUC	Area under the curve
BITC	Biotin isothiocyanate
Boc	tert-butyloxycarbonyl
BSA	Bovine serum albumin
CABG	Coronary artery bypass grafting
CAD	Coronary artery disease
CK	Creatine kinase
CK-MB	Creatine kinase MB-subunit, activity
CK-MBm	Creatine kinase MB-subunit, mass
CLSI	Clinical and Laboratory Standards Institute
CT	Computed tomography
cTn	Cardiac troponin
cTnI	Cardiac troponin I
cTnT	Cardiac troponin T
CV	Coefficient of variation
CVD	Cardiovascular diseases
C-CB	Committee on Clinical Applications of Cardiac Bio-Markers
DCM	Dichloromethane
DIPEA	N,N-diisopropylethylamine
DMF	Dimethylformamide
DTPA	Diethylenetriaminepentaacetic acid
ECG	Electrocardiography

EDTA	Ethylenediaminetetraacetic acid
eGFR	Estimated Glomerular Filtration rate
eNOS	Endothelial nitric oxide synthase
ESC	European Society of Cardiology
ESRD	End-stage renal disease
EtOAc	Ethyl acetate
Et_2O	Diethyl ether
Fab	Fragment antigen-binding region
FDA	US Food and Drug Administration
FH	Familial hypercholesterolemia
FIDD	Fibrin D-dimer
FPLC	Fast protein liquid chromatography
HAMA	Human anti-mouse antibodies
Hb	Hemoglobin
HBTU	Hexafluorophosphate benzotriazole tetramethyl uranium
HDL	High-density lipoprotein
HPLC	High-pressure liquid chromatography
HRMS	High-resolution mass spectrometry
hs-cTn	High-sensitivity cardiac troponin
ICP-MS	Inductively coupled plasma mass spectrometry
ICT	Intramolecular charge transfer
IDL	Intermediate-density lipoprotein
IFCC	International Federation of Clinical Chemistry
IFU	Instruction for use
IgG	Immunoglobulin G
IHD	Ischemic heart disease
IQR	Interquartile range rule
LD	Lactate dehydrogenase
LDL	Low-density lipoprotein
LDLox	Oxidized low-density lipoprotein
LiH	Lithium heparin
Ln	Lanthanide
LoB	Limit of blank
LoD	Limit of detection
LoQ	Limit of quantitation
LMW-ITC	Low molecular weight ITC complex
mAb	Monoclonal antibody
MALDI-TOF	Matrix-assisted laser desorption/ionization time-of-flight
MeOH	Methanol
MI	Myocardial infarction

MINOCA	Myocardial infarction with non-obstructive coronary arteries
MPO	Myeloperoxidase
NADPH	Nicotinamide adenine dinucleotide phosphate (reduced)
NcTnI	Cardiac-exclusive N terminal domain of cTnI
NMR	Nuclear magnetic resonance
NOX	NADPH oxidase
NSTEMI	Non-ST-elevation myocardial infarction
PCI	Percutaneous coronary interventions
PE	Petroleum ether
POC	Point-of-care
proBNP	Prohormone of brain natriuretic peptide
ROC	Receiver operating characteristic
ROS	Reactive oxygen species
RT	Room temperature
SAP	Stable angina pectoris
SMC	Smooth muscle cells
SR-B1	Scavenger receptor class B type 1
STEMI	ST-elevation myocardial infarction
skTn	Skeletal troponin
TEA	Triethylamine
TFA	Trifluoroacetic acid
THF	Tetrahydrofuran
TnC	Troponin C
TM	Tropomyosin
TRF	Time-resolved fluorescence
TSA	Tris-buffered saline with azide
UAP	Unstable angina pectoris
URL	Upper reference limit
UV-Vis	Ultraviolet-visible
WHF	World Heart Federation
WHO	World Health Organization
XO	Xanthine oxidase
ε	Molar extinction coefficient
$\varepsilon\varphi$	Brightness
φ	Quantum yield
$r\varphi$	Relative quantum yield
λ	Wavelength
λex	Excitation wavelength
λem	Emission wavelength
τ	Photoluminescence decay time

List of Original Publications

This dissertation is based on the following original publications, which are referred to in the text by their Roman numerals:

I Aalto R, Lahtinen A, Airaksinen KEJ, Vasankari T, Hellman T, Koskimäki L, Wittfooth S. Design and analytical evaluation of an immunoassay for long forms of cardiac troponin T. *J Appl Lab Med*, 2026; 11(1):36–47.

II Airaksinen KEJ, Aalto R, Hellman T, Vasankari T, Lahtinen A, Wittfooth S. Novel Troponin Fragmentation Assay to Discriminate Between Troponin Elevations in Acute Myocardial Infarction and End-Stage Renal Disease. *Circulation*, 2022; 146:1408–1410.

III Aalto R, Wang Q, Takalo H, Rosenberg J, Bamberg K, Koskimäki L, Soukka T, Wittfooth S. Synthesis and Characterization of Novel Highly Luminescent Europium(III) Chelates Excitable at Long-Wavelength Ultraviolet. [manuscript]

1 Introduction

Cardiovascular diseases (CVD) are the leading cause of death globally. According to the estimates by World Health Organization (WHO), almost 18 million lives are lost annually due to CVDs.[1] In addition, CVDs place an enormous health, mental and economical pressure on inflicted individuals and their relatives. Ischemic heart disease (IHD) which is most often caused by coronary artery disease is the most prevalent CVD. In 2019 the estimated global prevalence of IHD was 197 million cases with over 9 million deaths.[2] On a society level IHD causes economic burden that is a combination of treatment costs and productive years lost. In European Union alone, cardiovascular diseases are estimated to cause annual productivity losses of €48 billion, informal care costs of €79 billion and healthcare expenditure of €155 billion, which is around 11% of the total EU-healthcare expenses in 2021. Contribution of ischemic heart disease to this sum was estimated to be €77 billion.[3] In United States, the estimated figures were similar in 2016. Total annual CVD treatment expenses were $320 billion from which ischemic heart disease accounted for the largest part around $80 billion.[4]

Ischemic heart disease is caused by the narrowing of the coronary artery by atherosclerotic plaque. This condition can lead to acute coronary syndrome (ACS) where the coronary blood flow is suddenly decreased. In case of unstable angina pectoris (UAP) this process is usually reversible and no myocardial cell damage occurs. ACS can also lead to myocardial infarction (MI) where the plaque causes sudden and often irreversible occlusion of coronary blood flow, thus leading to myocardial ischemia and eventually necrosis. For some people myocardial infarction is the first sign of IHD.[5]

The MI diagnosis is composed by clinical symptoms, electrocardiography (ECG), imaging techniques and biomarker tests. Usually, the physician is alerted to consider myocardial infarction by clinical symptoms. These might include sudden chest pain, pain radiating to upper arms or jaw or difficulty to breath. Even though pain is a common MI symptom, not all patients experience same symptoms including pain. Also, similar clinical symptoms might be seen in multiple other conditions. Thus, clinical symptoms alone are non-specific and further clinical tests are needed. Depending on the tier of the treatment unit, not all diagnostic techniques might be

available at the location. This is especially true in case of different imaging equipment and trained personnel which are usually found in hospitals. ECG is commonly available in different treatment tiers including emergency medical service units like ambulances. With ECG, ST-elevation myocardial infarction (STEMI) can be rapidly diagnosed in most cases and correct actions implemented. In case of non-ST-elevation myocardial infarction (NSTEMI) ECG might be normal or inconclusive and thus definite diagnostic conclusions cannot be made.[6]

In suspected NSTEMI cases and other situations where the diagnosis needs further confirmation, clinicians can rely on biomarker tests to identify those that have ongoing or have recently experienced myocardial damage. Nowadays the most commonly used biomarker tests for MI are the cardiac troponin (cTn) tests.[6] cTn is a protein complex that is essential for myocardial muscle contraction. During myocardial cell damage, cTn is released into the blood stream. Even though cTn is extremely good marker for myocardial cell damage, it unfortunately has its shortcomings in MI diagnostics. Both cardiac troponin I (cTnI) and cardiac troponin T (cTnT) assays currently in use lack the capability to differentiate between MI induced cTn elevation and non-MI induced elevations, which can be encountered in multiple situations and conditions.[5]

In chronic conditions with cTn elevation, mainly highly fragmented forms of cTn have been encountered.[7] In contrast, in MI, mainly intact and almost intact forms of cTn are released and subsequently degraded into smaller troponin fragments.[8] Thus, by targeting specific structural forms of cTn, it may be possible to differentiate between cTn elevations resulting from MI and those associated with chronic conditions. Unfortunately, this improvement in clinical specificity requires highly sensitive assay, which may be achieved by developing and synthesizing new highly fluorescent immunoassay labels.[9]

In ACS diagnostics, speed and diagnostic accuracy are essential for preventing further myocardial damage.[6] By improving the clinical specificity of MI diagnostics, it might be possibly to improve treatment outcomes and to decrease the related long term treatment costs.

2 Literature Review

2.1 Historical Perspective of Atherosclerosis and MI

From early post-mortem observations to the onset of diagnostics era

Throughout history, atherosclerosis and associated diseases have been part of human life and death. Modern archaeology has revealed that the iceman Ötzi, ancient Egyptians and 16th century Inuit all endured the same atherosclerotic ailments that we modern-day humans do.[10–12] It is unclear if priests and healers at that time could identify these macroscopic vascular changes of the coronary arteries and aortas during embalming or autopsies and if so, understood the causal relationship between them and death due to "chest pain". Much of ancient knowledge has been lost, but for certain we know that many curious minds were needed to advance our understanding of blood circulation and atherosclerosis. One of these minds was that of Leonardo da Vinci who stated that "vessels in the elderly restrict the transit of blood through thickening of the tunics".[13,14] This early observation was followed by many others. In 1575, posthumously published texts of Italian physician and priest Gabriele Falloppio describe "degeneration of arteries into bone".[15,16] In 1628, physician extraordinary to James I of England, William Harvey, proved blood circulated and was moved by the heart, instead of lungs.[17,18] In 1740, Gottfried Reinhold under physician Johann Crell noted that coronary artery hardening was not merely bony, but derived from pus.[16] However, it was not until 1833 that a French-German surgeon and pathologist (and enthusiastic archaeologist) Jean Lobstein gave these observed changes of arteries a name "arteriosclerosis". Although in his definition these changes did not include ossification and were limited to large arterial trunks.[19,20] It was later in 1904 when a German professor of pathology Felix Marchand adopted the term "atherosclerosis" and later terminology discussions especially in the 1950s and 60s that molded the terminology we use today.[21,22]

It is evident that "thickening of the tunics", or atherosclerosis in modern terms, was seen as an unavoidable part of aging in early accounts.[23] Although, general understanding of anatomy and blood circulation was still lacking during the Renaissance, it can be assumed due to humoralism being the prevalent theory at the

time, that these vascular changes were seen as something that affects health through restricting blood flow as stated by Da Vinci.[13,14]

Due to the evolution of medical practices and instruments, surgeons and pathologists started to identify "thickening of the tunics" more widely as pathological in the latter half of the 18th century. In 1761, anatomist Giovanni Morgagni published De Sedibus, where he described in detail many anatomic structures and pathological findings, including those of coronary arteries. In addition, De Sedibus provided important information associating clinical symptoms to post-mortem findings.[24,25] A few years later in 1768, Physician William Heberden held his lecture where he associated the symptoms of angina pectoris and the sudden death that could follow.[26] His friend and colleague John Fothergill was one of the first to suspect heart as an origin of angina pectoris, but failed to conclude the role of coronary arteries.[27] The first to associate angina pectoris and sudden cardiac arrest with calcification of coronary arteries were the famous physicians Edward Jenner and Caleb Parry with whom Jenner shared his autopsy observations and who then reported them to the public in 1799.[28] Jenner stated that during the autopsy of a patient deceased due to angina pectoris, he could not find any cause after examining the heart, that is until his knife struck something hard and gritty. He first thought that some plaster had fallen down from the ceiling, but then understood that the coronary arteries had become bony canals. Jenner then concluded that coronary artery ossification was the culprit behind angina pectoris and death of the patient.[28,29] Similar conclusion was independently reached by Irish physician Samuel Black, who also associated his pathological findings with lifestyle habits: "the great majority of the subjects of it have belonged to better ranks of society, who were in the habit of sitting down every day to a plentiful table".[30–32]

In 1840, the 4th edition of "Pathology and Diagnosis of Diseases of the Chest" by physician Charles Williams was published and there he contemplated that the colour and structural changes observed in the hearts of the suddenly deceased could be due to the "altered state of nutrition of the organ, owing to a partial obstructions in the coronary vessels, rather than to the immediate influence of inflammation."[33,34] Later student and friend of his, Richard Quain, studied the microscopic structure of the myocardium and noticed that many suddenly deceased had lipid accumulations within muscle fibers, which they referred to as "fatty degeneration". Quain postulated that fatty degeneration, later known as myocardial steatosis, was due to coronary occlusion.[33,35]

Around the same time as Williams and Quain, pathologists Rudolf Virchow in Germany and Carl von Rokitansky in Austria-Hungary described cellular inflammatory changes in atherosclerotic vessel walls. According to Mayerl *et al.*, Rokitansky thought these changes were secondary in nature, whereas Virchow considered inflammation to have a primary role in atherogenesis.[36] In his

publication Cellular Pathology translated by Frank Chance, Virchow describes as follows: " …in the next place, a second series of changes, in which we can distinguish a stage of irritation preceding the fatty metamorphosis, comparable to the stage of swelling, cloudiness, and enlargement which we see in other inflamed parts. I have therefore felt no hesitation in siding with the old view in this matter, and in admitting an inflammation of the inner arterial coat to be the starting point of so-called atheromatous degeneration."[37]

Although several atherosclerotic changes and even lifestyle habits had now been associated with angina pectoris and sudden death, the importance of plaque rupture and occlusion of the coronary arteries were still somewhat hazy. In 1844, a few years after Williams published his work, the famous Danish artist Bertel Thorvaldsen died while attending a show in Copenhagen Royal Theatre. What made his case exceptional, was not only his prominent figure but also his autopsy report, which is commonly cited as the first described case of plaque rupture in the written medical history: "… the anterior [coronary artery] exhibited numerous atheromatous sections from one inch below its origin to its division. One of these was rather seriously ulcerated, and the atheromatous mass had drained into the arterial cavity".[13,38] After the death of Thorvaldsen, 33 years went by before the first clinical diagnosis of coronary occlusion was made by Adam Hammer in 1877 and confirmed post-mortem.[39] It took another 40 years until in 1912 physician James Herrick pointed out that plaque rupture followed by coronary occlusion was the probable cause of Thorvaldsen`s demise, and noted the significance of the autopsy report.[40] Herrick is also often described as the first one to point out that coronary occlusion was not necessarily fatal, but could resolve with rest. In fact, there were people such as Julius Cohnheim, a student of Virchow, who stated in 1881 that occlusion of smaller coronary artery branches was not inevitably fatal.[41] However, Dr. Herrick was the first to utilize a new invention called ECG to diagnose MI and to demonstrate that one could survive it, thus reinvigorating interest in research, diagnostics and treatment of myocardial infarction.

Era of MI diagnostics

It is safe to state that the era of MI diagnostics started when Augustus Waller recorded the first ECG of human heart in 1887 using Lipmann mercury capillary electrometer.[42] As this equipment was crude and far from practical or reliable, a Dutch physician and a Nobel laurate Willem Einthoven utilized string galvanometer and invented the first practical electrocardiograph machine in 1903.[43,44] In 1919, the already mentioned James Herrick adapted the new innovation to observe patients with severe non-fatal angina pectoris. Thus, first time in history there was a diagnostic method to identify myocardial infarction.[45]

In the following decades ECG was improved, which led to the standardization of 12-lead ECG in 1954.[46] Although the innovation of ECG was ground breaking, it was accompanied and followed by several other important advances in cardiac diagnostics and imaging. First of these advances was the accidental discovery of X-rays at the end of 19th century and the first clear cardiac X-ray images, which were enabled after the invention of "Blitzapparat" - a short exposure x-ray machine by physicist Friedrich Dessauer in 1909.[47,48] Although basic röntgenogram offered limited information on soft tissue, it was revolutionary invention. In 1929 Werner Forssmann, at the time a surgical resident, used cardiac X-ray imaging to confirm that he had successfully performed the first ever (self!) cardiac catheterization.[39,49] Few decades later in 1958 F. Mason Sones Jr. accidentally performed the first selective coronary angiography and initially feared he had doomed the patient.[50] The development of efficient contrast agents and a few daring or accidentally performed experiments allowed cardiac vasculature to be selectively visualized. The utilization of X-rays did not stop there as in 1971 the first patient underwent computed tomography (CT) scanning. The first CT machine engineered by Godfrey Hounsfield was solely crafted for head scans, but since then CT equipment have gradually improved to meet the needs of cardiac and cardiovascular imaging.[51,52]

After the discovery of X-rays and the first radioactive elements, early radionuclide imaging technologies were also starting to emerge. In 1927 Blumgart *et al.* published several papers depicting clinical results and a method where they injected sodium chloride solution infused with radium C (^{214}Bi) and observed diminished arm-to-arm circulation times for those individuals that were experiencing arteriosclerosis or heart failure.[53,54] This experiment was followed by a long chain of innovations that led to the utilization of myocardial perfusion imaging in combination of a stress test in 1973 by Zaret *et al*.[55,56] With myocardial perfusion imaging it was now possible to asses which myocardial areas were experiencing decreased blood circulation.

In the 1940s mitral valve stenosis could be operated by dilating (inserting a finger) to the mitral valve opening. If the patient had undiagnosed mitral insufficiency this operation could in turn deteriorate the condition of the patient. This clinical need led to the innovation of echocardiography in 1953 by cardiologist Inge Edler and physicist Hellmuth Hertz. This innovation enabled the visualization of heart movements and thus established a convenient way to diagnose mitral insufficiency and many other cardiac conditions.[57,58]

Almost simultaneously with the emergence of echocardiography, the era of cardiac biomarkers started to emerge. The first biochemical biomarker utilized for acute myocardial damage was aspartate aminotransferase (AST) in 1954 and followed shortly after in 1955 by lactate dehydrogenase (LD). Both of these enzymes were first studied and suggested as cardiac biomarkers by John Ladue, Felix

Wróblewski and in case of AST, also Arthur Karmen.[59,60] Both of these markers were far from optimal as AST, although providing somewhat good clinical sensitivity, lacked sufficient clinical specificity and LD, even though offering improvement compared to AST, faced similar specificity problems.[61]

In 1960 it was noticed by Dreyfus *et al*. that increased activity of creatine kinase (CK) was associated with myocardial infarction.[62] Total CK activity was not highly specific for MI, but offered another enzyme that could add diagnostic information. The true importance of this finding was that it led to the development of CK-MB activity (CK-MB) and CK-MB mass (CK-MBm) assays. In 1972 Roe *et al*. created electrophoretic method for CK-MB and established its usefulness in MI. The finding, although again offering improvements in clinical sensitivity and specificity towards MI, had its drawbacks as several preanalytical or analytical factors could affect CK-MB results.[61] Over decade later in 1985, the first immunoassay for CK-MB mass (concentration of CK-MB), was developed by Chan *et al*.[63] Measuring the actual concentration made the CK-MBm assay devoid of the same preanalytical and analytical problems that affected CK-MB enzyme activity. Still the measurement of CK-MBm could not change the fact that skeletal muscles contained CK-MB isoform in small amounts and thus could affect clinical specificity of the measurement.[64]

A few years after the usefulness of CK-MB had been established as a diagnostic marker for MI, the first results concerning the use of myoglobin in MI diagnostics were published by Stone *et al*. Although offering promising results, especially during the first hours after onset of MI, this assay took over 24h to perform.[65] Further development of myoglobin assays improved the turnaround times, thus enabling their use in clinical settings in mid 80s.[61]

The real breakthrough diagnosing myocardial damage came in 1980s with the introduction of first troponin I and T assays. “Tropomyosin like protein” or troponin complex as we name it today, was first discovered in 1965 by physiologist Setsuro Ebashi and Ayako Kodama.[66] Later in early 1970s, it was recognised by Greaser and Gergely that the protein was comprised of three distinct subunits that were later named as troponin I, T and C.[67] This finding was followed by several structural and sequencing studies that revealed the existence of troponin isoforms and their tissue specific distribution.[68–71] The first ever troponin assay and its diagnostic utility was reported in form of an abstract by Cummins and Auckland in 1983.[72] The comprehensive evaluation of this cTnI radioimmunoassay was published four years later in 1987.[73] The first troponin T immunoassay was developed by Katus *et al*. in 1989 and later in early 1990s transferred into automated ES-analysers (Enzymun-TestR system) by Boehringer Mannheim.[74,75] The new troponin I and T assays offered enhanced clinical specificity compared to previously established biomarkers of myocardial damage and thus started a new era of how we define and diagnose myocardial infarction.[76]

2.2 Atherosclerotic Coronary Artery Disease

Atherosclerosis is a pathological process where lipids accumulate into vascular tunica intima, disrupting the vascular structure and potentially obstructing flow of blood either by narrowing the vasculature or by producing unstable atherosclerotic lesions which after rupture or erosion may cause formation of a blood-lipid clot that may occlude the affected vascular area and cause an ischemic event.[5,77]

In 1910, a German chemist and Nobel prize laureate Adolf Windaus showed that atherosclerotic plaques were consisted of calcified connective tissue and cholesterol.[36,78] Few years later Nikolai Anichkov and Semen Chalatov were able to prove that cholesterol rich diet could induce atherosclerotic changes in rabbits.[79–81] The link between blood cholesterol levels and risk of myocardial infarctions in humans was established in 1938 when physician Carl Müller discovered familial hypercholesterolemia (FH), in which the affected individuals had 20-fold higher incidence of heart attacks during their adulthood when compared to normal population.[82,83] A decade later in 1949, biophysicist and Manhattan Project veteran John Gofman and his graduate student, Frank Lindgren, with the help of Edward Pickles, utilized ultracentrifugation to separate plasma lipoproteins into density fractions and showed that in patients with FH, the cholesterol elevation was mainly due to the elevation in low-density (LDL) and intermediate-density (IDL) lipoprotein fractions.[84] Although, the molecular mechanism behind atherosclerosis is complicated and still not fully understood, these early discoveries laid the foundation for further studies. Nowadays several risk factors and molecular interactions affecting the initiation and the progress of macroscopically visible atherosclerosis have been identified.

The atherosclerotic process is considered to start when lipoproteins containing apolipoproteins (Apo) such as ApoB100, ApoB48 or Apo(a) are transferred into vascular tunica intima.[85] From these apolipoproteins ApoB100 is considered be highly relevant as it is the main apolipoprotein of LDL.[86] The influx of lipoprotein particles into the tunica intima occurs via caveolae-mediated transcytosis involving scavenger receptor class B type 1 (SR-B1) and activin receptor-like kinase 1 (ALK1).[87–91] After the cholesterol rich LDL particles have journeyed though the endothelium into the tunica intima, retention and oxidation of LDL occurs. The retention of LDL is mediated through set of apolipoproteins, such as those mentioned previously, that bind into negatively charged proteoglycans, that are part of the vascular extra cellular matrix and affect the physicochemical properties of the vasculature.[92–97] Generally, it is thought that retention of LDL by proteoglycans extends exposure time at the intima and thus promotes enzymatic and oxidative changes of LDL.[98,99] Several oxidative enzymes have been proposed to contribute to the formation of LDLox at different stages of plaque formation. These include lipoxygenase, NADPH oxidases (NOX), uncoupled endothelial nitric oxide

synthase, xanthine oxidase (XO) and myeloperoxidase (MPO). [100–104] In addition, other factors such as heme iron from microbleeds and mitochondrial reactive oxygen species (ROS) have been suggested.[105,106] The accumulation of LDLox and other oxidative species induces inflammation response and activation of the immune system. This leads to the infiltration of immune cells and uptake of LDLox by macrophages and specialised smooth muscle cells (SMC) via scavenger receptors LOX-1, CD36 and SR-A.[107,108] Free cholesterol may be removed from the foam cells via HDL mediated efflux.[109–111] Imbalance between cellular influx and efflux of lipids leads to the formation of foam cells.[111–120] In time, this pathological process may lead to clinically manifesting coronary artery disease and in worst case myocardial infarction and death.

The process leading to the development of atherosclerotic plaque and clinically manifesting coronary artery disease starts at early age and can take decades to evolve.[121,122] This was first demonstrated by US Armed Forces Institute of Pathology in 1950 when young soldiers killed in the Korean war were autopsied. With the average age of 22 years, 77% of the deceased showed some level of atherosclerotic changes in their coronary arteries.[123]

2.2.1 Classification of Atherosclerotic Lesions Based on Morphological Differences

Morphological changes of arteries were the first observational findings of atherosclerosis made centuries ago. These findings laid the base for later research and understanding of the disease. In the end of 1960s, AHA Committee on Grading Lesions of the Council on Arteriosclerosis first introduced two sets of colour photographs of arteries arranged in increasing severity of atherosclerosis as a method to grade the severity of atherosclerosis in human coronary arteries and aortas.[124] In the early 1990s AHA Committee on Vascular Lesions of the Council on Arteriosclerosis, introduced their definitions of atherosclerotic lesions. Type I (intima thickening) and II (fatty streaks) are defined as initial changes. Type III is classified as intermediate lesion that is a sign of progressive disease. Type IV, V, VI, VII and VIII are classified as advanced lesions with increasing severity and signs of risk factors for plaque integrity.[125,126] Diverting from the original classification, subdivisions of lesions (IIa, IIb, Vb…) were later removed and updated classification scheme is shown in Figure 1.[127]

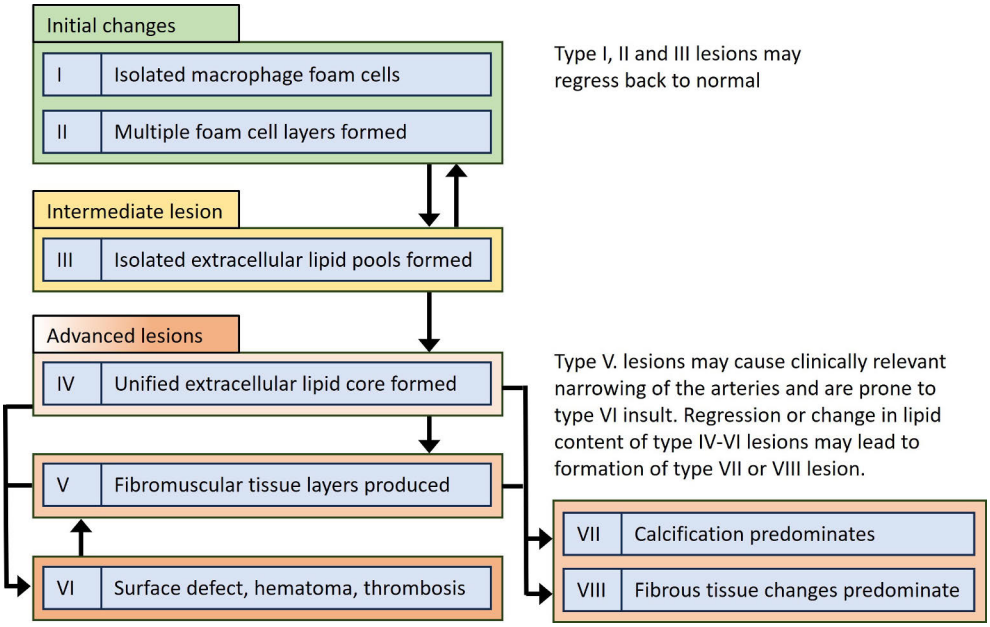

Figure 1. The updated lesion classification scheme adapted from AHA Committee on Vascular Lesions.[127]

Type I

The initial histological changes are minimal. Small, isolated groups of macrophage derived foam cells and lipid deposition can be identified by microscopy or by biochemical means. In coronary arteries these changes can be seen in intima at regions that have an adaptive intimal thickening of the eccentric type.[125]

Type II

Microscopic composition determines whether a lesion is classified as type II. This kind of lesions consists primarily of macrophage foam cells arranged into adjacent layers, whereas type I lesions have only isolated groups of these cells. Increased amounts of macrophages without lipid accumulation are also present. In addition to macrophages, first signs of T cell infiltration, increased amount of mast cells and intimal SMC containing lipid droplets can be detected. Although, most of the lipid accumulation in the lesion is inside cells, extracellular space contains small amounts of dispersed lipid droplets and vesicular particles of different sizes. In addition, there are smaller extracellular lipoprotein particles that are not visible by routine microscopy. The lipid content consists primarily of cholesterol esters (77%), cholesterol and phospholipids. Fatty streaks, a first visible morphological change in atherosclerosis, are considered type II lesions. However, lesions can fulfill the

microscopic criteria of type II lesion without fatty streak formation. These changes are clinically benign, but they may later develop into clinically relevant lesions. Fatty streaks manifest regardless of age and have been identified even in infants and young children. In the original classification type II lesions were further divided into subgroup IIa (progression-prone type) and IIb (progression-resistant type). In the updated version this subdivision was removed. Now it is emphasized that mechanical forces cause adaptive intimal thickening in areas that are most affected by these forces. These sites are associated with intimal lipid accumulations and lesions that are prone to progression.[125,127]

Type III

The characteristic feature of type III lesion is microscopically visible extracellular lipid droplets that reside among SMC below the layer of macrophages and macrophage derived foam cells. These extracellular lipid accumulations disrupt the intimal smooth muscle structure and replace intercellular matrix proteoglycans and fibers. In type III lesion a lipid core has not yet developed. The extracellular lipid droplets can be bound to membrane or be free, but in larger quantities than in some more immature lesions. When compared to type II lesion, type III lesions contain more free cholesterol, fatty acids, sphingomyelin, lysolecithin and triglycerides. Type III lesion may progress to advanced lesion or regress.[125,127]

Type IV

Type IV is the first lesion considered advanced. The lipid core, which is the hallmark of type IV lesion, is formed by the dense accumulation of extracellular lipid in the intima. The lipid core causes severe intimal disorganization, but the intima layer above the core is mainly unchanged when compared to earlier lesion types. Also, within the core, calcium particles can often be found. However, no fibrous tissue formation or other complications of endothelial integrity can be seen. The intima above the lipid core contains macrophages and SMC, which can be either infused with lipids or be without lipid accumulations. Lymphocytes and mast cells are also present. Even though usually visible to the naked eye and possibly even obstructive, type IV lesions don`t generally narrow the vascular lumen to great extent. [126,127]

Type V

Type V lesions are characterized by extensive formation of new fibrous connective tissue, which disrupts the normal intercellular matrix. They may contain multiple lipid cores in various arrangements, separated by fibrous connective tissue. Type V

lesions are considered clinically highly relevant as they can cause narrowing of the arteries and are prone to develop fissures, hematoma and thrombus.[126,127]

Type VI

Type VI lesions are associated with hematoma, hemorrhage and/or thrombosis. Atherosclerosis related morbidity and mortality are largely due to type IV and type V lesions which develop disruption of endothelium. However, any type of lesion or intima without lesion can precede type VI lesion.[126,127]

Type VII and VIII

In a type VII lesion calcium mineralization is the dominant feature. The lesion consists of increased fibrous connective tissue and large calcium deposits, which may replace even lipid cores. In case of type VIII lesion, the lipid content is generally minimal and the lipid core is thus absent. The normal intima is usually thick and replaced by extensive amount of fibrous connective tissue.[126,127]

2.3 Myocardial Infarction

2.3.1 Definition and Pathophysiological Classification of MI

The way acute coronary syndrome and myocardial infarction are defined has always followed the diagnostic capabilities at our disposal. The pre-ECG era relied heavily on clinical symptoms and findings on post-mortem autopsies. This changed after Dr. James Herrick adopted the use of ECG and thus modernized MI diagnostics.[45] Since then, the development of imaging technologies and diagnostic biomarkers, especially cTn, have altered how we define ACS and MI.

In 1959 WHO launched its first definition of MI and updated it actively in the following decades.[128,129] In 2000 ESC and ACC collaborated to redefine the definition of MI by utilizing troponin biomarkers.[130] In 2018 the fourth iteration of Universal Definition of Myocardial Infarction by ESC/ACC/AHA/WHF was released and is at the moment the newest iteration of the universal definition.[5]

MI is defined as a condition that leads to myocardial cell death due to myocardial ischemia.[5] Diagnostically elevation of circulating cTn above 99th percentile upper reference limit (URL) has been used to detect myocardial injury. As there are several chronic non-ischemic conditions that may cause cardiac injury and thus lead to elevated, but quite stable levels of cTn during relevant time frames, rise or fall of cTn values are required for the detection acute myocardial damage. To differentiate between acute non-ischemic and acute ischemic conditions, at least one additional

sign of ischemia must be present for the diagnosis of MI. These signs include clinical symptoms of ischemia, new ischemic ECG alterations, development of pathological Q waves in ECG, imaging evidence consistent with an ischemic etiology or identification of a clinically relevant coronary blockage. In addition, MI can be divided into subtypes based on factors such as different pathological mechanism or treatment related incidences.[5]

Myocardial infarctions are classified based on pathophysiology. These are referred as type 1 MI, type 2 MI etc. and the precise criterion for each type is given in the fourth universal definition of myocardial infarction.[5]

Type 1 MI

In type 1 MI full or partial thrombotic occlusion of the coronary artery occurs, leading to necrotizing myocardial ischemia.[5] The formation of thrombus is initiated either by sudden plaque rupture or by slower eroding process, where vascular endothelium is unable to prevent platelets coming into contact with subendothelial matrix.[131] In a study by Saaby *et al*., 72% of the 553 Danish patients hospitalized with myocardial infarction had type 1 MI.[132]

Type 2 MI

Type 2 MI happens due to imbalance between myocardial oxygen supply and demand that is sufficient to cause myocardial damage, but without acute atherothrombotic plaque disruption. Factors that might cause type 2 MI are for example: occlusion of coronary artery by atherosclerotic plaque without rupture, coronary artery spasm, coronary microvascular dysfunction, coronary embolism, coronary artery dissection, severe hypertension or shock, respiratory failure, severe anaemia, sustained tachyarrhythmia (abnormally fast heartbeat) or severe bradyarrhythmia (abnormally slow heartbeat).[5] According to a study by Saaby *et al*., around 26% of hospitalized MI patients had type 2 MI.[132]

Type 3 MI

The diagnosis of type 3 MI is set when the suspicion of MI is high, but the patient succumbs before reliable cardiac biomarker sample can be obtained. If other type of MI is confirmed post-mortem, the diagnosis is reclassified.[5]

Type 4a, 4b and 4c MI

Coronary interventions are associated with a risk of postprocedural MI due to intervention related coronary injury. Type 4 MIs happen due to percutaneous coronary interventions (PCI) and are subdivided into a, b, and c. The diagnosis of type 4a MI is usually set based on sufficient post-operational rise of cTn and additional evidence of ischemia. As it is statistically difficult to define cut-off values for a cTn rise in type 4 MI, they are arbitrarily defined. The diagnosis can also be established regardless of cTn, based on new pathological postprocedural Q waves or autopsy. Type 4b MI is diagnosed when the postprocedural MI is associated with stent/scaffold thrombosis utilizing criteria identical to type 1 MI and confirmed with either angiography or autopsy. Diagnosis of type 4c MI is set when MI happens during angiography, in-stent restenosis or if the infarct area is under restenosis following balloon angioplasty and no other culprit lesion or thrombus is found.[5]

Type 5 MI

Type 5 MI is associated with myocardial injury that happens due to coronary artery bypass grafting (CABG). The diagnosis is usually set based on sufficient post-operational rise of cTn and additional evidence of ischemia, such as ECG, angiography or imaging evidence. The cTn cut-off values of both type 4 and type 5 MIs are arbitrarily selected.[5]

2.3.2 Diagnostics of ACS and MI

Several guidelines have been published for the management of suspected ACS and for the treatment of confirmed ACS subtypes: STEMI, NSTEMI and unstable angina pectoris. The latest guideline iterations from different bodies include: ACC/AHA/ACEP/NAEMSP/SCAI (2025), ESC (2023), Käypähoito (2022).[6,133,134]

The suspicion of ACS often arises due to suggestive clinical symptoms. The most common associated symptom of ACS is the onset of sudden chest pain, angina pectoris, which is often described as sudden onset of pain, pressure or discomfort that may radiate from chest to arms, neck, jaw, shoulders and/or upper back.[135] Although pain is a common symptom of MI, it is not highly specific symptom nor is it always expressed with MI. Silent or atypical myocardial infarctions where no chest pain is felt are estimated to represent approximately one-tenth to one-third of all MI cases.[136–138] In addition, patients may also express symptoms that are vague and highly unspecific such as fatigue, dizziness, breathing difficulties, cold sweating, vomiting and general malaise.[139]

To investigate the possibility of MI further, the standard 12-lead ECG is usually acquired as soon as possible. In addition, leads such as V3R, V4R and posterior V7–

V9 can be utilized if required.[6,133,134] The use of additional leads is usually beneficial as they improve the sensitivity of ECG study and may reveal changes that would otherwise be missed or misinterpreted.[135] If the patient is located outside hospital or other appropriate medical facility, it is common practice in the developed countries that the first ECG is usually recorded by the emergency medical services unit within 10 minutes of arrival. If the initial ECG is inconclusive and symptoms persist or worsen, further ECG recording and surveillance is recommended.[6,133,134] It is noteworthy to mention that ECG alterations can evolve over time as the pathophysiological state of the myocardium changes.[140] Around 15% of patients that end up with STEMI diagnosis do not show ST-elevation in the initial ECG.[141] The amplitude and direction of the ECG changes in different leads can also vary depending on the location and extent of the ischemia. This can be exploited to locate the affected area or to assess risk of adverse outcomes, as patients presenting with ST-segment elevation in 8–9 of 12 leads have three to four times higher mortality compared to those with ST-elevation only in 2–3 leads.[77] The initial ECG may also be completely normal after transient episode of angina pectoris or change into normal due to pseudonormalization.[140] Ischemic changes in ECG can appear for example as hyperacute or inverted T waves, ST-segment elevation or depression, Q wave abnormalities, decrease of precordial R wave amplitude, cardiac arrhythmias or U wave inversion.[5,77,140] Hyperacute T waves and ST-segment changes can be the earliest pathological ECG alterations in MI.[142] Pathological Q waves usually take longer to appear, from few up to 24 hours or they might not appear at all, and thus MIs can be divided into Q-wave and non-Q-wave infarctions.[142] The significance of this division arises from the worse short-term prognosis of Q-wave infarctions.[5,143] Q waves can also indicate previously occurred MI.[142] T wave inversions due to MI may occur few hours up to 1–2 days after the onset of ischemia or they may occur as a positive sign after achieving reperfusion of the affected area.[77] Unfortunately, many other conditions can cause similar ECG changes as ischemia, and thus no single ECG change is specific to MI. For more precise description of possible ECG findings during ischemia or listing of possible alternative causes for different ECG changes can be found from several sources including literature work by Mann *et al*. and handbook of cardiology by Airaksinen *et al*.[77,135]

During suspected episode of ACS, initial diagnosis of either STEMI or NSTEMI is usually established when supported by sufficient evidence. If the ECG recording is consistent with ST-segment elevation as shown in Figure 2, fulfills criteria mentioned in Table 1 and there is no suspicion of a STEMI mimicking condition, initial diagnosis of STEMI is set. If no ST-segment elevation is detected in the ECG utilizing additional leads, but clinical symptoms in combination with other possible ECG findings suggest ischemic origin, initial diagnosis of NSTEMI is usually

made.[6] Patients are also divided into risk categories to guide their treatment. For the risk stratification, assessment tools like GRACE and TIMI risk scores can be utilized in addition to clinical and diagnostic information.[6,133,134]

ST-segment elevation is an indicator of severe transmural ischemia and is commonly associated with complete occlusion of affected part of coronary artery.[77] Thus ST-segment elevation is an important indicator which usually triggers the use of rapid reperfusion treatment options such as PCI or fibrinolytic therapy.[6,133,134] The diagnosis of STEMI can be confirmed later if necessary with high-sensitivity cTn (hs-cTn) measurement, although reperfusion should not be postponed due to pending biomarker results.[133,134] Similarly patients with indication of very high risk (GRACE 2.0 risk score >140) NSTEMI should undergo immediate invasive treatment strategy regardless of missing cTn results.[6]

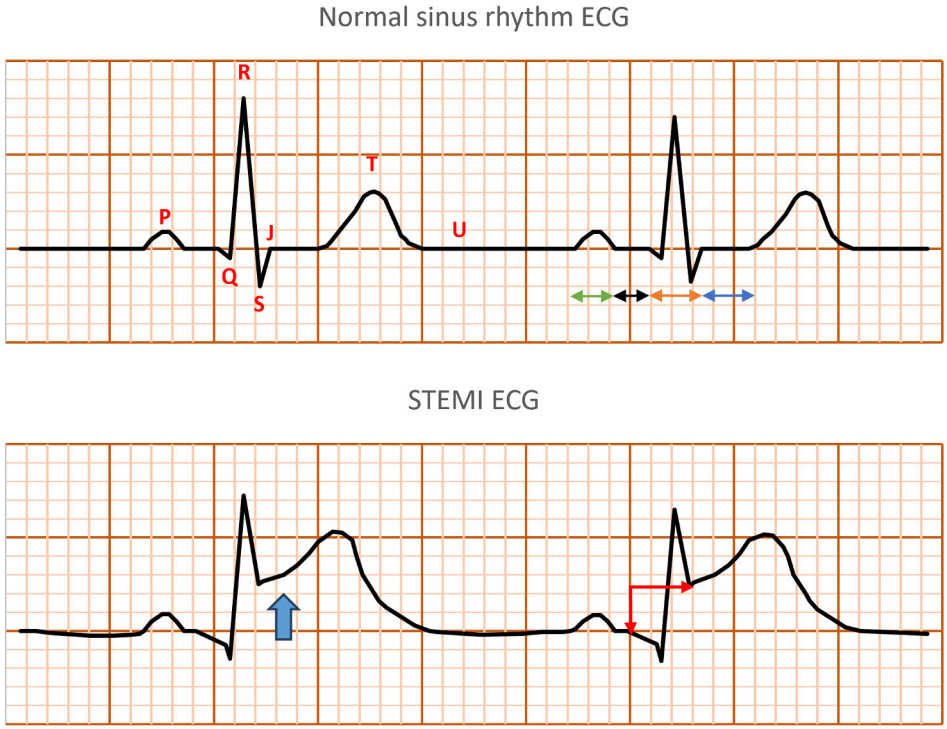

Figure 2. Approximated presentation of normal sinus rhythm ECG (upper graph) and STEMI ECG (bottom graph) in lead II. Letters: P wave, Q wave, R wave, S wave, J point, T wave and possible location of U wave. Double-headed arrows: P wave duration (green), PR segment (black), QRS duration (orange), ST segment (blue). Elevation of ST-segment (shown by the blue arrow) is measured based on the difference of J point and the initial onset of the Q wave (red arrows). Scale: 1 mm = one small square.

Table 1. **ECG** criteria of STEMI according to käypähoito recommendation [134]

New ST-segment elevation in 2 anatomically contiguous leads…	
Other than V2-V3 or V4R, V7-V9 leads: and/or	≥ 1 mm
In V2-V3 lead: and/or	≥2.5 mm in men <40 y ≥2 mm in men ≥40 y ≥1.5 mm in women regardless of age
In V4R, V7-V9 leads:	≥0,5 mm

ECG findings in NSTEMI are more varied as the group is clinically more heterogenous than STEMI.[135] ECG can be normal, atypical or show ST-segment depression or T wave inversions. Generally, ST-segment depression of 0.5 mm or 1 mm, depending on the guideline and leads in question, is considered to be indicative of ischemia when present in two or more contiguous leads.[6,133,134] If the ECG does not show ST-elevation consistent with STEMI or other highly indicative pattern for immediate reperfusion therapy, further diagnostic methods can be utilized to distinguish between NSTEMI, UAP, stable angina pectoris (SAP) and other conditions that might cause symptoms without ischemic origin. Usually this means in the context of suspected ACS the utilization of cardiac biomarkers cTnI or cTnT.

Ischemia induced myocardial damage induces the release of cTn biomarkers into the circulation. Assay results above the 99th percentile URL are indicative of myocardial injury. For rapid rule-in and rule-out several algorithms have been created and evaluated.[144] Usually nowadays with modern hs-cTn assays, the use of ESC 0h/1h algorithm (as shown for Roche Elecsys hs-cTnT in Figure 3) is recommended as a primary protocol.[6,133,134] Alternatively, 0h/2h or 0h/3h algorithms can be utilized for hs-cTn assays. Prolonged time intervals are required for assays not achieving high sensitivity. In practise these algorithms utilize assay specific cut-off values and repeated cTn measurements to guide decision making. Sufficient elevation or decrease of cTn values indicate recent or ongoing myocardial damage, whereas stable cTn levels indicate chronic origin. Although chronic elevations may sometimes be high, initial cTn measurements at or above rule-in cut-off value can be used to indicate high probability of MI.[6] On the other hand, if the initial cTn measurement is very low, generally near the limit of detection (LoD), the use of another cut-off value may be utilized to rule-out MI.[6] The usability of rule-out cut-off value is dependent on time between sampling and the onset of symptoms as myocardial damage and troponin elevation may require some time to evolve.[145] Generally, the time threshold from symptom onset is considered to be three hours, but käypähoito recommends threshold of two hours when a cTn measurement below

LoD is complemented by normal ECG and asymptomatic patient.[6,133,134] If these conditions for single cTn measurement rule-out cannot be met, serial cTn measurements must be utilized according to the algorithm. If subsequent cTn results (third measurement at 3h) show no sufficient change between cTn measurements, the likelihood of ongoing MI is considered to be extremely low.[6,133,134] When cTn assay results do not indicate myocardial damage, further imaging studies and additional laboratory tests can be utilized to establish the correct diagnosis.

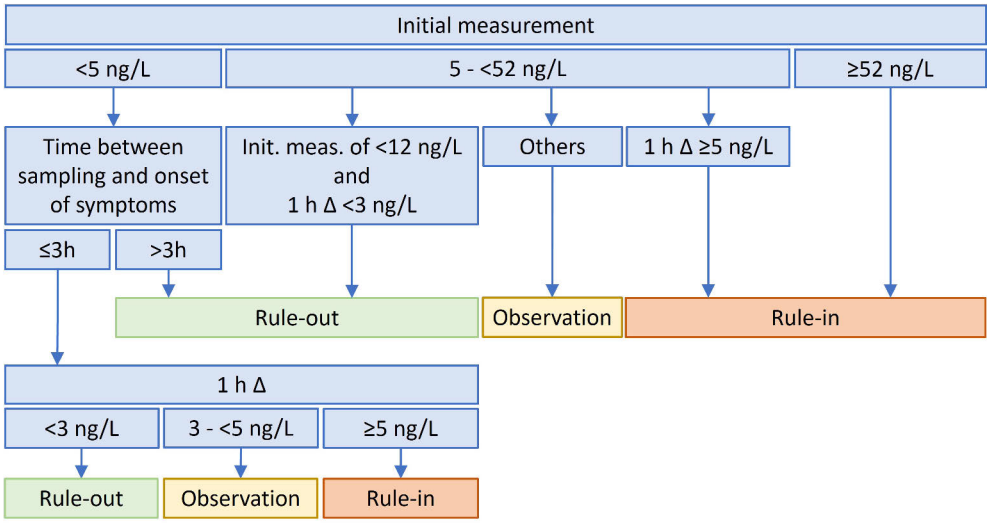

Figure 3. ESC 0h/1h Roche Elecsys hs-cTnT algorithm for suspected NSTEMI

For all patients ruled-in and those at observation, echocardiography is recommended.[6] Echocardiography is commonly acquired before coronary angiography or to help establish differential diagnosis of thoracic aortic dissection, pericarditis, cardiomyopathies including takotsubo, pulmonary embolism, cardiac tamponade, heart failure or aortic valve disease.[134,146] Invasive coronary angiography is performed for all patients prior to PCI or CABG. During the angiography a contrast agent is injected to the coronary artery, which reveals and pinpoints the culprit lesion(s). Around 8-19% of the patients show no relevant occlusion, which may indicate myocardial infarction with non-obstructive coronary arteries (MINOCA) – a type 2 MI or depending on other evidence some non-ischemic condition.[135] Although chest roentgenogram has low utility in diagnosing MI, it is useful detecting potential alternative diagnosis such as fractures of the rib cage, pneumonia, pneumothorax or other thoracic conditions.[6] In some situations CT angiogram may be performed for low-risk patients to help rule-out conditions like pulmonary embolism or aortic dissection or to identify atherosclerotic lesions in

the coronary artery.[6] Similarly in special cases cardiac MRI may be performed when inflammatory heart disease is suspected.[134,135] Myocardial perfusion imaging may also be utilized in specific situations during suspected ACS to exclude type 1 MI, or to supplement the information gathered from coronary angiography.[134] In Finland perfusion imaging in acute setting is mainly used to identify decreased perfusion after the episode.[135] Additionally, those in the observation zone and without indication of other serious condition or elevated risk may benefit from stress testing in combination for example with ECG.[6] Additional laboratory testing may also be required. Elevated proBNP may indicate heart failure, whereas normal fibrin D-dimer (FIDD) testing can help rule-out pulmonary embolism and aortic dissection.[77] Full blood count including hemoglobin (Hb) and leukocytes may help identify anaemia induced ischemia or infection.[6,147] If these additional tests indicate transient ischemia without myocardial damage to be the culprit, diagnosis of UAP is usually established, although in some cases diagnosis of SAP may also be considered.[134,147]

Diagnosis of stable and unstable angina are both normally associated with the sensation of chest pain, discomfort or pressure. However, these symptoms are not required for the diagnosis of SAP or UAP as either can present atypical symptoms without characteristic angina pectoris features.[135,148] SAP manifest with reversible and well predictable symptoms that are often induced by physical exertion, whereas in UAP the symptoms usually differ in severity and may be triggered even at rest or after rather mild exertion. During these ischemic episodes, no observable myocardial cell damage occurs in either SAP or in UAP. [135,148] The diagnostics and treatment of SAP follow its own guidelines, not further discussed here.[147,148] In case of UAP, diagnostic evaluation and clinical assessment guide the risk assessment, which decides further course of action.[6,133,134] Although patients with UAP do not show markers of acute myocardial damage, their sudden increase in symptom severity or decrease in angina threshold can indicate among other causes a plaque rupture or erosion with incomplete venous blockade or progression of the atherosclerotic disease.[149] Thus episodes of UAP may precede further complications and MI and careful risk assessment is warranted.[134,148]

2.4 Cardiac Troponin

2.4.1 Cardiac Troponin Complex

Troponin is a regulatory protein of a skeletal and heart muscle contraction. It is bound to tropomyosin (TM) and distributed in repetitive manner along actin filament; one to every seven actin monomers.[150] The function of troponin is regulated by intracellular calcium ion concentration. At low calcium concentration

troponin with TM inhibits myosin-actin interaction, thus preventing muscle contraction. At higher calcium concentrations, the inhibiting effect is removed after calcium ion bounds to troponin and induce conformational changes that enable actin-myosin interaction as seen in Figure 4.[151] Troponin consists of three structurally and functionally different subunits: I, T and C; thus commonly referred to as the troponin ITC complex.

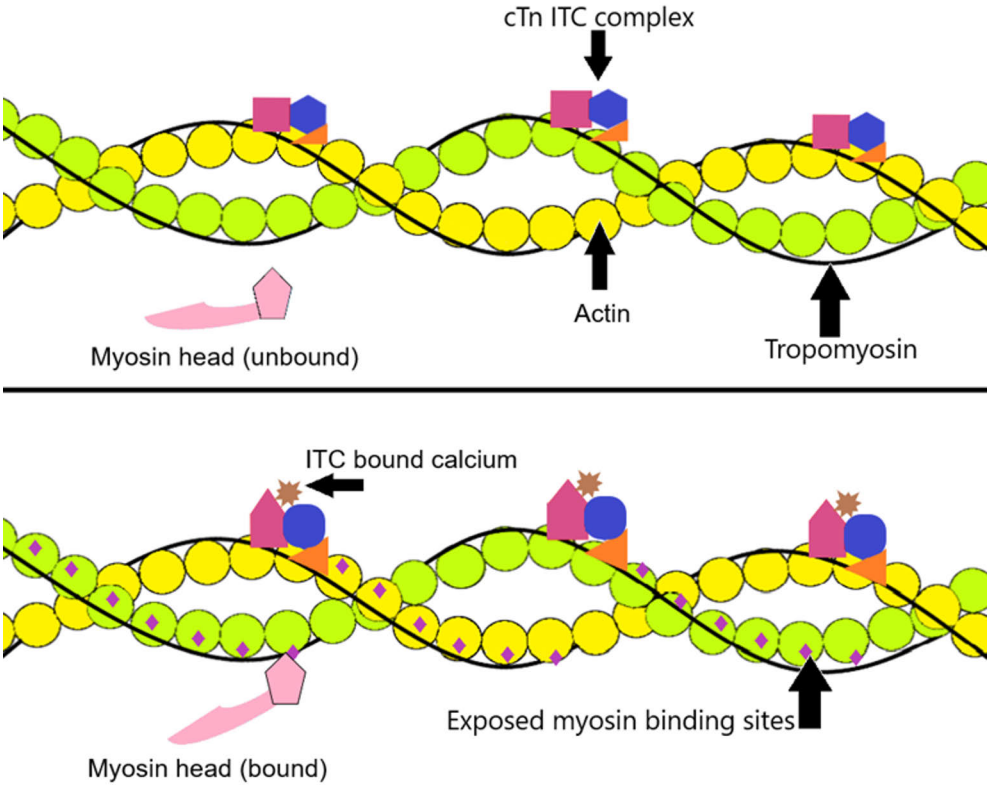

Figure 4. Interactions between troponin, tropomyosin, actin and myosin. Calcium induces conformation change in cTn, which enables tropomyosin to move and expose myosin binding sites of actin. Binding of myosin into actin leads to muscle contraction.

Troponin C

Troponin C (TnC) is the sensing part of troponin complex that binds calcium ions which induce the structural changes of troponin complex during muscle movement. In humans, TnC is present in two isoforms that are encoded by *TNNC1* and *TNNC2* genes.[152] *TNNC2* encodes TnC that is part of fast skeletal muscles, whereas *TNNC1* encodes TnC for both cardiac and slow skeletal muscle. *TNNC1* (UniProt entry: P63316) product is 18 kDa protein with 161 amino acid residues that make up nine

α-helices (Figure 5) which in turn form two globular domains that are connected with a flexible hydrophobic linker region.[153] These globular domains contain the cation binding sites of TnC. In cardiac muscle, TnC contains one inactive, one active and two structural binding sites. Structural binding sites (III aar 92-127; IV aar 128-161) are always occupied under physiological conditions and can bind both Ca^{2+} (K_A ~10^7 M^{-1}) and Mg^{2+} (K_A ~10^4 M^{-1}) ions and tether TnC to the rest of the cardiac troponin (cTn) complex.[153,154] Unlike in skeletal troponin (skTn), binding site I (aar 16-51) has been shown to be inactive in cardiac TnC.[153] Binding site II (aar 52-87) is the regulatory site for cardiac muscle contraction.[153] Although, site II binds both Ca^{2+} (K_A ~10^5 M^{-1}) and Mg^{2+} (K_A ~10^3 M^{-1}) ions, only Ca^{2+} induces a conformational change upon binding during systolic concentration increase (400–1000 nM).[155,156] TnC is not utilized as an effective cardiac biomarker due to the fact, that heart and slow skeletal muscle TnC have homological amino acid sequence.[157]

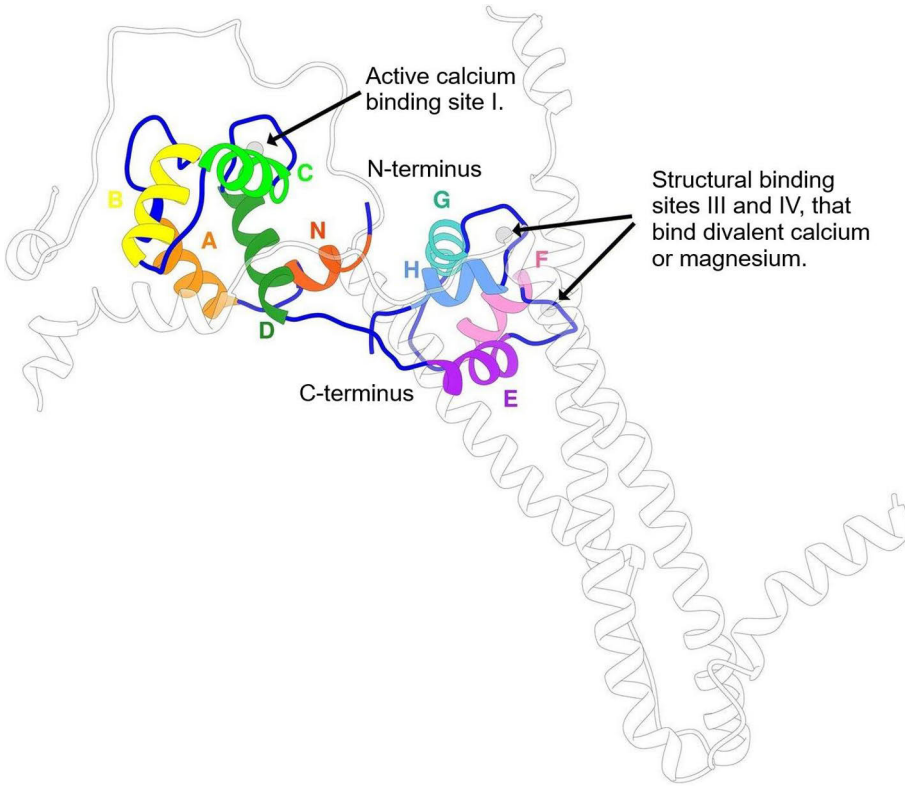

Figure 5. Structure of TnC in cTn with structural α-helices (A-H, N) and cation binding sites. Edited from Marston and Zamora[153] under the terms of the Creative Commons Attribution 4.0 International License.

Troponin I

The function of troponin I (TnI) in troponin ITC complex is to sterically inhibit the formation of actin-myosin bridge at low cytosolic Ca^{2+} concentrations, thus inhibiting muscle contraction. The inhibiting effect is achieved when the C terminus of TnI (cTnI aar 163–210) binds to actin and adjusts TM into position where it blocks the myosin binding sites of actin filament.[153,158] Upon systolic Ca^{2+} concentration increase in cytosol and binding of Ca^{2+} ions at TnC regulatory binding site(s), the troponin complex undergoes intra-molecular conformation change. This opens a hydrophobic surface at the N terminus of TnC and enables the switch peptide part of TnI (cTnI aar 149-163) to interact with the revealed area. This in turn retracts C terminus of TnI away from actin, thus allowing TM to shift and reveal myosin binding sites of actin filament.[153,158] In human body, three different TnI isoforms are encoded: Slow skeletal TnI that is encoded by *TNNI1*, fast skeletal muscle TnI by *TNNI2* and cardiac muscle TnI (cTnI) by *TNNI3* (UniProt entry: P19429).[159] From these isoforms the cTnI is the largest (24 kDa) with total length of 210 amino acid residues or 209 after the removal of a methionine residue at the N-terminus. It contains two larger structural cTnI α-helices H1 (aar 43–79) and H2 (aar 90–135) which form the IT arm domain that serves as an area for C-terminal area of TnC to attach.[153] cTnI also incorporates a specific part called cardiac-exclusive N terminal domain (NcTnI; aar 1–32) that is not found in other TnI isoforms.[153,159] This unique area contains two adjacent serine amino acids (aar 23 and 24) that are readily phosphorylated by protein kinase A. This phosphorylation leads to a decreased affinity between cTnI and TnC subunits, decreased Ca^{2+} binding affinity at the TnC regulatory binding site II and thus increase the rate of relaxation and diastolic function of the cardiac muscle.[160–162] In patients with heart failure, phosphorylation of these specific serine residues has been found to be decreased.[163,164] In addition, cTnI also contains several other phosphorylation sites (e.g. Ser-43, Ser-45 and Thr-145).[159,165] It is noteworthy to mention that the main TnI isoform found in cardiac muscles of newborn babies is not the cTnI, but that of a slow skeletal muscle isoform. The isoform expression changes between later fetal development and the first 9 months of postnatal development, after which the main isoform of the heart muscle is the cTnI.[166] No alternative splicing has been shown to affect cTnI.[167] Three-dimensional structure of cTnI is presented in Figure 6.

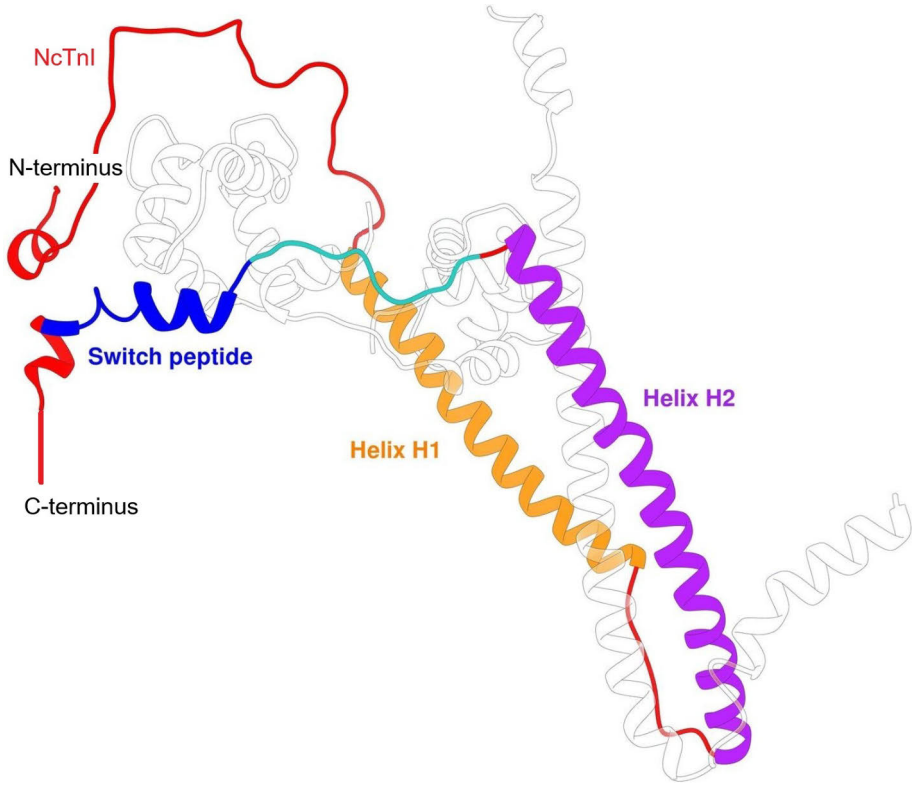

Figure 6. Structure of cTnI. Edited from Marston and Zamora[153] under the terms of the Creative Commons Attribution 4.0 International License

Troponin T

The function of troponin T in cTn complex is to bind cTn into TM. Three distinct TnT isoforms are encoded in humans: *TNNT1* encodes TnT for slow twitch skeletal muscle, *TNNT2* (UniProt entry: P45379) for cardiac muscle (cTnT) and neonatal skeletal muscles and *TNNT3* for fast twitch skeletal muscles.[168] In addition at least 12 different cTnT isoforms are produced through alternative splicing of TNNT2 transcripts. Isoform 6 (also sometimes referred as TnT3) is the predominate form found in normal healthy adult heart.[165,169] Isoform 1 is a 298 aar protein, whereas isoform 6 has undergone deletion between aar 24–33 thus incorporating 288 amino acid residues (287 after removal of N terminal methione). Isoform 6 has a calculated mass of 34-35 kDa and usually reported mass somewhere between 35–40 kDa.[170,171] Altogether most of the cTnT structure is quite conserved, with the exception of N-terminal hypervariable area (aar 1-79), which is the site where main isoforms (1, 6, 7, 8) differ. This area can drastically affect the activation strength of cardiac myofilaments.[165] Next to the N-terminal hypervariable area is the first TM binding

site of cTnT (around aar 98-136).[172] Both of these areas are located in T1 domain (aar 1–168) of cTnT which is connected via linker area (169–200) to cTnT T2 domain (aar 201–288) that consists of α- helices H1 (aar 201-225) and H2 (arr 226–277) and c-terminal T2 site (aar 278–288).[153] The second TM binding site (aar 197–239) is located in T2 domain overlapping H1 α- helix.[172] Interactions between cTnT and TM function as an anchor to keep the troponin complex in correct position on the thin filament. TnT also closely interacts with other cTn subunits and forms the structurally rigid IT arm with cTnT H2 α-helix interacting mainly with cTnI H2 α-helix but also with cTnI H1 α-helix.[153] Three-dimensional structure of cTnT is shown in Figure 7. As in case of cTnI, cTnT can exhibit posttranslational modifications. Phosphorylation of Ser-2 has been proven in vivo, but although several in vitro studies have identified multiple phosphorylation sites, in vivo studies have not.[165,173]

The expression of different cTnT isoforms can change both in heart muscle and in skeletal muscles during development. In fetal cardiomyocytes, isoforms 7 and 1 are mainly expressed and in lesser extent isoform 8.[169,174,175] The developmental shift towards isoform 6 causes alterations in calcium affinity of TnC and actomyosin ATPase activity, therefore decreasing maximal force of the myofibrils.[176] During adulthood healthy skeletal muscles do not contain significant amounts of cTnT. In contrast, in fetal skeletal muscles small amounts of cTnT can be found.[169,174,175] cTnT isoform expression can also be altered also due to disease. Several skeletal muscle disorders like skeletal myopathies or muscle dystrophies can cause upregulation of TNNT2 gene in skeletal muscles and thus lead to diagnostically relevant increases of total cTnT concentration in plasma.[177] The expression of cTnT isoforms can also shift during heart failure, which has been shown to promote the expression of fetal isoform 7.[174,175]

Whereas disease can affect cTnT isoforms, the opposite is also true. Over 100 different mutations in cTn have been associated with hereditary cardiomyopathies.[178] Of these mutations 15-30% originate from cTnT and they do not necessarily need to be at specific area of cTnT structure, thus underlining the importance of the whole structure.[153,179]

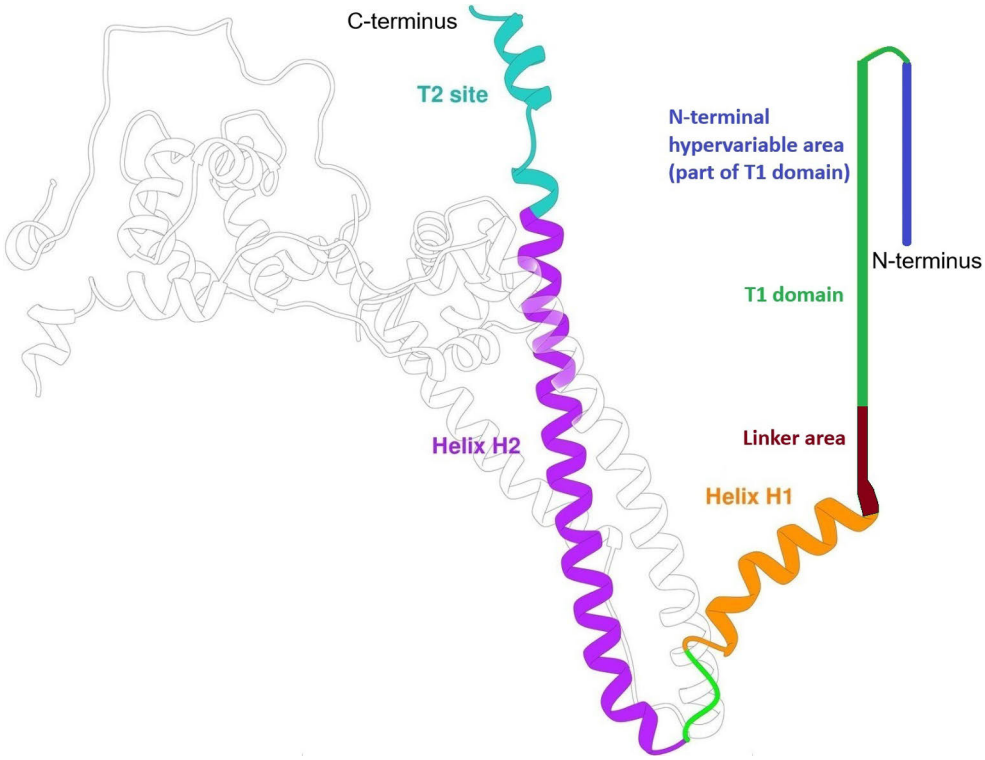

Figure 7. Structure of cTnT. Edited from Marston and Zamora[153] under the terms of the Creative Commons Attribution 4.0 International License.

2.4.2 Cardiac Troponin Kinetics and Fragmentation

Cardiac troponins are released into the circulation during MI due to myocardial damage that is induced by decreased perfusion and lack of oxygen at the affected part of myocardium.[157] The release patterns of cTnI and cTnT are dependent on the underlying condition. During stress and reversible ischemia, a fast and transient rise of cTn can be detected. This rise often resolves and returns back to baseline during 24 hours.[157] Several hypotheses have been presented for this kind of release pattern including proteolytic degradation and exocytotic release of cTn fragments, change in the permeability of cardiomyocyte membrane, formation and release of blebs or apoptosis by caspase pathways.[157,180]

The concentration kinetics of cTn following MI are quite well established. cTn elevation and its duration depend on infarct size, possible treatment measures and clearance speed.[181–184] The release of cTnI usually occur in monophasic manner, whereas with cTnT a biphasic release is often observed, especially if reperfusion has been performed, as illustrated in Figure 8.[184,185] cTnI released after the onset of MI usually stays elevated between 4–10 days (median of 7 days) and peaks between 6–

13 hours (median of 9–10 h) after PCI or around 24h without successful reperfusion.[186–188] cTnT stays elevated between 5–14 days and peaks similarly between 6–11h (median of 9–10 h) after PCI or around 48h without reperfusion.[184,187,189] The second cTnT peak occurs independent of reperfusion status around day four after symptom onset.[184] The difference between cTnI and cTnT kinetics is still unclear, but it is suggested that the initial cTnT release is due to cytosolic free pool (6 ± 1.1% of cTnT) and the secondary cTnT release is suspected to originate from dying cardiomyocytes.[184,190] When assessing cTn release it must be kept in mind that in addition to one or more release pathways, there are also simultaneously acting degradation and elimination pathways. In addition, differences between assays might contribute, not only because of lack of standardization, but also depending on other factors concerning assay design, monoclonal antibodies (mAb(s)) being utilized, the epitopes identified and cTn autoantibodies interfering with the elimination kinetics.[191] Kristensen *et al.* ingeniously addressed the problem of simultaneous release and elimination on their study by storing STEMI plasma after acute revascularization and later readministering the plasma to the same individuals.[192] As seen in Table 2, five different hs-cTn assays were compared, which provided comprehensive picture on elimination kinetics. Half-lives between 134–239 minutes were determined for cTnI assays whereas the sole cTnT assay showed a half-live of 134 minutes. The difference seen in cTnI half-lives underlines the importance of assay selection and molecular degradation when making interpretations and data comparisons on cTn release or elimination kinetics.

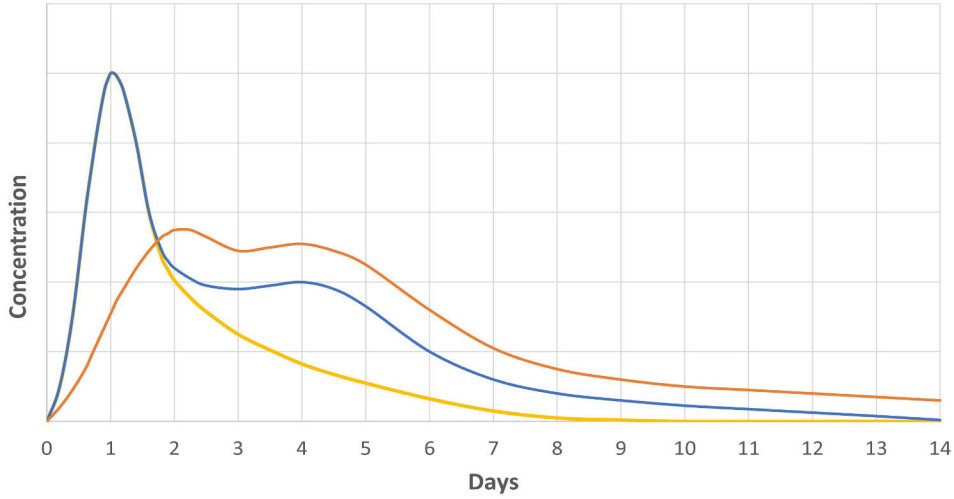

Figure 8. Illustration of cTn kinetics with reperfusion (cTnI, yellow; cTnT, blue) and without reperfusion (cTnT, orange).

Table 2. cTn assay epitope and median cTn elimination half-life comparison.

Assay		Manufacturer	Epitopes (aar)*				Median elimination half-life (min)***
			Capture mab(s)		Tracer mab(s)		
Vista	hs-cTnI	Siemens	29–34	–	41–50	171–190	199.3
Vitros	hs-cTnI	Ortho	87–91	–	24–40	41–49	239.7
Alinity	hs-cTnI	Abbott	Not published				212.6
Atellica IM	hs-cTnI	Siemens	41–50	171–190	29–34	–	134.4
Elecsys	hs-cTnT	Roche	136–147**	–	125–131**	–	134.1

*cTnI epitopes received from IFCC document[193] **cTnT epitopes[194–196]; cTnI and cTnT aar not comparable. ***Kristensen *et al.*[192]

The earliest reports in the late 1990s disclosed that cTnI and cTnT were found in the bloodstream after MI not as a single entity but as a spectrum of different forms.[197–199] It was thus noted that the antibody selection could drastically affect assay performance due to different forms being detected.[197] This sparked further interest to map different cTn fragments, fragmentation pathways and time-dependent changes in association with different conditions. Now it is established that troponin composition undergoes dynamic change after MI.[8] It is still debated into which extent these changes happen upon ischemia inside the damaged myocardium or post-release in the circulation.[200,201] It has been speculated and experimented in vitro that several proteases, most notably thrombin, are able to degrade different sections of cTn.[202]

Several methods have been utilized to study cTn fragmentation. These include immunoassays, gel filtration chromatography, immunoprecipitation, gel electrophoresis, western blotting and mass spectrometry. Although several minor cleavage sites and corresponding fragments have been identified, the most important cleavage sites lay at aar 68–69 and 189–223 in cTnT and around aar <34 and >126 in cTnI as shown in Figure 9.[201,203] Higher portion of intact cardiac troponin ITC complex is detected shortly after MI.[201] The N-terminal hypervariable area of cTnT is readily cleaved at least due to thrombin (aar 68–69), but possibly also intracellularly by calpain-I (aar 68–69) and/or caspase-3 (aar 88–89).[169,202,204,205] It has been shown that both calpain and caspase cleave the mentioned sites only when cTnT is part of ITC complex.[204,205] After cTnT has been cleaved at aar 189–223, low molecular weight ITC complex (LMW-ITC) and free cTnT fragments are formed.[8,201] These free cTnT fragments include the rather stable cTnT mid fragment between aar 69–189.[201] LMW-ITC further degrades into IC complex after the C-terminal cTnT fragment has been detached or degraded. Although it is currently unknown how this C-terminal cTnT fragment is detached from LMW-ITC, there is evidence that the Lys residue at 288 is readily cleaved at least in vitro and that the

area between aar 189–223 has several cleavage sites that in theory could contribute to the removal of C-terminal cTnT.[201] The IC complex can undergo further structural changes by both N- and C-terminal fragmentation of cTnI (aar <34 and >126), thus leaving the most stable central fragment attached into TnC.[203] To date, no free intact cTnI has been reported in any significant extent. Whether free intact cTnT is released during MI is still debated.[8,200]

The exact kinetics of cTn fragmentation in vivo is hard to establish. Several factors including interfering autoantibodies, post-translational modifications and simultaneous release of new cTn affect the results.[165,191] It is assumed that the release of intact cTn continues as long as damage in the myocardium keeps progressing. Although new intact cTn is released into circulation, the proportion of intact cTn starts to decline after the initial first hours as progressively smaller cTn fragments are produced.[8]

Also, preanalytical sample handling and the chosen matrix can affect troponin fragmentation. It is now well known that the N-terminal cleavage of cTnT mediated by thrombin is also evident in serum samples due to the activation of coagulation pathway during serum preparation.[170,206,207] Similarly, it has been shown recently that ethylenediaminetetraacetic acid (EDTA) samples exhibit enhanced degradation when compared to lithium heparin samples, probably due to chelating effect exerted upon structural stabilizing calcium ions.[208] Although, the analytical significance of C-terminal lysine cleavage of cTnT is rather miniscule or non-existent, it is known that this lysine is removed in vitro upon incubation of lithium heparin samples.[201] To avoid major degradation due to the chosen matrix, lithium heparin plasma, citrate plasma and hirudin plasma are thus preferred.[208–210]

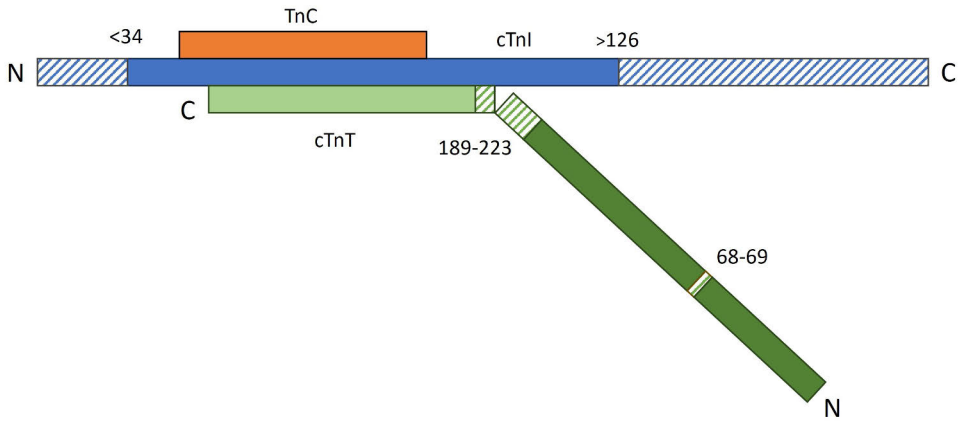

Figure 9. Illustration of the main cTn fragmentation sites / areas (dashed). TnC (orange), cTnI (blue), cTnT (green). Area in cTnT aar 189-223, cTnI aar <34 and aar >126 all contain multiple cleavage sites.

2.4.3 Commercial Cardiac Troponin Assays

Cardiac troponin assays have undergone several iterations and developmental steps since Cummins *et al*. and Katus *et al*. introduced the first cTnI and cTnT assays respectively.[72,74] The analytical sensitivity has improved from µg/L to the level of ng/L or even below.[211,212] The analytical specificity has similarly improved after implementation of monoclonal antibodies that do not show significant cross-reactivity with skeletal troponin isoforms.[211] These and other advancements in analytical capabilities of cTn assays have altered diagnostic cut-offs, algorithms and even how we define MI.[5,76,213] However, there are still several challenges regarding modern cTn assays such as interference caused by cTn autoantibodies, heterophile antibodies such as human anti-animal antibodies and rheumatoid factor and the intake of high-dose biotin supplements.[214–216] In extremely rare cases some cTn immunoassays might, at least in theory, be also affected by paraproteins, anti-ruthenium antibodies, anti-streptavidin, anti-biotin etc.[217] Additionally, elevated cTn results can be measured in several conditions not related to MI and are frequently observed among hospitalized patients.[218,219] Also, standardization of especially cTnI assays has long been sought, but due to the fact that cTn assays utilize different epitopes and calibration materials, it has been proven to be extremely challenging.[220,221] Thus, cardiac troponin assays from different manufacturers are not comparable. Similarly, different assay generations or different assay platforms from the same producer might not produce comparable results.[5,220]

All modern commercial cTn assays utilize the same principal method for analyte identification, monoclonal antibodies, most often immunoglobulin G (IgG), or their fragment antigen binding (Fab) portions specific for the cardiac isoforms of troponin (from here on both are referred to as antibodies).[212,222,223] An assay must utilize at least one capture and one tracer antibody, but may use more than one to enhance sensitivity and/or to decrease the effects of interfering cTn autoantibodies. A capture antibody is usually bound onto a solid surface or magnetic particles. Although several different coupling methods exist, it is often established with biotinylated antibodies that are anchored via specific interaction with streptavidin.[216,224] If magnetic particles are utilized, they can be controlled during analysis via electromagnetism and concentrated onto a specific surface area when necessary.[225] After the sample is introduced, the capture antibody binds into cTn. Similarly, the labelled tracer antibody with different target epitope binds into cTn, thus forming a so-called sandwich complex. As all unbound material is washed away in the course of the analysis, only bound material is measured. Different cTn assay platforms utilize different detection technologies and labels. Many of the modern methods utilize some form of chemiluminescence, fluorescence or enzymatic reaction.[226] The measured signal is generated by a specific label that has been conjugated to the tracer antibody. The final cTn concentration in a sample is calculated when the signal

is compared to the calibration curve which is calculated based on signals from calibrators of known concentrations.[227]

In general, cTn assays can be divided based on different factors. Most notably they are divided into cTnI or cTnT assays, based on the cTn subunit targeted by assay antibodies. The test systems and related assays can also be divided based on intended users and user location into core laboratory or point-of-care (POC) tests. In practice, POC test are usually easy to use and thus suitable to be used by non-laboratory professionals outside the laboratory, but most POC tests do not offer similar performance in comparison to core laboratory platforms. However, in recent years the first high sensitivity cTn POC assays have been introduced into the market.[228] As different assays inherently have different characteristics and analytical performance, they are often divided into high sensitivity or contemporary assays depending on their analytical sensitivity. Task Force on Clinical Applications of Cardiac Bio-Markers (now the IFCC Committee on Clinical Applications of Cardiac Bio-Markers, C-CB) of the International Federation of Clinical Chemistry (IFCC) has stated that a hs-cTn assay must adhere to following rules[229]:

- The 99th percentile URL of the assay should be measured with an analytical imprecision (coefficient of variation; CV) of ≤ 10%.
- cTn should be measured above the limit of detection in ≥ 50% of healthy subjects.

According to the recommendations of IFCC C-CB the 99th percentile URL for the assay should be derived from assumingly healthy individuals.[229] With hs-assays the use of sex-specific 99th percentiles are recommended, whereas age specific URLs are not.[226,229] Reporting of cardiac troponin results below concentration with total imprecision of 20% is prohibited by US Food and Drug Administration (FDA) and thus minimum total imprecision of 20% at the 99th percentile is deemed acceptable for contemporary assays.[226,230] The majority of both contemporary and hs-cTn assays have been listed in cTn Biomarkers Reference Tables by IFCC.[231,232] These tables also include some basic information about analytical characteristics, accepted sample matrix and in some cases about the exploited cTn epitopes. For further info about a specific assay, manufacturers Instruction for Use (IFU) should be consulted. Further recommendations for laboratories using cTnT assays are presented by IFCC C-CB.[214,230]

2.4.4 Clinical Specificity of cTn Assays

Since the release of hs-cTn assays cTn has been by far the most sensitive biomarker for diagnosis of MI. Simultaneously the increased assay performance and utilization of lower concentrations have introduced the problem of decreased clinical specificity of cTn regarding the diagnosis of acute MI. With modern hs-cTn assays it is not uncommon to obtain results over 99th percentile URL without MI. These non-MI related cTn elevations are typically associated with other morbidities or conditions as listed in Table 3 and increased age.[5,218,233–240]

Mechanisms behind elevated cTn levels are varied, and in some cases somewhat unknown. In many conditions the elevation is attributed to acute myocardial damage that may or may not be related to myocardial ischemia. Some conditions cause collateral damage that also affects myocardium, whereas in others direct cardiac involvement is the culprit. The speed in which the myocardial damage processes also vary in different conditions. In some, rapid elevation of cTn can be expected, whereas in others rather slow ongoing damage results in a stable elevated level of cTn.[241] In addition, decreased renal clearance may also affect the clearance of circulating cTn fragments.[183,209] Thus, both cardiac damage and decreased clearance of cTn may contribute to the elevated cTn levels in circulation.

As already stated, several cleavage sites have been identified in both cTnT and cTnI.[8,203] The cleavage of cTn can occur during circulation or during sample preparation, thus affecting the structural composition of measured cTn.[201,209,210] It is also becoming evident that in different conditions, the release mechanism of cTn can differ, thus possibly producing different structural compositions of circulating cTn pool.[188] The composition of the pool can also be affected by continuous release, degradation and clearance, thus temporal dependence of different cTn forms in circulating pool can be observed.[8,242]

Different hs-cTn assays are affected differently by cTn fragmentation due to the distinct epitope utilization and design choices regarding these epitopes, as already insinuated by median cTn elimination half-lives presented in Table 2 and fragmentation studies of cTnT and cTnI.[8,203] cTn elevations between cTnT and cTnI assays also show different prevalence in non-ACS conditions as presented in Table 4, which may reflect both analytical and mechanistic differences.[243–245] The epitope selection has previously been driven by factors like assay sensitivity, skTn cross-reactivity, epitope interference and patents.[226,246,247] In Roche Elecsys hs-cTnT assay both capture and tracer antibody epitopes are located in the stable middle fragment of cTnT and no major cleavage site is located between the epitopes.[226] This selection has the inherent ability to detect cTnT even after extensive degradation, thus increasing assay sensitivity. On the other hand, this selection of epitopes is not able to detect differences in composition of cTn pool between different conditions and morbidities.

Table 3. Non-MI related conditions that cause elevated plasma cTn levels.

Cardiac conditions
Heart failure
Cardiomyopathies
Cardiac inflammation e.g. Endocarditis, Myocarditis, Pericarditis
Atrial fibrillation
Sustained brady- or tachyarrhythmia
Takotsubo syndrome
Cardiac contusion following e.g. blunt chest trauma

Vascular and hemodynamic conditions
Ischemic stroke
Pulmonary embolism
Pulmonary hypertension
Severe hypertension
Hypotension or shock
Gastrointestinal bleeding
Subarachnoid and Intracerebral hemorrhage
Severe anemia
Microvascular dysfunction
Vasculitis
Coronary artery spasm
Coronary artery dissection

Other causes
Respiratory failure e.g. COPD
Strenuous exercise
Birth complications in infants

Systemic diseases
Acute renal failure
Chronic kidney disease
Diabetes
Severe hypothyroidism
Systemic sclerosis
Systemic lupus erythematosus
Skeletal myopathies
Amyloidosis
Sarcoidosis
Hemochromatosis
Infectious diseases and sepsis
Acute complications of inherited disorders e.g. Neurofibromatosis, Klippel-feil syndrome

Treatment related
Cardioversion
Lithotripsy
Coronary revascularization procedure
Catheter ablation
Other cardiac surgeries
Defibrillator shocks

Drugs and other substances
Chemotherapeutic agents and other medication e.g. verpamil, fenoterol, colchicine
Drug abuse e.g. cocaine + fentanyl use
Carbon monoxide poisoning
Venomous animal bites

Table 4. Prevalence (%) of cTn elevation in non-ACS patient groups.[244,245]

	Roche Elecsys hs-cTnT	Dimension Vista hs-cTnI	Architect i2000SR hs-cTnI
ESRD	99.0% (n=198)	-	34.5% (n=69)
Infection	42.7% (n=41)	8.3% (n=8)	–
Cancer	57.9% (n=11)	10.5% (n=2)	–
Gastrointestinal	36.8% (n=89)	5.0% (n=12)	–
All non-ACS conditions	40.8 (n=362)	7.4% (n=66)	–

2.5 Europium(III)Chelate Labels for TRF Assays

The performance of an immunoassay can be improved by introducing labels with enhanced signal generation. The basic concepts necessary to understand the principles of phosphorescence, fluorescence and time-resolved fluorescence (TRF) are covered in short manner as these have been thoroughly covered in multiple books and journals.[248,249] Lanthanide chemistry and europium(III)chelate labels utilized in TRF immunoassays are abruptly covered.

2.5.1 Fluorescence, Phosphorescence and Time-Resolved Fluorescence

Fluorescence is a type of photoluminescence, where a photon is absorbed and subsequently emitted at higher wavelength (λ). The difference in wavelength between the absorption and emission peaks is called Stokes shift.[249] The energy difference between the peaks and the reason for Stokes shift is the non-radiative decay that happens according to Kasha`s rule, which states that relaxation occurs from the lowest excited electronic state (S_1, D_1, T_1 etc.) of each multiplicity (S, D, T etc.).[250] As presented in Figure 10, fluorescence emission happens without change in spin multiplicity (S » S), whereas another type of photoluminescence, phosphorescence, happens when emission involves a change in spin multiplicity (T » S), which is forbidden by quantum-mechanical selection rules (in electric-dipole allowed process the spin of the electrons must remain the same).[248,251] For the same reason intersystem crossing from singlet state to triplet state is often not preferred. Additionally, the triplet state of organic molecules is readily quenched by molecular oxygen.[252] However, it is well established that heavier elements such as lanthanides (Ln) are able to stabilize the triplet state and increase the intersystem crossing rate considerably.[248] In practise, fluorescence processes are more probable and happen in smaller timescales than those of phosphorescence, which generally occur within milliseconds to seconds or even longer. Most fluorescent compounds have emission lifetimes at nanosecond timescale.[248] Some lanthanide salts and organometallic lanthanide chelates, especially europium chelates, have prolonged course of fluorescence emission that can last up to several milliseconds and is thus referred as TRF.[253] As most compounds and materials have short fluorescence emission lifetimes, this prolonged emission offers the advantage of better signal-to-noise ratio as illustrated in Figure 11. Thus, TRF has been utilized in combination with appropriate labels and dyes in various applications, including immunoassays.[254,255]

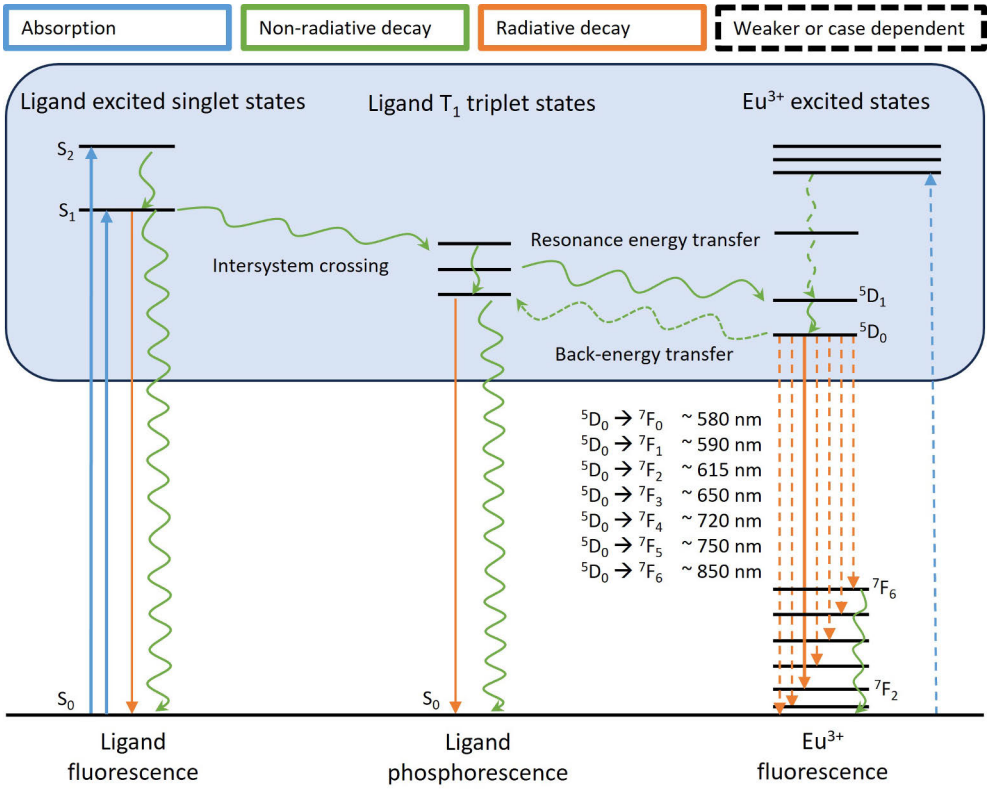

Figure 10. Jablonski diagram showing principles of fluorescence (S_1 » S_0), phosphorescence (T_1 » S_0) and TRF of Eu(III)chelate label ($^5D_0$ » $^7F_{0\text{-}6}$).[253,256,257] Absorption (blue), non-radiative decay (green), radiative decay (orange), weaker or case dependent energy transfer (dashed line).

The TRF process starts with the ligand absorbing a photon which results S_0 » S_{n+1} excitation. The introduction of a heavier element such as europium stabilizes the ligand triplet states and makes intersystem crossing a more favourable process, resulting in intra-ligand S_{n+1} » T_{n+1} transition.[248] A narrow energy cap between S_1 and T_1 energy states favours fast transition. Typically, k_{ISC} of $>10^9$ s^{-1} are needed to efficiently compete with fluorescence decay k_f which is around 3×10^8 s^{-1}.[258] As the spin selection rules make T_1 » S_0 transition forbidden and thus a rather slow process, the energy then flows from ligand triplet state to the Eu^{3+} ion.[248] The ligand-metal energy transfer to actually happen, a wave function overlap between the chromophore and Eu^{3+} ion must exist. In practice, the chromophore needs to have an integral electron donor such as a pyridine nitrogen or an anionic oxygen atom.[258] This electron donor must be located in close vicinity of the Eu^{3+} ion for an efficient energy transfer to occur via Dexter electron exchange mechanism.[258] In special cases, the energy transfer is assumed to happen via excited intramolecular charge

transfer (ICT) state rather than via triplet state. This kind of situation might arise when strong electron donating groups are located on the aryl ring.[258] After the energy transfer has occurred, the energy then decays non-radiatively into $^5D_0$ energy level from which relaxation occurs and light is emitted.[257]

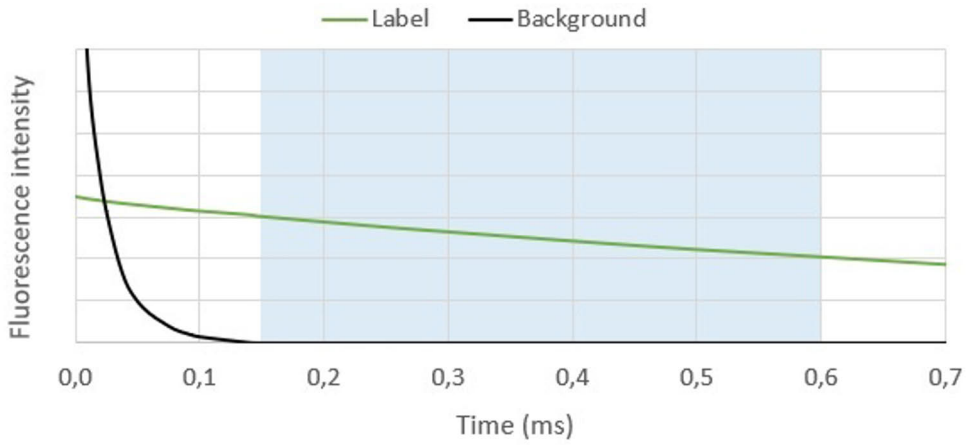

Figure 11. Illustration of background vs TRF-label emission decay kinetics. Delayed measurement window (e.g. 0.15-0.6 ms; light blue area) enables high S/N ratio.

TRF measurement and the performance of TRF-label depends on factors such as absorption, emission lifetime and quantum yield of the label. Absorbance is determined in relation to wavelength and it follows Beer-Lambert equation (Eq.1) in unsaturated non-turbid/homogenous matrix. In practice, it is measured as transmittance and converted into absorbance according to Eq.2 The fluoresence excitation spectrum often closely resembles absorption spectrum.[259]

$$A = \varepsilon\, c\, l \qquad \text{Equation 1.}$$

$$A = -log_{10}(T) \qquad \text{Equation 2.}$$

A, (absorbance), ε (molar absorption coefficient), c (concentration), l (path length), T (transmittance)

The absorbance in a solution is affected by the solvent matrix: polarity, pH, matrix absorbance and other interactions with other components. One of the most common causes of measurement error is the chromophore saturation and the subsequent formation of aggregates. Although, the reliable range of different instruments vary, it is commonly between 0.1–2 AU, while recommended absorbance area is below 1 AU (90% of light absorbed).[260]

The fluorescence quantum yield (φ) depicts how well the compound is able to convert absorbed photons into emitted photons. Thus, it is defined as the ratio of

photons that are emitted divided by photons that have been absorbed. In practice, determining quantum yield of a compound can be intensive, and if similar compound with known quantum yield exists, relative quantum yield (rφ) is often determined instead (Eq. 3).[253,261] According to Kasha–Vavilov rule, fluorescence quantum yield is independent of excitation wavelength.[262] But is affected by temperature and molecular environment.[263,264]

$$r\phi_a = \phi_{std} \times \frac{\int Em_a}{\int Em_{std}} \times \frac{A(\lambda ex)_{std}}{A(\lambda ex)_a} \qquad \text{Equation 3.}$$

Equation 3. can be utilised when solvent matrix has the same refractive index. std (known compound), ∫Em (integral of fluorescence emission), A(λex) (absorbance at excitation wavelength)

The fluorescence lifetime (τ) is defined as the time for fluorescence intensity to reach $1/e$ of its original value.[248] Fluorescence lifetime is usually independent of excitation wavelength, but similarly to quantum yield, it is affected by temperature and molecular environment.[265,266] Fluorescence brightness (εφ) is combination property of absorption of the molecule at specific wavelength, which is presented by the molar extinction coefficient ε multiplied with the molecules ability to convert the absorbed energy into fluorescence emission presented by quantum yield.[267]

2.5.2 Lanthanides

Lanthanoids also known as lanthanides (Ln), are rare earth minerals from lanthanum ($_{57}$La) to lutetium ($_{71}$Lu). Most of the lanthanides have, with the exception of lanthanum, occupied 4f orbitals, which have odd parity.[257] These f orbitals are well shielded by other orbitals and thus do not participate significantly in binding. Generally, lanthanides behave chemically very similarly and they tend to adopt +3 oxidation state in aqueous solution.[257] Formation of hydroxide complexes is also readily observed above pH 6 in aqua.[268] Lanthanides usually form complexes with coordination numbers 6–12, but lower numbers have also been reported. Empirical studies suggest that Eu^{3+} ion readily adopts nine-coordinate structure in aquatic environments. However, coordinating ligands affect highly to the coordination chemistry and the physiochemical properties of Ln^{3+} ions.[257] The influence goes both ways, as the Ln^{3+} ions also affect the energy levels and photophysical properties of the ligand. Most of the Ln^{3+} ions, including Eu^{3+}, have unpaired electrons in their orbitals and are thus paramagnetic. Due to the paramagnetic nature of many Ln^{3+} ions, distance dependent NMR-shifts are readily observed in organic ligands.[257] Paramagnetism of Ln^{3+} ions also contribute to medical imaging. Gadolinium compounds are the preferred contrast agents due to high magnetic moment (many unpaired electrons), isotropic magnetic field and relatively long spin relaxation time.[257] Although highly toxic in free ionic form, organic ligands decrease the

toxicity of the Gd^{3+} ion. Ln^{3+} ions, like almost all positive metallic ions, prefer electronegative anionic ligands and multidentate ligands generally offer enhanced stability to the complex.[257]

Some Ln^{3+} ions absorb visible electromagnetic radiation (λ 380–760 nm), but usually in an extremely weak manner due to Laporte-forbidden f-f transitions.[257] To explain this in a simplified manner: In a centrosymmetric system (electron orbitals that have center of inversion) the wavefunctions of the electron orbitals have definite parity (either odd or even). When a photon interacts with the wavefunction via electric-dipole operator (which is odd inversion operator), a wavefunction must change sign (parity) or otherwise the spatial coordinate inversion operation ends up being odd, which means the integral is 0 and thus the energy transition is forbidden as illustrated in Eq.4.[257,269] As a simple analogy this process can be thought (somewhat incorrectly) as interfering waves that either cancel or amplify each other after electron has interacted with them.

$$\langle \psi_f | \hat{\mu} | \psi_i \rangle \rightarrow \langle even | odd | even \rangle = \text{odd} \qquad \text{Equation 4.}$$

Ψ_f (wavefunction of the final state), μ (electric-dipole operator), Ψ_i (wavefunction of the initial state),

Much of the centrosymmetric nature of 4f orbitals is also retained even after the addition of ligands, as 4f orbitals are well shielded and do not participate in binding. For the same reason emission peaks of Ln^{3+} ions are not readily affected by the molecular environment and thus they also produce quite sharp peaks.[270] In TRF-assays the most commonly used lanthanide is Eu^{3+} due to its long fluorescence lifetime, bright emission and sharp $^5D_0$-$^7F_2$ peak.[253,271] Terbium (Tb^{3+}) is often complementary option and if needed, for example for multiplexing assays, dysprosium (Dy^{3+}) and samarium (Sm^{3+}) can be added. All of these cations also emit at visible wavelength (Tb^{3+}, λ540; Dy^{3+}, λ570; Eu^{3+}, λ615; Sm^{3+}, λ640 nm), in contrast to some other lanthanides like ytterbium (Yb^{3+}, λ980 nm), neodymium (Nd^{3+}, λ1060 nm) and erbium (Er^{3+}, λ1540 nm).[253]

The emission of europium is slow due to the same forbidden nature of f-f transitions that prevent absorption of light directly by europium.[257] If the energy cap between the ligand and europium is too narrow, the energy may flow back and quench the TRF signal. The triplet or ICT state should be at least 2500 cm^{-1} higher in energy at RT than Eu $^5D_0$ to prevent energy backflow.[256] The fluorescence intensity is also lowered if the ligand structure offers several rotational and vibrational degrees of freedom, and thus a rigid structure is often preferred.[248] The same is true if the solvation sphere of europium is filled with water molecules. Water molecules enable vibrational energy decay through oscillating O-H bonds and consequently decrease the fluorescent lifetime and quench the TRF signal.[272] For these reasons chelating groups that efficiently displace water molecules from the

solvation sphere of Eu show improved fluorescence lifetimes.[9] The fluorescence intensity and quantum yields can also be quenched due to an electron transfer process from the ligand containing electron-rich groups to the Eu ion.[258]

2.5.3 Europium(III)Chelate Labels

Several different chelator molecules for europium have been synthesized.[9,255,273,274] In immunoassays, these organic chelator molecules function as a bridge that crosslinks the Eu^{3+} to the tracer antibody. The covalent label-antibody conjugation is often achieved via an active group such as isothiocyanato or dichlorotriazinyl, that target free amine groups in lysine and N-terminus.[253] Alternatively, iodoacetamido activated chelates can be used to target free sulfhydryl groups in cysteines.[274]

Some labels function as Eu^{3+} carriers, whereas some are intrinsically fluorescent. When utilizing the carrier approach, the Eu^{3+} must be released to form a new complex with organic molecules capable of absorbing and transferring energy to the europium. One example of this kind of a label is the N1-chelate that utilizes enhancement solution, which may incorporate molecules such as β-diketone derivates (Figure 12).[275,276] There are downsides in this approach, when compared to intrinsically fluorescent labels. For example:

- The measurement is done in solution and an extra solution handling step is needed due to the use of enhancement solution.[271]
- After the addition of the enhancement solution, short equilibrating time is needed.[271] The time is dependent on dissociation conditions and strength of the chelates.
- The measurements cannot be made at later time after the enhancement solution has been added.[277]
- EDTA, citric acid or other chelators may interfere with the results, especially if the light absorbing chelators have low denticity.[278]
- For multiplex assays, enhancement solutions with different chelating chromophores are needed for different lanthanides.[271]
- Not usable in applications where localized signals are needed.[274]

Intrinsically fluorescent Eu labels have one or more chromophores directly attached to the chelating moiety, thus fundamentally eliminating the need to dissociate the Eu with any kind of ES. In intrinsically fluorescent Eu labels, the structural design of the chromophore is extremely important for the signal generation of the label. The chromophore must have a good absorptivity at the desired excitation wavelength and the energy levels must be in optimal range with the levels of the Ln ion for efficient energy transfer.[271,275]

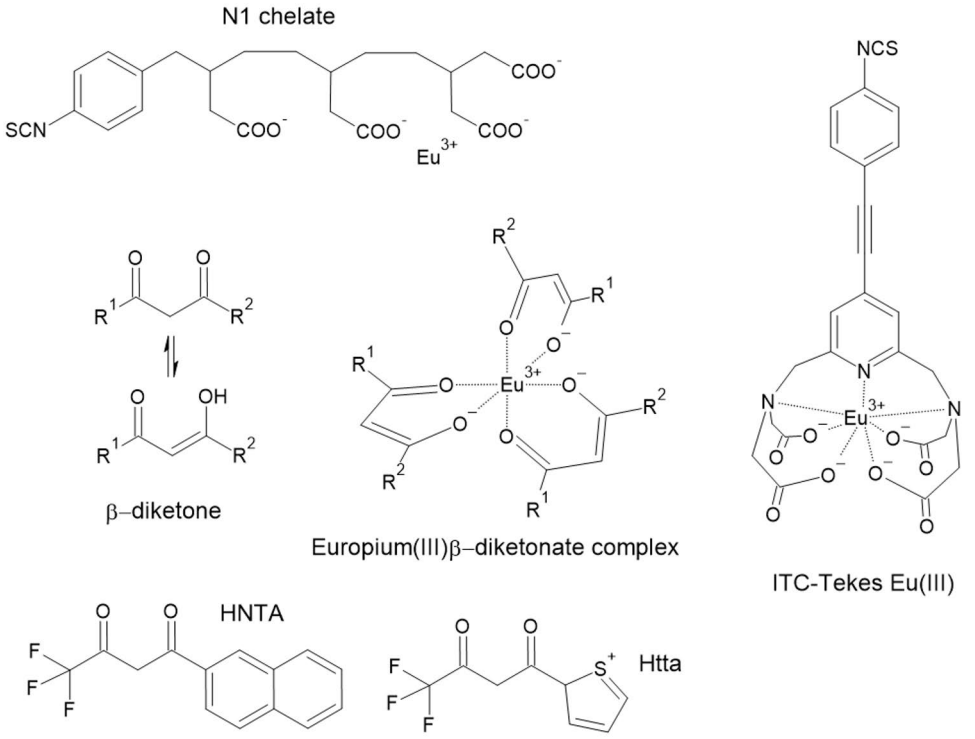

Figure 12. Illustration Eu(III) chelating moieties.

In contrast to many fluorescent labels that relay on S_1 » S_0 transitions, time-resolved-fluorescence applications relaying on lanthanides commonly have very large Stokes shift.[271] The exact excitation maximum of the organic ligand can vary, but the emission wavelength of each lanthanide stays almost constant. Slight variation in emission can be attributed on the ligand – lanthanide interaction and the effects on lanthanide f4 orbitals.[257] The ligand excitation wavelength often resides at UV-B/A area (UV-B, λ280–315; UV-A, λ315–400 nm), most notably at the lower end of UV-A where many conjugated organic molecules absorb. Increased size of the conjugated system shifts the absorption towards longer wavelengths.[279] Lower wavelengths are not used due to the facts that many organic molecules start to exhibit photodissociation below 200–250 nm and below wavelengths of 300 nm background fluorescence is also increased considerably, especially in clinical applications.[280]

The sensitivity of an immunoassay is not solely dictated by the intrinsic performance of the label, but is also affected among other things by the labelling degree, which depicts how many labels there are conjugated per antibody. The labelling degree can be affected, in addition to the labelling conditions and reagent ratios, by the label size and structure.[271] Different activating groups have different

kind of reactivity towards their targets, thus affecting the degree.[253] Although high labelling decree intuitively means more signal and is often desired, too many labels or labels in wrong places may affect antibody binding affinity towards antigen, thus decreasing the effectiveness of the tracer antibody. Efficient method to increase the labelling degree without endangering the effectiveness of antibody is to use labelled polypeptides, nanoparticles or other macro complexes that can be attached in antibody with simple chemistry.[271] Good example of peptide based approach is the use of SpyTag / SpyCatcher protein ligation technology that has been successfully utilized in cTnI immunoassay.[281] Similarly, labels having more than one chelating moiety or more than one chromophore per Eu can be used to increase labels performance.[271]

Although several factors affecting the properties of intrinsically fluorescent Eu chelating labels are known, the design of an optimal ligand is not a straightforward process nor is there an easy way to predict the properties of a chosen structure. Even a small structural change may have significant consequences for the fluorescent properties or structural stability of the label. The final tracer antibody effectiveness and signal generation is a combination of the properties of the lanthanide ion used, structure of the organic chromophore and chelating moieties, utilized activation chemistry and other labelling technologies, conditions and processes, assay buffer components and of course antibody properties, including antigen affinity. Additionally, assay design, sample matrix and measurement equipment affect the sensitivity of the assay.

3 Aims of the Study

The aim of this PhD thesis was to develop an immunoassay capable of identifying a cTnT form that differentiates between chronic and MI-related acute cTnT elevations, while also improving the immunoassay by designing and synthesizing novel antibody labels with improved performance and excitation at 360 nm.

The aims of individual studies were:

Study I: To design and develop a TRF immunoassay method able to identify the forms of cTnT that have not been cleaved at the C-terminal cleavage area of aar 189–223 (long cTnT). The study also aimed to evaluate the basic analytical performance of the novel assay.

Study II: To evaluate the clinical specificity of the novel long cTnT assay and the usability of the long/total cTnT ratio which was innovated and brought forth in this study. The results were compared to Roche Elecsys hs-cTnT assay which was also used to produce the total cTnT results. The ability of the novel methods to differentiate between STEMI, NSTEMI and ESRD patients was evaluated.

Study III: To design and synthesize a highly fluorescent europium(III) chelate that could be excited at 360 nm, thus enabling the use of high-power LED excitation sources, which would offer a cost-effective means for small measurement systems with improved excitation efficiency. The study also aimed to characterize the luminescence properties of the novel chelate and to assess its usability in TRF immunoassay.

4 Summary of Materials and Methods

The materials and methods used in publications I–II and manuscript III are summarized here. In addition, unpublished data is presented on synthesis and characterization of novel europium chelate that was investigated in this thesis.

4.1 Clinical samples

Samples from seemingly healthy volunteers were collected in Laboratory of Turku University of Applied Sciences. Patient samples were collected in Turku University Hospital as part of the TROPOnin FRAGMentation in Myocardial Injury Study (Tropo-Fragm, ClinicalTrials.gov Identifier: NCT04465591). The study complies with Declaration of Helsinki as revised in 2013 and the study protocol was approved by the Medical Ethics Committee of the Hospital District of Southwest Finland. Samples were collected after participants provided their written informed consent.

4.1.1 Patient Selection

The patient recruitment was conducted at the TYKS Heart Center and the TYKS Kidney Center. The STEMI and NSTEMI patient samples were collected during hospitalization based on the initial diagnosis. The final analyses were conducted based on confirmed diagnoses. ESRD patients were on maintenance hemodialysis and samples were collected pre- and post-dialysis.[282] No patients under the age of 18 were included in the study.

4.1.2 Sample Acquisition Protocol

Blood samples were collected into Vacuette CAT Serum Separator Clot Activator (Greiner Bio-One GmbH) and Vacutainer LiH (BD Biosciences) tubes. Plasma was centrifuged (15 min; 2200×g) and aliquoted into polypropylene microtubes (Sarstedt AG&Co. KG). Serum samples followed the same protocol after a coagulation period of 30 min. All samples were stored at -70 °C. For plasma samples the median time

from sample acquisition to centrifugation and from centrifugation to freezing was 20 [15–27] min and 20 [18–23] min, respectively. Prior to analysis, samples were thawed at room temperature (RT), vortexed and spinned briefly. During the same blood draw, a separate LiH plasma tube was collected and sent for routine cTnT analysis (Roche Elecsys hs-cTnT) at the laboratory of Turku University Hospital.

4.1.3 Samples Utilized in Studies I-II

In study I, serum and LiH plasma samples of NSTEMI (n=40), STEMI (n=72) and seemingly healthy volunteers (n=5) were utilized. In study II, LiH plasma collected from patients with NSTEMI (n=46), STEMI (n=71) or ESRD (n=40) was used.

The patient cohort used in study II for the clinical evaluation of the long cTnT assay had the following characteristics. In the NSTEMI group, coronary angiography was performed in 44 patients (95.7%), of whom 36 (78.3%) underwent percutaneous coronary intervention (PCI) and 6 (13.0%) were treated with coronary bypass surgery. The NSTEMI samples were collected before angiography in 24 (54.5%) patients and after in 18 (40.9%) patients. All STEMI patients underwent coronary angiography and primary PCI. All but three STEMI samples were acquired after angiography. All ESRD samples included in the clinical evaluation were collected prior to hemodialysis. The median time between symptom onset and sample acquisition was 23 [17–33] h for the NSTEMI cohort and 25 [21–33] h for the STEMI cohort. The collected patient data included additional demographics, clinical characteristics and laboratory parameters some of which are presented at Table 5.

Table 5. Baseline Characteristics of the Patients in Study II.

	ESRD (n=40)	NSTEMI (n=46)	STEMI (n=71)
Age; median (IQR)	72 (59-76)	73 (66-77)	65 (57-72)
Female	17 (42.5)	12 (26.1)	15 (21.1)
Hypertension	39 (97.5)	32 (69.6)	27 (38.0)
Diabetes	25 (62.5)	16 (34.8)	9 (12.7)
Prior coronary artery disease	18 (45.0)	23 (50.0)	9 (12.7)
Prior myocardial infarction	12 (30.0)	8 (17.4)	5 (7.0)
Heart failure	25 (62.5)	3 (6.5)	1 (1.4)
Atrial fibrillation	16 (40.0)	7 (15.2)	6 (8.5)
LMWH*	0 (0)	38 (82.6)	65 (91.5)
Heparin*	0 (0)	1 (2.2)	5 (7.0)
LMWH and heparin*	0 (0)	2 (4.3)	0 (0)
eGFR ml/min; median (IQR)	8 (6-10)	72 (60-90)	90 (76-96)

Data presented as cases (percentage, or median interquartile range = IQR), as indicated. Low molecular weight heparin (LMWH); estimated glomerular filtration range (eGFR; calculated using CDK-EPI formula); *administered prior to sample collection.

4.2 Total cTnT

Total cTnT results utilized in studies I–II were produced by the FINAS accredited laboratory (T124) of Turku University Hospital. Roche Elecsys high sensitivity cTnT assay (5th gen) was used in combination with the Roche Cobas 8000 system e801 module. The Elecsys hs-cTnT assay utilizes a chimeric capture antibody (5D8) that recognizes epitope at aar 136–147 and a tracer antibody (M7) that recognizes the epitope at aar 125–131.[194–196] The Elecsys hs-cTnT assay utilizes chemiluminescence with a tris(2,2'-bipyridyl)ruthenium(II) label and is calibrated against Elecsys Troponin T STAT assay, which in turn is standardized against Enzymun-Test Troponin T method as stated in the assay IFU (08469873500). The analytical characteristics of the assay are presented in IFCC Biomarkers Reference Tables and in assay IFU.[232]

4.3 Long cTnT Assay

4.3.1 Antibody Biotinylation and Labeling

The capture antibody (mouse monoclonal IgG 7E7; HyTest Ltd) was conjugated with 30-fold molar excess of biotin isothiocyanate (BITC, in-house) in a sodium carbonate-bicarbonate buffer [50 mM; pH 9.8]. The solution was incubated for 4h at RT while protected from light. After incubation, the buffer was changed to tris-buffered saline with azide (TSA) buffer (tris-HCl [50 mmol/l] pH 7.75; NaCl [150 mmol/l]; NaN_3 [0.5 g/l]) with buffer exchange columns (NAP-10, PD-10; GE Healthcare). The mAb concentration and yield of collected eluate was determined with ultraviolet-visible (UV-VIS) spectrophotometer, after which 0.1% of diethylenetriaminepentaacetic acid (DTPA) purified bovine serum albumin (BSA) (PerkinElmer) was added and the solution filtered through a 0.22 µm pore size filter. Biotinylated mAb was stored at +4°C.

Each tracer antibody (mouse monoclonal IgGs 1C11cc, 329cc and 7G7; HyTest Ltd) was separately conjugated in sodium carbonate-bicarbonate buffer [50 mM; pH 9.8] with 30- to 35-fold molar excess of [2,2′,2″,2‴-{[2-(4-isothiocyanatophenyl)-ethylimino]bis(methylene)bis{4-{[4-(alfa-galactopyranoxy)-phenyl]ethynyl}pyridine-6,2-diyl}bis(methylenenitrilo)}tetrakis(acetato)] Eu(III) chelate (Eu-9d; in-house).[255] The solution was incubated for 18–20h at RT while protected from light. The antibodies were purified with fast protein liquid chromatography (FPLC; Pharmacia Ab.) on a Superdex 200 HR 10/30 gel filtration column (Cytiva) and TSA buffer as an eluent. The mAb concentration of pooled fractions was calculated based on the TRF measurements conducted with Arcus 1230 fluorometer (Wallac Oy). The labeling degree of the mAb was estimated using Eu-standard (in-house; verified with

[1 nM] DELFIA Eu std. (B119-100; PerkinElmer)) diluted in enhancement solution. DTPA-purified BSA was added into the pooled fractions and the solution was filtered. Labeled mAbs were stored at +4 °C.

4.3.2 Assay Design

In comparison to the Roche Elecsys hs-cTnT, which measures even highly fragmented forms of cTnT, the long cTnT assay was designed to monitor the C-terminal cleavage area of cTnT at aar 189–223, as illustrated in Figure 13. The assay is based on sandwich-type immunoassay format with one monoclonal capture antibody and three monoclonal tracer antibodies. The assay utilizes TRF (λex 340 nm) for analyte quantification.[255] The biotinylated capture antibody 7E7 targets cTnT at epitope aar 223–242 (UniProt entry P45379-6). The labeled tracer antibodies (1C11cc, 329cc and 7G7) recognize cTnT towards the N-terminus at aar 171–190, 119–138 and 67–86 respectively. In addition to the mAbs that were chosen, several different mAbs and mAb combinations were tested during the development of the long cTnT assay. Human cardiac troponin ITC-complex (Hytest Ltd; Cat# 8T62) diluted into TSA-BSA buffer (7.5% Probumin, Merck Millipore; pH 7.75) was used as a multipoint calibrator for the long cTnT immunoassay. Other assay reagents are presented at Table 6 and the complete assay protocol is described in Table 7.

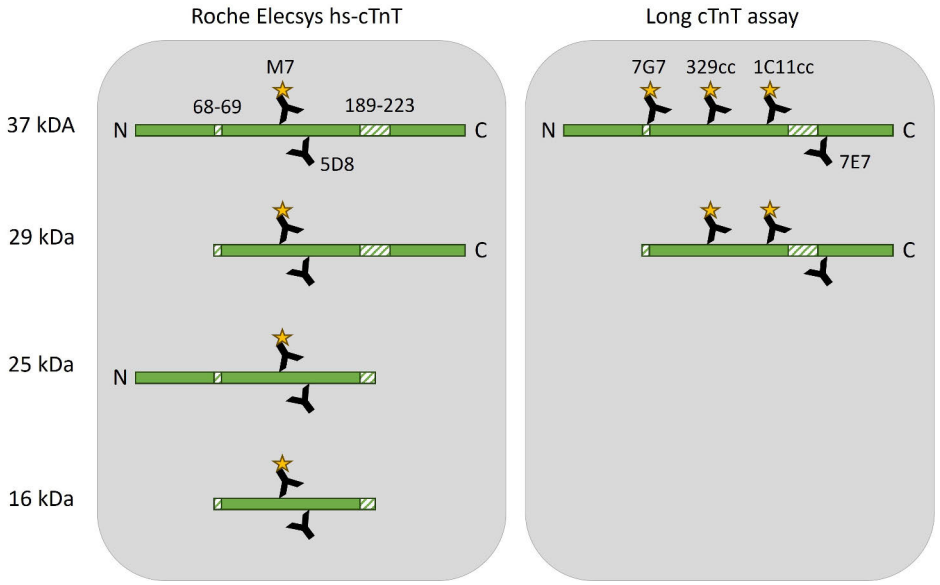

Figure 13. Illustration of the main molecular forms detected by the Roche Elecsys hs-cTnT and long cTnT assays.[194–196]

Table 6. Long cTnT assay reagents.

Microtiter plate	Streptavidin coated 96-well plate (yellow); Kaivogen Oy
Capture mAb	Biotinylated mAb 7E7
Tracer mAbs	Eu-9d labelled mAbs 7G7, 329cc, 1C11cc
Buffer for capture mab	Buffer Solution Red; Kaivogen Oy
Assay buffer	Tris-HCl [100 mmol/L] pH 7.75; NaCl [600 mmol/L]; NaN_3 [0.5 g/L]; BSA, [25 g/L]; casein, Calbiochem, Merck Millipore [4 g/L]; bovine-γ-globulin, Sigma-Aldrich [0.6 g/L]; native mouse IgG, Meridian Life Science Inc. [0.8 g/L]; denaturated mouse IgG [0.05 g/L]
Wash solution	Wash solution; Kaivogen Oy

Table 7. Long cTnT assay protocol.

Preparation of capture mAb solution	The capture buffer and capture mAb (for all wells) is mixed in Eppendorf tube. Capture buffer (25 µl/well), capture mAb (200 ng/well).
Immobilization of capture mAb	Capture mAb solution is added into each well of the microtiter plate (25 µl/well). Short shaking for few seconds with plate shaker is applied to the plate after which it is placed into humidity chamber. Incubated for 1h at RT.
Preparation of tracer mAb solution	The correct amount of assay buffer and each of the tracer mAbs for all wells is mixed in Eppendorf tube. Assay buffer (40 µl/well), each tracer mAb (100 ng/well).
1st Wash	The capture mAb solution is removed with plate washer and wells washed two times with wash solution.
Addition of tracer mAb solution	Tracer mAb solution is added into each microtiter well (40 µl/well).
Addition of calibrator or sample	Either calibrator or sample (30 µl/well) is added into each well. Microtiter plate is then carefully covered with sealing tape and placed into plate incubator for 1h at +36 °C, 900 rpm.
2nd Wash	The solution containing assay buffer and either sample or calibrator is removed from all wells with plate washer and wells are washed six times with wash solution.
Drying of microtiter plate	The microtiter plate is dried under stream of hot air from hot air blower for 5 minutes at +60 °C.
Cooling the microtiter plate	The microtiter plate is moved into chamber with silica bead pouch (humidity remover). Cooled passively into RT.
TRF measurement	Measurement of the microtiter plate conducted with VictorX4 Multilabel counter (PerkinElmer). λex 340 nm, λem 615 nm, meas. delay 250 µs, meas. window 750 µs.

4.3.3 Evaluation of Assay Performance

The evaluation of analytical performance of the long cTnT assay included limit of blank (LoB), limit of detection (LoD), limit of quantitation (LoQ) and dilution linearity. LoB, LoD and LoQ were defined as follows:

- LoB - the highest measurement result expected for a blank sample with 95% probability.
- LoD - the lowest analyte concentration that can be distinguished from the blank with 95% probability.
- LoQ - lowest amount of an analyte in a material that can be quantitatively determined with accuracy of 10% CV.

Both LoB and LoD were determined according to the Classical Approach of Clinical and Laboratory Standards Institute (CLSI) guideline EP17-A2 with single deviation as just one reagent lot was used.[283] LoB was determined by measuring five batches of TSA-BSA buffer on five non-consecutive days as triplicates (n=75). Due to non-Gaussian distribution of data points, nonparametric data analysis was conducted. LoD was determined by measuring six pools of LiH plasma samples with low concentrations of long cTnT (6.2–14.3 ng/L). Samples were analysed as triplicates on four non-consecutive days (n=72). Due to Gaussian distribution of data points, parametric data analysis methods were used.

Roche Elecsys hs-cTnT assay refers to LoQ as functional sensitivity with an intermediate precision CV of ≤10%.[284] Although our assay is not a hs-cTnT assay, we also adopted this terminology and adhered to CLSI guideline EP17-A2 to determine LoQ.[283] In addition, we determined LoQ with 20% CV as required in US by the FDA.[230] Long cTnT was measured from 10 plasma sample pools (5.5–44.0 ng/L) on four days as triplicates (n=120).

The LiH plasma pools used to determine the LoD and LoQ were prepared from LiH plasma obtained from STEMI patients and diluted with LiH plasma from healthy volunteers, which was confirmed to contain undetectable levels of long cTnT.

Dilution linearity was assessed with two sets of experiments. The first experiment was performed using pooled LiH plasma collected from three STEMI patients. The second experiment was conducted with cTn ITC complex calibrator material in pooled LiH plasma of healthy individuals. Both dilution experiments were conducted using 2-fold dilutions and healthy plasma as a diluent.

The temporal trends of long cTnT and long/total cTnT ratio during type 1 MI were investigated in study I. Visual comparison was made between long cTnT, total cTnT and long/total cTnT ratio by analysing data from STEMI and NSTEMI patients (n=106) and plotting each variable against time after symptom onset. This data set

was also investigated by dividing results into timeframes of 0–24h (n=53), >24h–48h (n=43) and >48–74h (n=10) and comparing their median trends.

The clinical evaluation of the long cTnT assay was conducted by investigating its ability to distinguish the STEMI (n=71) and NSTEMI (n=46) patient cohorts from the ESRD (n=40) cohort. The long cTnT results were compared to the fifth-generation Roche Elecsys hs-cTnT assay (total cTnT) as an individual parameter and in combination with total cTnT as long/total cTnT ratio.

In addition, the effect of hemodialysis on long cTnT and long/total cTnT ratio was also evaluated by measuring LiH samples acquired from ESRD patients before and after hemodialysis.

4.3.4 Matrix Comparison and Evaluation of Analyte Stability

Preliminary comparison of serum and lithium heparin (LiH) plasma matrix was conducted by comparing the measured long cTnT concentrations of serum and LiH samples taken from STEMI patients (n=3) at the same instance. The *in vitro* stability of endogenous long cTnT was evaluated by spiking both TSA-BSA buffer and pooled LiH plasma from healthy volunteers with LiH plasma collected from a STEMI patient to a final concentration of 200 ng/L. The aliquoted samples were then subjected to either +4 °C, +21 °C, or +37 °C for 24h or 7 days and stored at -20 °C until measured shortly after day 7. The stability was also evaluated by subjecting separate aliquots to 1, 3, or 5 freeze–thaw cycles between -20 °C and room temperature. All the results were then compared to a baseline measurement conducted at the start of the experiment.

4.4 Europium Chelate

4.4.1 Europium Chelate Synthesis

All the reagents and solvents used in the synthesis of the target compounds and their intermediates were obtained as reagent grade and used without further purification. All the intermediates were stored between subsequent synthesis steps at -18 to -20 °C and the final target compounds at -70 °C and protected from light and moisture.

Synthesis of 2,2'-(((6-(((2-(bis(carboxylatomethyl)amino)ethyl)-(carboxylatomethyl)amino)methyl)-4-((5-((4-isothiocyanatobenzyl)amino)-pyrazin-2-yl)ethynyl)pyridin-2-yl)-methyl)azanediyl)diacetate europium(III)

Compound (6) was synthesized according to scheme 1. By utilizing microwave assisted synthesis 2,5-dibromopyrazine was coupled with 4-(Boc-amino)benzylamine to achieve compound (1). This was followed by subsequent substitution of bromine with ethynyltrimethylsilane group with bis(triphenylphosphine)palladium(II) dichloride ($Pd(PPh_3)_2Cl_2$) catalyst and copper(I) iodide (CuI) co-catalyst to achieve compound (2). The reaction was performed with microwave equipment under argon atmosphere. Compound (3) was achieved by removal of trimethylsilane protection with potassium carbonate in methanol. Compound (4) was synthesized according to the procedures found in literature.[9] Sonogashira cross-coupling reaction was used to produce Compound (5) in a similar manner as compound (2). Trifluoroacetic acid was then used to remove tert-butyloxycarbonyl (Boc) protection and all the tert-butyl groups from compound (5). Europium(III) ion was then introduced in the form of europium trichloride. This was followed by the conversion of the primary amine into isothiocyanate group with thiophosgene to yield compound (6).

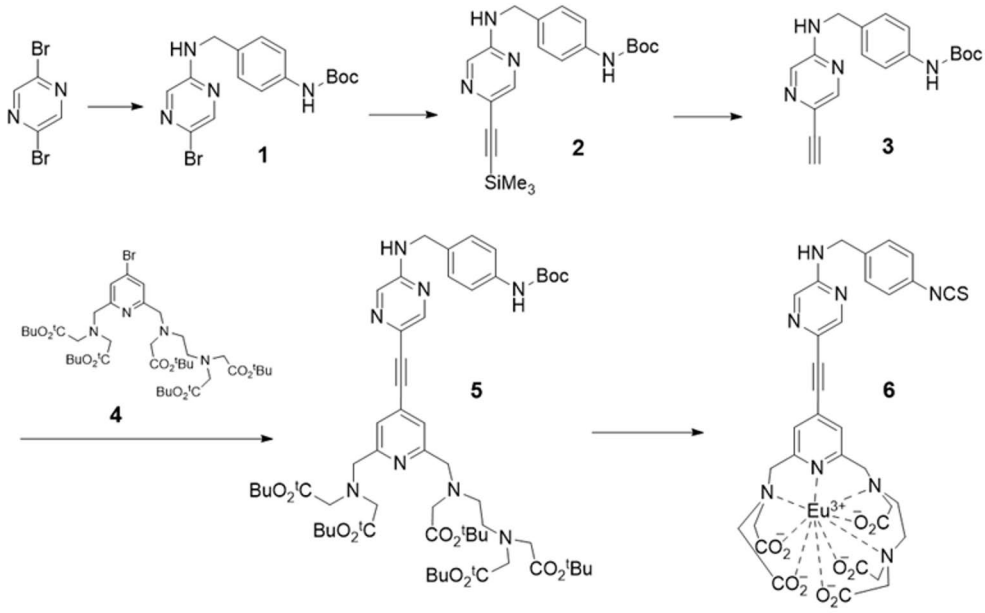

Scheme 1. Synthesis pathway of 2,2'-(((6-(((2-(bis(carboxylatomethyl)amino)ethyl)-(carboxylatomethyl)amino)methyl)-4-((5-((4-isothiocyanatobenzyl)amino)-pyrazin-2-yl)ethynyl)pyridin-2-yl)methyl)azanediyl)diacetate europium(III); referred as compound (6).

Synthesis of 2,2'-(((6-(((2-(bis(carboxylatomethyl)amino)ethyl)(carboxylatemethyl)amino)methyl)-4-((5-((4-isothiocyanatobenzyl)amino)-6-methoxypyrazin-2-yl)ethynyl)pyridin-2-yl)methyl)azanediyl)diacetate europium(III)

Compound (13) was synthesized according to scheme 2. To achieve compound (7), 5-bromo-3-methoxypyrazin-2-amine and 4-nitrobenzoylchloride were coupled together under dry conditions. The nitro group in compound (7) was reduced into an amine with stannous chloride to achieve compound (8). [1 M] Borane-tetrahydrofuran (THF) solution under strict anhydrous conditions was used to reduce carbonyl group to produce compound (9). Thereafter synthetic steps followed similar synthesis pathway as with target compounds (2) to (6).

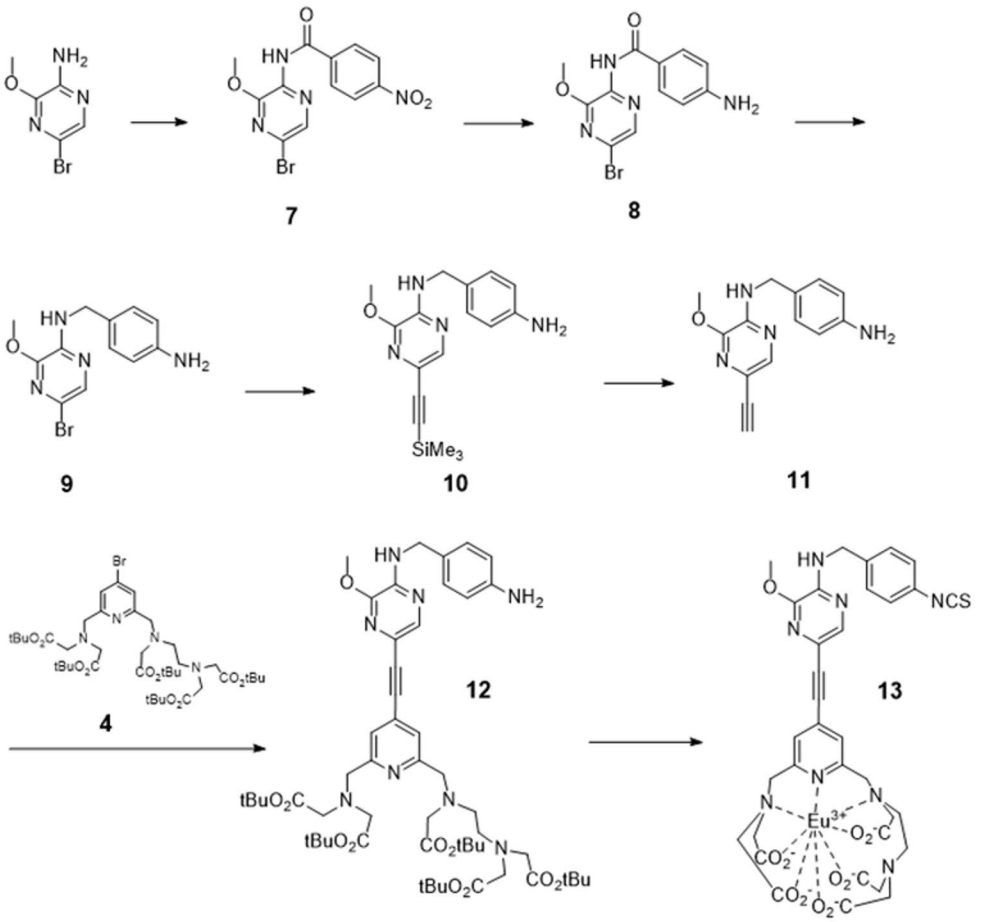

Scheme 2. Synthesis pathway of 2,2'-(((6-(((2-(bis(carboxylatomethyl)amino)ethyl)-(carboxylatomethyl)amino)methyl)-4-((5-((4-isothiocyanatobenzyl)amino)-6-methoxypyrazin-2-yl)ethynyl)pyridin-2-yl)methyl)azanediyl)diacetate europium(III); referred as compound (13).

Synthesis of 2,2'-(((4-((5-amino-6-((4-isothiocyanatobenzyl)carbamoyl)pyrazin-2-yl)ethynyl)-6-(((2-(bis(carboxylatomethyl)amino)ethyl)(carboxylatomethyl)-amino)methyl)pyridin-2-yl)methyl)azanediyl)diacetate europium(III)

Compound (19) was synthesized according to Scheme 3. A detailed description of the synthesis is provided in this thesis, as it was not included in Manuscript III. Methyl 3-amino-6-bromopyrazine-2-carboxylate (0.55 g; 2.4 mmol) was treated with [5 M] sodium hydroxide (10.5 ml) in methanol (50 ml), to convert the methyl carboxylate into carboxylic acid. The reaction was conducted at RT with stirring for 3 hours. The product was extracted with ethyl acetate and after drying the extract with sodium sulfate, evaporated to dryness.

Compound (14) (0.35 g; 1.6 mmol) was combined with tert-butyl (4-(aminomethyl)phenyl)carbamate (0.38 g; 1.7 mmol) to achieve compound (15). This was accomplished by dissolving compound (14) and hexafluorophosphate benzotriazole tetramethyl uranium (HBTU) (0.64 g; 1.7 mmol) into dimethylformamide (DMF) (30 ml) and by adding N,N-diisopropylethylamine (DIPEA) (0.34 ml; 1.9 mmol) into the mixture while stirred at ice bath. After few minutes, N,N-diisopropylethylamine (DIPEA) (0.34 ml; 1.9 mmol) was added. The ice bath was shortly after removed and the mixture was kept overnight at RT and then purified with silica gel column (5% methanol (MeOH)/dichloromethane (DCM)).

Similarly, as with compounds (2) and (10), Sonogashira cross-coupling reaction was utilized to achieve compound (16). The mixture of compound (15) (0.97 g; 2.3 mmol), $Pd(PPh_3)_2Cl_2$ catalyst (0.07 g; 0.1 mmol) and CuI co-catalyst (0.02 g; 0.1 mmol) were loaded into a flame dried microwave tube and sealed. Oxygen was flushed with dry argon for five minutes via septum. 1:1 (v/v) mixture of dry THF and triethylamine (TEA) (9 ml) was added via septum. The solution was again flushed with dry argon. Trimethylsilylacetylene (0.42 ml; 3.0 mmol) was mixed with THF:TEA (1.3 ml) and added into the reaction mixture via septum with heavy stirring. Tube was heated with Biotage Initiator Microwave Synthesizer for one hour at 60 °C. Product was purified with long silica gel column with 30% ethyl acetate (EtOAc) / petroleum ether (PE) eluent.

To remove the trimethylsilane protection, compound (16) (0.20 g; 0.46 mmol) was added into a flask with potassium carbonate (0.03 g; 0.22 mmol). The flask was sealed and flushed with argon via septum. MeOH (15 ml) and diethyl ether (Et_2O) (5 ml) were added via septum. The mixture was stirred for one and half hours at RT. The solution was filtered through Celite® and washed with MeOH/diethyl ether (Et_2O). Solution was then evaporated into dryness in vacuo and compound (17) was obtained.

To synthesis compound (18), compound (4) (0.30 g; 0.36 mmol), $Pd(PPh_3)_2Cl_2$ catalyst (0.012 g; 0.017 mmol) and CuI co-catalyst (0.003 g; 0.014 mmol) were sealed into a flame dried microwave tube and flushed with argon for five minutes via septum. A small amount of THF:TEA (1:1) was added via septum to dissolve the solids. Compound (17) (0.16 g; 0.43 mmol) was dissolved with THF:TEA and added slowly in to the mixture via septum while stirring. The tube was heated with microwave synthesizer for one and half hours at 65 °C. The mixture was cooled down to RT and filtered. The filtride was washed with THF:TEA and all volatiles were evaporated in vacuo. The product was then dissolved into a small amount of DCM and washed three times with water. The organic layer was dried with sodium sulfate and evaporated in vacuo. The product was then purified with two consecutive silica gel column runs. First was conducted using dry loading and 20–40% EtOAc/PE. In the second column 5–10% MeOH/DCM followed by 10% MeOH/DCM with 4% (v/v) TEA was used.

Compound (19) (0.113 g; 0.101 mmol) was synthesized by three consecutive steps: removal of protecting Boc and tert-butyl groups, introduction of Eu(III) and activation by introducing isothiocyanate group. Compound (18) and chloroform (1.5 ml) were transferred into a flame dried flask under argon. The flask was put into an ice bath and trifluoroacetic acid (TFA; 2 ml) was slowly added with heavy stirring. The ice bath was removed and stirring was continued at 24–25 °C for two hours. Small amount of MeOH/acetone mixture was placed into rotavapors solvent collection flask and all volatiles were evaporated in vacuo without any heating. The mixture was dissolved into ultra-pure water (3.5 ml) and the pH was adjusted around five with sodium bicarbonate. Solid $EuCl_3$ (0.039 g; 0.106 mmol) was added, after which the mixture was stirred for 10 minutes. The pH was then adjusted between 8.0–8.5 with sodium bicarbonate and sodium carbonate, which caused the product to precipitate. The solution was stirred for additional five minutes after which the mixture was transferred into a falcon tube and the precipitate was removed by centrifugation. Acetone (30 ml) was added into the solution and solid precipitate formed, which was again collected by centrifugation, washed with acetone (4 × 3 ml) and dried in vacuo. The precipitate was dissolved into water (0,5 ml) and chloroform (0.5 ml) and thiophosgene (12 µl, 0.16 mmol) were added and the mixture was stirred vigorously for 5 min. The pH was kept around 7.0 with sodium bicarbonate. The chloroform was carefully removed with pipette and acetone (45 ml) was added. After mixing, the precipitate was isolated by centrifugation, washed with acetone (2 × 40 ml) and dried in vacuo.

To obtain the glycine conjugated chelate for luminescence characterization, compound (19) (10 mg) was allowed to react with glycine (100 mg) in aqueous solution at pH 9.8 for overnight. The product was purified by high-pressure liquid chromatography (HPLC) similarly as with compound (13).

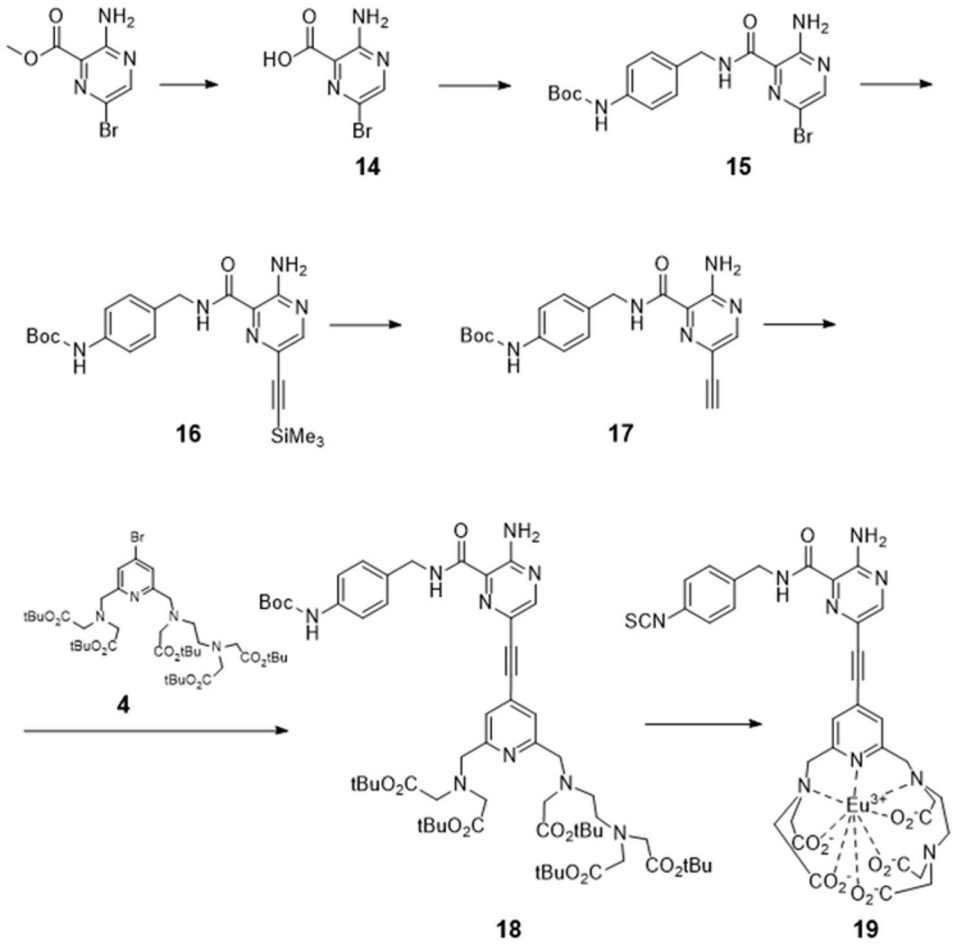

Scheme 3. Synthesis pathway of 2,2'-(((4-((5-amino-6-((4-isothiocyanatobenzyl)carbamoyl)-pyrazin-2-yl)ethynyl)-6-(((2-(bis(carboxylatomethyl)amino)ethyl)(carboxylatomethyl)-amino)methyl)pyridin-2-yl)methyl)azanediyl)diacetate europium(III); referred as compound (19).

4.4.2 Europium Chelate Structural Analysis

For the structural analysis of the compounds mass spectrometry and nuclear magnetic resonance (NMR) analyses were utilized. Matrix-assisted laser desorption/ionization time-of-flight (MALDI-TOF) analyses were acquired with Bruker Daltonics Ultraflex II mass spectrometer. High resolution mass spectra (HRMS) measurements were conducted with Bruker Daltonics microTOF mass spectrometer. Calculated m/z values were acquired with ChemDraw Professional v.23 (Revvity). ^{1}H and ^{13}C NMR spectra were recorded on a 500 MHz Bruker Avance-III spectrometer and analysed with SpinWorks 4 (v4.2.12.0; Kirk Marat, University of Manitoba). Both HRMS and NMR measurements were conducted at the Turku Centre for Chemical and Molecular Analytics. No NMR measurements were conducted on compounds containing europium, due to the nature of paramagnetic europium(III) to shift and alter resonances.[285,286] Therefore, pre and post glycine conjugation HPLC data was acquired and compared to confirm successful conjugation. All molecular structures were drawn either with ChemDraw Professional v.23 or Marvin JS (Chemaxon).

4.4.3 Characterization of Luminescence Properties

The novel europium(III) chelates (compounds 6, 13 and 19) were conjugated to glycine, dissolved into TSA [50 mmol/l; pH 7.75] and characterized for their luminescence properties. As a reference, a well-established europium chelate {2,2',2",2"'-{[2-(4-isothiocyanatophenyl)ethylimino]bis(methylene)-bis{4-{[4-(galactopyranoxy)-phenyl]ethynyl}-pyridine-6,2-diyl}bis-(methylenenitrilo)}-tetrakis(acetato)} europium(III) was used (Eu-9d; Figure 14).[255] The characterization included absorption spectrum, fluorescence excitation spectrum, fluorescence emission spectrum and fluorescence decay profiles at 20 °C, 40 °C and 60 °C. UV-Vis absorption spectra were recorded on a Shimadzu UV1800 or with Molecular Devices UV-Vis Spectrophotometer. The fluorescence emission and excitation spectra and emission decay profiles were acquired with Varian Cary Eclipse Fluorescence Spectrophotometer. Temperatures of the fluorescence measurements were controlled with Varian Peltier. The concentration of glycine conjugated compounds (6) and (13) were determined by SGS Belgium NV I.A.C. with ICP-MS and with an in-house method with Wallac Arcus 1230 using PerkinElmer DELFIA europium standard (B119-100) as a calibrator.

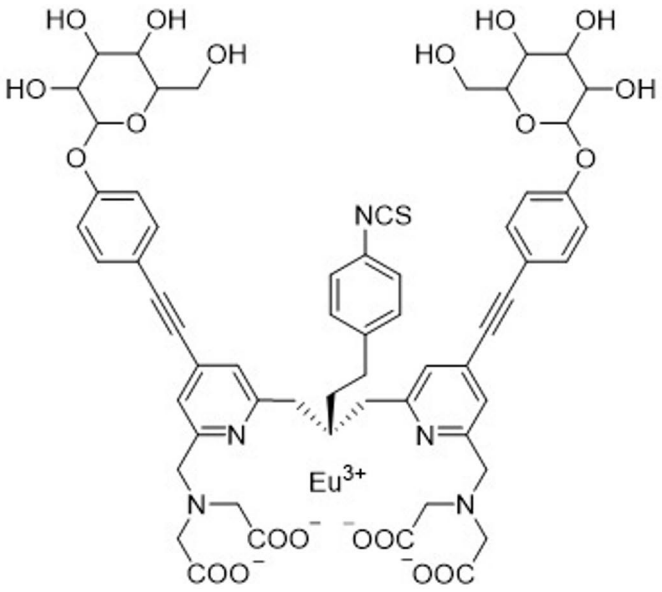

Figure 14. The structure of reference chelate Eu-d9.[255]

4.4.4 Performance of Synthesized Labels in cTnI Assay

Compounds (6), (13) and (19) were each individually conjugated with cTnI mAb 625 (Hytest Ltd.) in sodium carbonate-bicarbonate buffer [50 mM; pH 9.8] with 30- to 140-fold molar excess of label and used as a tracer antibody in a sandwich-type cTnI immunoassay based on earlier work.[287] The assay utilized a 3+1 format with three capture antibodies (Fabs 4C2, MF4 and mAb 19C7; Hytest Ltd.) and one tracer antibody. The assay was measured using excitation wavelength of 340 nm with Victor X4 Multilabel counter (PerkinElmer; λem 615 nm, meas. delay 250 µs, meas. window 750 µs) and excitation wavelength of 365 nm excitation using LED excitation fluorometer (Labrox). The LoD estimates were calculated according to Eq.5 using the background signal and the slope of the calibration curve, with an assumption of blank 10% CV, due to limited number of blank results per label. Human cardiac troponin ITC-complex (Hytest Ltd.; Cat# 8T62) was used as a calibrator.

$$Estimated\ LoD = 3\ x\ 0.1\ x\ \frac{average\ blank\ signal}{slope\ of\ calibration\ curve}$$ Equation 5.

4.5 Statistical Analyses

Study I

For the detection of outliers 1.5 times IQR was used. The distributions of measured values were examined visually and by using the Shapiro–Wilk test. Results were presented as median [25^{th}–75^{th} percentiles] for continuous variables with skewed distributions. Dilution linearity and other linear regression analyses were conducted with Origin 8 or OriginPro 2024 (OriginLab). For the analyte stability evaluation and for sample matrix comparison studies, means ± propagated SD values were reported. The functional sensitivity (LoQ) of the assay was determined by utilizing an exponential decay function in SigmaPlot 16 (Grafiti LLC).

Study II

The normality of continuous variables was examined visually and analysed using Shapiro-Wilk and Kolmogorov-Smirnov tests. Results were presented as median interquartile range rule (IQR) for continuous variables with skewed distributions. Mann-Whitney U test was used to compare continuous variables with two skewed distributions. Kruskal-Wallis test was utilized to test for significance between multiple groups. With significant difference, analyses were continued with Dunn test to identify between which groups the difference was significant. To improve the validity of findings, Bonferroni correction was applied. To evaluate how well long cTnT and long/total cTnT ratio could separate ESRD and NSTEMI patient groups, receiver operating characteristics (ROC) curves and area under the curve (AUC) were established. The comparisons between the total and long cTnT levels before and after hemodialysis in the ESRD group were performed using the Wilcoxon signed rank test. Analyses were performed using IBM SPSS Statistics software version 26.0 (IBM Corporation).

Study III

Linear regression analyses were utilized when determining fluorescence lifetimes with Origin 8 or OriginPro 2024.

5 Results and Discussion

5.1 Long cTnT Assay

Novel long cTnT assay that only detects intact and N-terminally truncated cTnT was successfully developed and evaluated according to CLSI guidelines. For the first time ever, it was shown that by measuring specific forms of cTnT it is possible to differentiate between patient groups with chronic non-MI related cTnT elevation and type 1 MI.

5.1.1 Analytical Performance

The long cTnT assay produced a linear response (R^2 = 0.993; slope = 19.66 ± 0.65; residual sum of squares = 10.5) in the range of 5 to 5000 ng/L. The assay achieved LoB, LoD, and LoQ (10% CV) of 4.4 ng/L and 10.8 ng/L and 30.8 ng/L (R^2 = 0.986) respectively. Concentration at 20% CV was 18.8 ng/L. Although Roche Elecsys 5th gen hs-cTnT assay has a measuring range up to 100 000 ng/L as reported in the IFU, the upper limit of quantitation of long cTnT assay was more than sufficient for quantifying the majority of MI samples in our cohort (median 221 [44–687] ng/L). The analytical sensitivity of our assay was acceptable for studying the selected cTnT forms and their diagnostic potential. However, the long cTnT concentration of some samples fell under the LoQ, thus emphasizing the need for more sensitive assay. During different stages of assay development and thesis progression, multiple approaches were considered to ensure the finalized assay achieved good sensitivity, given that only a fraction of circulating cTnT was targeted. First, a combination of three different tracer antibodies was utilized in the design to improve long cTnT assay sensitivity. Several antibodies with known epitopes and negligible (<1%) cross-reactivity with skTnT were screened. mAbs 329cc and 1C11cc presented excellent performance characteristics during preliminary screening and were thus selected. Although mAb 7G7 was known to be affected by N-terminal cleavage, it was chosen due performance characteristics, epitope availability and because it emphasizes the freshly released N-terminally intact cTnT.[288] A second approach to increase sensitivity was investigated in study III, where a highly fluorescent europium(III) chelate label was developed. Although the new label outperformed the

existing label, utilization in long cTnT assay was hampered by signal background problems and time constraints. The third approach which was considered but not acted upon in this thesis, included using polylysine peptides to increase the labelling decree of the tracer antibodies.[281] Subsequently a more sensitive long cTnT assay using upconverting nanoparticle was developed by Salonen *et al.* based on the long cTnT assay presented in this thesis.[289]

5.1.2 Assay Interference

The dilution linearity of the long cTnT assay was investigated to establish whether the assay produces linear results upon dilution or if the results are affected by interfering matrix components. The dilution linearity of the assay was acceptable with endogenous long cTnT (R^2 = 0.998; slope = 1.094 ± 0.017; *y*-intercept = −0.43 ± 0.049; residual sum of squares = 21.2) and troponin ITC-complex calibration material (R^2 = 0.989; slope = 1.047 ± 0.042; *y*-intercept = −0.18 ± 0.14; residual sum of squares = 132.7) when serially diluted into LiH plasma pool within the range of 20 to 5000 ng/l. Healthy plasma was tested to contain no detectable amounts of long cTnT. The long cTnT assay showed good dilution linearity, indicating that basic plasma matrix components do not cause concentration-dependent interference in the tested range. Also, importantly both endogenous cTnT and ITC calibration material behaved similarly, thus supporting our choice of calibration material. However, due to the limited number of used samples, it cannot be excluded that rare individual features such as troponin autoantibodies, heterophilic autoantibodies or cTnT mutations may affect the long cTnT assay.[290,291]

The long cTnT assay uses three tracer antibodies. The use of multiple tracers simultaneously makes the assay more robust towards cTn autoantibodies, but also increases the risk of false positive results due to cross-linking by heterophilic antibodies such as human anti-mouse antibodies (HAMA) and rheumatic factor.[292] However, the long cTnT assay buffer contains both native and denaturated mouse IgG, which helps to mitigate the detrimental effects of both HAMA and rheumatic factor on the mouse mAbs used in the assay.[290] To further improve the assays resistance to heterophilic antibodies the assay mAbs would need be replaced for example by Fabs or F(ab`)$_2$ fragments.[293] However, the prevalence of interfering heterophilic antibodies in general population has been estimated to be rather low ranging from 0.1 to 3%.[294]

The epitope of the capture mAb 7E7 is suspected to be affected by cTn autoantibodies.[292] The presence of autoantibodies may lead to falsely decreased results or prolonged elevation due to decreased clearance of cTnT due to macrotroponin formation.[191] Most of the cTn autoantibody studies address cTnI autoantibodies, while there are limited number of studies regarding the prevalence

of cTnT autoantibodies. In general, it seems that the prevalence of cTn autoantibodies is affected differently depending on the associated morbidity.[295] In healthy population the prevalence of cTnT autoantibodies has been estimated to be around 10%.[296] However, as with cTnI, not all cTnT autoantibodies bind into the same epitopes, nor is the extent of interference always clinically relevant.[297] As the long cTnT assay utilizes just one capture antibody, identifying and selecting an epitope that is minimally affected by cTn autoantibodies is an important consideration for further long cTnT assay development.[298]

5.1.3 Long cTnT Sample Matrix

The measured long cTnT concentration of serum samples were 59 ± 6%, 66 ± 10%, and 75 ± 9% of the respective LiH plasma concentrations. Earlier studies have revealed that thrombin causes cleavage of cTnT at aar 68–69.[170,206] This cleavage does not happen in such extent in heparin plasma samples, due to thrombin-heparin-antithrombin complex formation which inactivates thrombin.[299,300] Moreover, it has been recently demonstrated, that serum samples are affected by accelerated degradation beyond thrombin-mediated cleavage, which leads to the formation of smaller 16 kDa cTnT fragments.[208] Regardless of the small sample size, the preliminary results presented in study I are in line with these findings. In addition, serum sample preparation takes longer due to the necessary coagulation time. Thus, LiH plasma was chosen as the preferred sample matrix when measuring long cTnT with our assay. However, additional matrixes have been recently considered in other studies. EDTA plasma showed a higher degree of fragmentation compared to LiH plasma, whereas hirudin plasma prevented any in vitro fragmentation of cTnT during 48h study period.[208,209]

5.1.4 Analyte Stability in Plasma

When compared to the baseline measurement conducted at the start of the experiment, incubation of endogenous long cTnT in healthy LiH plasma at +4 °C resulted in relative concentrations of 82 ± 9% at 24h and 67 ± 5% at day 7. As expected, incubation at higher temperatures led to a decreased analyte stability. Incubation at RT showed relative concentrations of 65 ± 4% at 24h and 28 ± 2% at 7 days. When subjected to incubation at +37 °C fast analyte loss was observed leading to relative concentration of 21 ± 3% at 24h and almost total analyte loss (2 ± 0.5%) at day 7 as shown in Figure 15.

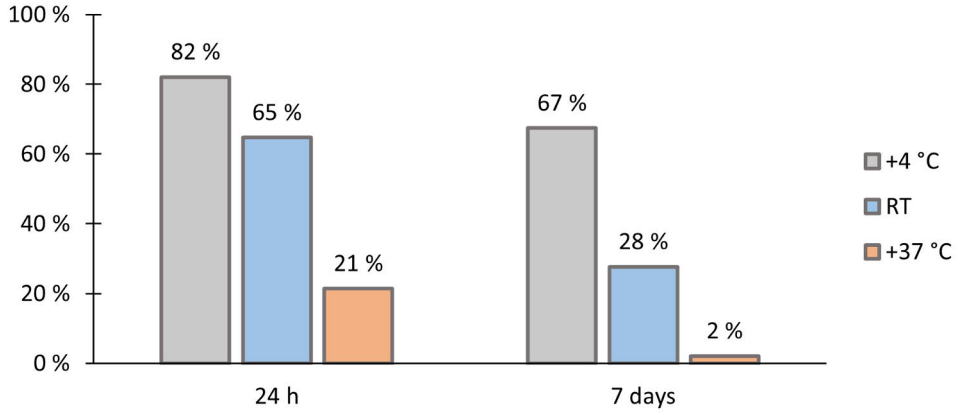

Figure 15. Stability of endogenous long cTnT spiked into long cTnT-negative LiH plasma and incubated at +4, RT or +37°C for 24h or 7 days. Relative concentrations were expressed as a fraction of the baseline measurement obtained at the beginning of the experiment.

Previously several studies have assessed cTnT stability in serum or LiH plasma by measuring concentration with Roches hs-cTnT assays.[301,302] These studies however are not valid when studying long cTnT stability as different forms of cTnT are measured. Thus, only a limited number of studies have been conducted, where *in vitro* stability of cTnT in LiH plasma has been assessed with western blotting or gel filtration studies. Mingels *et al*. found no time-dependent degradation when NIST cTnT Standard Reference Material 2921, a human myocardial tissue-derived purified ITC complex, was incubated in cTn-negative LiH plasma at +4 °C or +37 °C for 3 days.[303] Recently Vroemen *et al*. investigated cTnT fragmentation by spiking healthy LiH plasma with intact cTnT (40 kDa) and incubating it at 37 °C for up to 48 h. They reported that only 10% of cTnT had degraded to 25-29 kDa fragments during the 48h time period.[208] These reports appear to contradict results obtained in study I. However, in a recent study by Riabkova *et al*. cTn immunoassay was utilized with Tcom8 and 7E7 mAbs, and after incubating the ITC-complex in various matrices at +4, RT or +37 °C for 24 h, they similarly observed a clear decrease in measured values. They then tested LiH plasma with western blotting and found no cTnT degradation.[210] This clearly supports the findings of study I and could indicate, that although cTnT remains rather intact in LiH plasma, prolonged incubation at elevated temperatures can cause reduced immunochemical activity which is observed with immunoassays, including long cTnT assay.

In regard to long cTnT assay, these results indicate that prolonged storage at RT can cause decrease in measured concentrations within 24 h. However, ESC recommends that cTn results should be obtained within 60 minutes of blood sampling.[6] Moreover, median laboratory turnaround times (defined as the time from

sample acquisition to reporting) presented by French national survey in 2025 and Kuopio University Hospital in 2008 were 81 and 69 minutes respectively.[304,305] It can be assumed that within these time frames, the relative concentration change of long cTnT in LiH plasma *in vitro* is significantly less than that observed after 24 h. Nevertheless, results of study I demonstrate that long cTnT samples should be analysed as soon as possible after blood draw, and the immunochemical activity of long cTnT should be carefully validated within clinically relevant time frames, taking into account potential reanalysis and small unforeseen delays in routine laboratory workflow.

5.1.5 Analyte Stability in Buffer

When compared to the baseline measurement, incubation of endogenous long cTnT in TSA-BSA buffer at +4 °C resulted in relative concentrations of 112 ± 10% at 24h and 99 ± 12% at day 7 as illustrated in Figure 16. Incubation at RT showed a rather modest decrease in relative concentration, with values of 88 ± 10% at 24h and 62 ± 6% at 7 days. Incubation at +37°C resulted a significantly poorer analyte stability with relative concentrations of 45 ± 5% at 24h and 33 ± 3% at day 7.

The *in vitro* stability of long cTnT in TSA-BSA buffer was excellent when kept at +4 °C and good stability was also observed after incubation at RT. Across temperature range of +4 °C to +37 °C and selected time points, better analyte stability was observed in buffer than in plasma. Therefore, these results indicate that long cTnT stability is enhanced after sample is added into buffer, thus suggesting that the most critical phase concerning cTnT stability is prior to analysis.

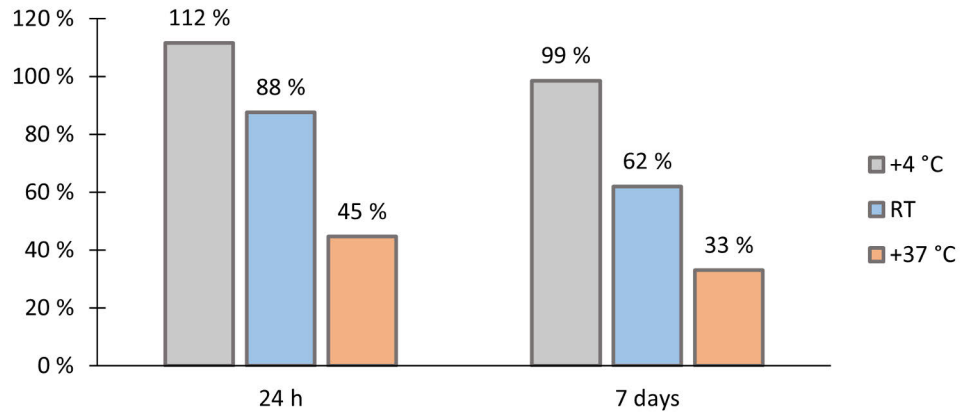

Figure 16. Stability of endogenous long cTnT spiked into TSA-BSA buffer and incubated at +4, RT or +37 °C for 24h or 7 days. Relative concentrations were expressed as a fraction of the baseline measurement obtained at the beginning of the experiment.

5.1.6 Analyte Stability After Freeze–Thawing

All stability results concerning freeze-thawing were compared to the baseline results obtained prior to first cycle. Endogenous long cTnT spiked in LiH plasma resulted in relative concentrations of 98 ± 10% after the first freeze-thaw cycle and results of 107 ± 11% and 83 ± 9% after the third and fifth cycles respectively. Endogenous long cTnT spiked into TSA-BSA buffer showed similar results with relative concentrations of 96 ± 15%, 92 ± 7% and 90 ± 11% after the first, third and fifth cycles respectively. Results illustrated in Figure 17.

Reports concerning cTnT stability in frozen samples or as subjected to freeze-thawing have focused heavily on Roche cTnT assays.[306,307] As explained previously these studies are somewhat invalid when considering long cTnT. Therefore, the effect of freeze-thawing on long cTnT stability was evaluated for the first time in study I. The results indicate that even multiple freeze-thaw cycles had rather minor effect on the stability of endogenous long cTnT in both plasma and buffer. Although, these results demonstrate the excellent short-term stability of long cTnT after multiple freeze-thaw cycles, no conclusion can be made about the long-term stability after being frozen. Even though in clinical context, long-term stability might be less critical parameter, it becomes highly important in research due to prolonged storage of different sample cohorts. Therefore, future studies should investigate the long-term stability of cTnT or include stability control in each sample cohort to be measured and followed with the same method.

5.2 Clinical Evaluation of Long cTnT Assay

5.2.1 Temporal Trend of Long cTnT and Long/Total cTnT Ratio in MI Patients

In study I, the temporal trend of long cTnT and long/total cTnT ratio during type 1 MI was investigated and compared to total cTnT as shown in Table 8. Patients whose samples were taken within 24h from symptom onset (NSTEMI n=23 (43.4%); STEMI n=30 (56.6%)) showed higher long/total cTnT ratios than those with >24h delay. This was also true when both NSTEMI ([≤24 h] 0.29 (0.20–0.72); [>24h] 0.15 (0.10–0.20); $p<0.001$) and STEMI ([≤24h] 0.62 (0.41–0.93); [>24h] 0.22 (0.11–0.38); $p<0.001$) cohorts were examined individually. The median long/total cTnT ratio also steadily declined after the onset of symptoms (≤24h 0.52, >24–48h 0.25, >48–74h 0.08). Total cTnT median value kept rising in relation to time (≤24h 355 ng/L, >24–48h 981 ng/L, >48–74h 1820 ng/L), whereas the median value of long cTnT peaked between 24–48h and decreased considerably thereafter (≤24h 226 ng/L, >24–48h 293 ng/L, >48–74h 155 ng/L).

Based on these data, it can be speculated that long cTnT, and especially the long/total cTnT ratio, might work best as MI biomarker during the early hours after onset of MI. Moreover, if measured long cTnT concentrations decrease faster than concentrations of those cTn forms measured with current cTn assays, long cTnT may offer improvement in perioperative diagnosis of MI or in reinfarction diagnostics. A recent study by Katrukha *et al.* supports the findings of study I, as they confirmed that in a period of 2–37h after the onset of MI the intact cTnT decreases from fraction of 64.9% to 25.5%.[201] In comparison, measured cTnI and cTnT values may remain elevated for up to 10 and 14 days, respectively, after the onset of MI.[184,186,189] Similarly, cTn values can be elevated perioperatively for example after PCI, CABG or other heart related surgery, thus complicating the detection of new myocardial injury.[5] However, as cTnT may show biphasic release kinetics independent of reperfusion, it is extremely important to conduct a more precise evaluation of long cTnT kinetics and the cTnT forms released on the second phase, which can be achieved by serial sampling from the same patient(s). To study long cTnT elimination kinetics free of continuous release of new cTn, a similar protocol than was used by Kristensen *et al*. to study cTnI could be adapted.[192] The decrease in analytical activity of long cTnT could be followed after the cTn concentration of a patient has returned to the suspected baseline level and a retransfusion of plasma that was collected during the early release phase.

Table 8. Temporal composition trend of circulating cTnT in patients with type 1 MI.

Time after symptom onset	n	Long cTnT (ng/L)	Total cTnT (ng/L)	Long/total cTnT ratio (ng/L)
0–24 h	53	226 [44–972]	355 [115–1480]	0.52 [0.27–0.76]
24–48 h	43	293 [70–627]	981 [333–2370]	0.25 [0.16–0.38]
48–74 h	10	155 [32–552]	1820 [237–5960]	0.08 [0.06–011]

Results presented as median [25th-75th percentiles]

5.2.2 Diagnostic Performance of the Long cTnT Assay in Discriminating Between ESRD and NSTEMI Patients

In our study cohort, total cTnT measured with 5th gen Roche Elecsys hs-cTnT assay did not differ between the ESRD (76 [50–124] ng/L) and the NSTEMI (NSTEMI 141 [62–312] ng/L; p=0.063) patient cohorts. However, when measured with the developed long cTnT assay, the ESRD cohort (3 [1–6] ng/L) differed significantly from both the NSTEMI (30 [10-186] ng/L; p< 0.001) and the STEMI (STEMI 442 [154–1235] ng/L; p< 0.001) cohorts. When only patients whose samples were taken within 24h from symptom onset were included, the total cTnT measurement failed

to differentiate between ESRD and NSTEMI (111 [56–299] ng/L; p< 0.155) cohorts, whereas long cTnT again showed statistically significant difference (44 [10–226] ng/L; p< 0.001) between these groups as shown in Figure 17. However, even more pronounced difference was achieved using long/total cTnT ratio.

When the samples were acquired within the first 24h after the onset of symptoms, the long/total cTnT ratio showed excellent capabilities to differentiate the ESRD (0.04 [0.02–0.08] cohort from the NSTEMI (0.29 [0.21–0.66]; p< 0.001; Figure 17) and STEMI (0.66 [0.43–0.93]; p< 0.001) cohorts. Even among patients with over 24h from the start of the symptoms, the long/total cTnT ratio was able to differentiate between chronic cTnT elevation seen in ESRD and acute cTnT release in NSTEMI (0.15 [0.10–0.19]; p< 0.001).

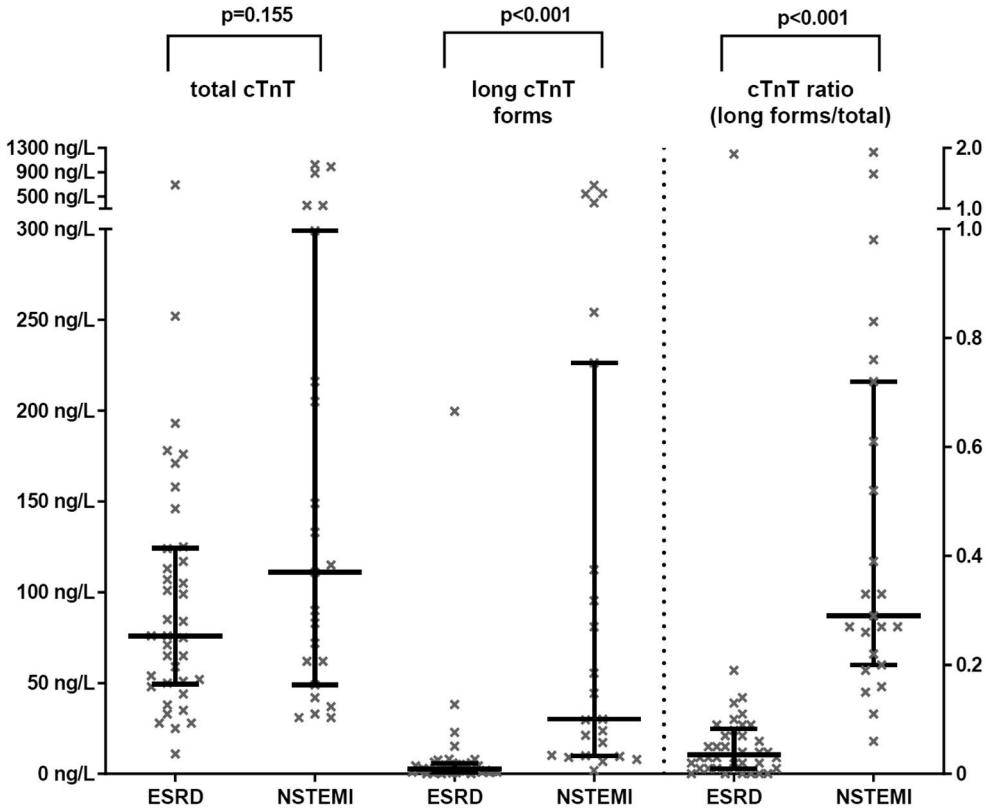

Figure 17. The ability of total cTnT, long cTnT and long/total cTnT ratio to differentiate between ESRD and NSTEMI patient cohorts whose samples were taken withing the first 24h after the onset of symptoms. Republished from the original publication II with permission from Wolters Kluwer Health, Inc.

The ability of long/total cTnT ratio to discriminate between ESRD and NSTEMI patients was assessed using ROC curve analyses. When all NSTEMI patients were included, AUC of 0.906 (CI95% 0.837–0.975) was achieved, with an optimal cut-off point of 0.105 and sensitivity of 84.4% and specificity of 86.8%. The power of long/total cTnT ratio to discriminate between ESRD and NSTEMI was increased when the analysis focused on NSTEMI patients whose samples were taken within the first 24h after the onset of MI. In this case, AUC of 0.955; (CI95% 0.899–1.0; Figure 18) was obtained, with an optimal cut-off point of 0.145 and excellent sensitivity (91.3%) and specificity (94.7%). By comparison, the total cTnT only achieved AUC of 0.688 (CI95% 0.575–0.800) when all NSTEMI patients were included and 0.609 (CI95% 0.454–0.764) when including only those who had their samples taken within the first 24h of MI.

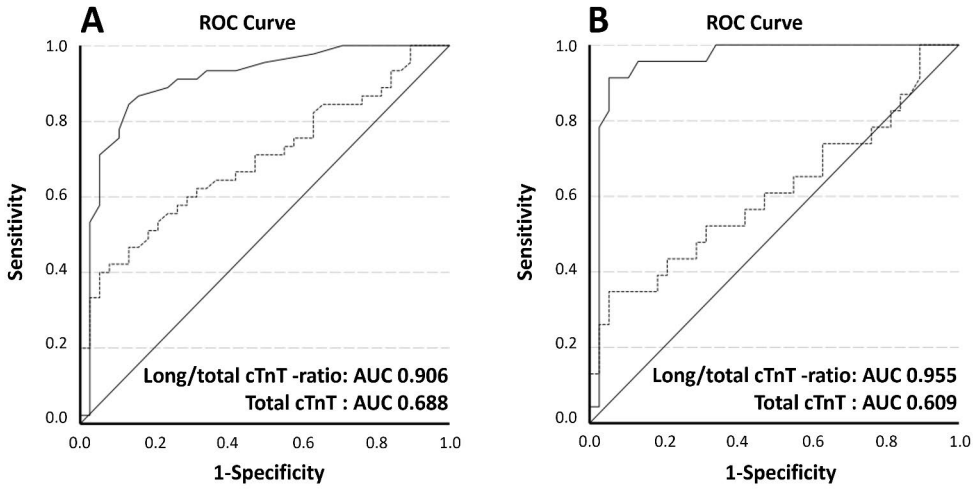

Figure 18. ROC curves depicting the ability of long/total cTnT ratio (solid) and total cTnT (dotted) to discriminate between ESRD and NSTEMI. A). All NSTEMI patients. B). NSTEMI patients whose samples were taken within first 24h of MI. Original picture made by Tapio Hellman.

In study II, the diagnostic potential of the first developed long cTnT immunoassay was successfully evaluated. For the first time ever, it was shown that specific forms of cTnT (long cTnT) can be measured to differentiate between cTnT elevations seen in ESRD and NSTEMI patients.[7,8,288] Non-MI related chronic cTn elevations often encountered in emergency departments, pose a diagnostic challenge, especially in relation to NSTEMI, thus requiring the use of algorithms that rely on serial measurements of cTn over a period of 1–3h.[6,308,309] By measuring and utilizing both long cTnT and long/total cTnT ratio, a major diagnostic improvement might be achieved due to improved diagnostic specificity for MI.

The long cTnT assay, and especially the long/total cTnT ratio, showed excellent diagnostic performance in separating between ESRD and NSTEMI patient cohorts. The performance of long/cTnT ratio exceeded that of total cTnT analysed by the Roche Elecsys hs-cTnT assay, regardless of the time frame between sampling and the onset of MI symptoms. However, as the release of cTnT continues for as long as myocardial damage progresses, and the intact or almost intact cTnT forms are degraded during circulation, the long/cTnT ratio shows optimal performance when utilized during the critical early hours after the onset of MI, as presented in Figure 18.[192,201]

In this study, the temporal cut-off value of 24h was arbitrarily chosen, when assessing the diagnostic performance of long/total cTnT ratio. However, according studies by Ritzmann *et al*. and Nilsson *et al*., a median total pre-hospital delay among MI patients was 3.1h and 5.1h respectively.[310,311] Therefore, in future studies the optimal timeframe of long/total cTnT ratio should be determined statistically with larger MI patient cohorts. Another factor to consider when using the long/cTnT ratio is the absolute value of total cTnT. If the absolute concentration of total cTnT is low, minor absolute change can cause large variation in ratio, thus in low absolute concentrations, the use of absolute long cTnT values might be preferred. However, more sensitive cTnT assays measuring intact forms of cTnT have been recently developed.[289,298] These assays may offer lower limits at which to utilize long/total cTnT ratio effectively.

5.2.3 Effect of Hemodialysis on cTnT

Hemodialysis had minor effect on the circulating total cTnT concentration (76 [51–124] ng/L vs 58 [40–89] ng/L; $p<0.001$). Whereas no significant effect on circulating long cTnT concentration was detected. Similarly, only a minor increase in long/total cTnT ratio (0.04 vs 0.06, $p=0.002$) was observed due to the change in total cTnT concentration.

These results indicate that long cTnT assay can be utilized both before and after hemodialysis, and that the use of samples collected before hemodialysis does not cause any major bias when evaluating the clinical potential of long cTnT or long/total cTnT ratio.

5.2.4 Future Consideration Regarding Long cTnT Research

Immunoassay interference among some individuals is almost unavoidable in routine analytics. However, every measure must be taken to avoid such factors that may cause incorrect results and harm to the patient. In study II, one ESRD, two NSTEMI and one STEMI samples had long/total cTnT ratio higher than 1.5, thus indicating

that these samples might be affected by possible interference that may affect either long cTnT assay or Roche Elecsys hs-cTnT assay. To degrease possible interference, the utilization of different antibody constructs, such as the use of Fabs or F(ab`)$_2$ fragments, should be considered.[293] Moreover, as antibody 7E7 is known to experience interference with some individuals due to autoantibodies targeting the epitope of 7E7, further capture epitope options should also be evaluated to avoid possible negative assay interference.[292,298]

In study I and II, most of the STEMI and NSTEMI patient samples were acquired after the patients had received LMWH (n=103), heparin (n=6) or both (n=2). Therefore, the effect of these anticoagulants should be investigated. Although LMWH has a relatively low inhibitory effect on thrombin, unfractionated heparin might efficiently form thrombin-heparin-antithrombin complex and thus inhibit thrombin activity and slow down thrombin mediated degradation of intact cTnT.[299,300,312]

Since the development of the first long cTnT assay presented in this thesis, a more sensitive assay using the 7E7-1C11cc antibody combination and upconverting nanoparticles has been developed.[289] This represents an important advancement for further studies regarding long cTnT and its potential application in clinical use. However, before long cTnT or long/total cTnT ratio can be accepted into diagnostic use, extensive validation of long cTnT is required. Further studies should include patient groups with different conditions associated with elevated cTn concentration.[313,314] Preferably, these studies should be conducted with the same heterogeneous patient population as encountered in emergency departments.[315] Moreover, thorough analysis must be conducted to establish diagnostic cut-offs and carefully consider what are the appropriate diagnostic protocols when incorporating long cTnT alongside total cTnT. In addition, it would be advantageous if long cTnT and total cTnT were analysed on the same automated platform for improved workflow and analytical consistency.

5.3 Europium Chelate Synthesis

Three new europium(III) chelates (compounds 6, 13 and 19) were successfully synthesized. The new Eu(III) chelate labels presented good to excellent fluorescence characteristics and succeeded in enabling the efficient use of high-power LED excitation. All relevant MALDI-TOF, HRMS, ^{1}H and ^{13}C NMR spectra and their interpretations for compounds (6) and (13) and/or their intermediates are presented in the supplementary of manuscript I. In addition, all available structural data of compound (19) and its intermediates are presented in the supplementary I of this thesis (Figures A1–A17). Structures of compounds (6, 13 and 19) are presented in Figure 19.

- Compound (6):
  2,2'-(((6-(((2-(bis(carboxylatomethyl)amino)ethyl)(carboxylatemethyl)-amino)methyl)-4-((5-((4-isothiocyanatobenzyl)-amino)pyrazin-2-yl)-ethynyl)pyridin-2-yl)methyl)azanediyl)diacetate europium(III)
- Compound (13):
  2,2'-(((6-(((2-(bis(carboxylatomethyl)amino)ethyl)(carboxylatemethyl)-amino)methyl)-4-((5-((4-isothiocyanatobenzyl)amino)-6-methoxypyra-zin-2-yl)ethynyl)pyridine-2-yl)methyl)azanediyl)diacetate europium(III)
- Compound (19):
  2,2'-(((4-((5-amino-6-((4-isothiocyanatobenzyl)carbamoyl)pyrazin-2-yl)-ethynyl)-6-(((2-(bis(carboxylatemethyl)amino)ethyl)(carboxylatemethyl)-amino)methyl)pyridin-2-yl)-methyl)azanediyl)diacetate europium(III)

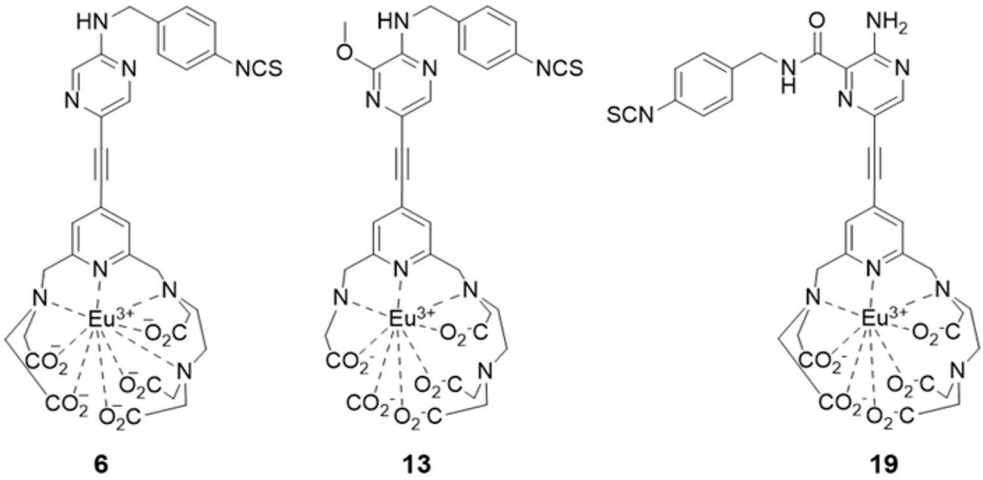

Figure 19. From left to right the structures of compound (6), (13) and (19).

5.3.1 Characterization of Luminescence Properties

All characterized compounds were studied for their luminescence properties as lysine conjugates. Characterization results are summarized in Table 9.

Characterization of the luminescence propoerties of compound (6)

Compound (6) exhibited excellent luminescence properties at both 340 nm and 360 nm excitation wavelengths. At the excitation wavelength of 360 nm, the label presented more than 10-fold increase in molar absorption when compared to the reference chelate Eu-d9 and higher relative quantum yield (11 vs. 7%). The label also had almost comparable characteristics at 340 nm excitation wavelength. However, only 2% higher brightness was achieved with compound (6) at 340 nm as the reference chelate expressed 20% higher molar absorption than compound (6) at this wavelength. At RT, the photoluminescence decay time (τ 0.98 ms) was comparable with the reference chelate (τ 1.05 ms), however the fluorescence signal decay profile presented high temperature dependence.

Characterization of the luminescence propoerties of compound (13)

Compound (13) expressed higher brightness at 360 nm excitation wavelength than the reference chelate (3000 vs 400 M^{-1} cm^{-1}). However, the reference chelate showed higher brightness at 340 nm, slightly higher relative quantum yield and noticeably longer photoluminescence decay times across temperature range of +20 °C to +60 °C. Similarly to compound (6), photoluminescence decay presented high temperature dependence with bi-exponential decay.

Characterization of the luminescence propoerties of compound (19)

Compound (19) exhibited the longest photoluminescence decay time at RT among the newly developed labels. However, at higher temperatures the photoluminescence decay time decreased markedly, as was the case with compounds (6) and (13), although to a lesser extent. The fluorescence decay profile of compound (19) is shown in Figure 20 and presented numerically in Table 9. Due to technical difficulties and Covid-19 shutdown, reliable absorbance measurement could not be obtained. Thus, molar absorptivity, relative quantum yield and brightness could not be determined. The fluorescence excitation spectrum is presented in Figure 21, with a maximum at 325 nm.

Table 9. Luminescence properties of glycine conjugated europium(III) chelates in TSA buffer.

	Comp. 6	Comp. 13		Comp. 19	Ref. chelate Eu-d9
λabs max (nm)	361	360		-	320
λex max (nm)	361	362		325	323
τ (ms) at 6°C	1.12 R^2= 0,9997	not measured		not measured	not measured
τ (ms) at 20°C	0.98 R^2= 0,999	τ1: 0.51 R^2= 0,998	τ2: 0.83 R^2= 0,996	1.04 R^2= 0,999	1.05 R^2= 0,999
τ (ms) at 40°C	0.64 R^2= 0,999	τ1: 0.36 R^2= 0,992	τ2: 0.59 R^2= 0,999	0.80 R^2= 1.000	1.00 R^2= 0,999
τ (ms) at 60°C	0.35 R^2= 0,999	τ1: 0.21 R^2= 0,974	τ2: 0.37 R^2= 0,998	0.55 R^2= 0,999	0.95 R^2= 0,999
ε (M^{-1} cm^{-1}) at 360 nm	42400	43000		-	4600
ε (M^{-1} cm^{-1}) at abs max	42500	43000		-	51000
Φ (%)	11[a]	7[a]		-	9[b]
εΦ (M^{-1} cm^{-1}) 360 nm	4700	3000		-	400
εΦ (M^{-1} cm^{-1}) abs max	4700	3000		-	4600

Table abbreviations: Absorption max (λabs), excitation max (λex), photoluminescence decay time (τ), molar absorption coefficient (ε), brightness (εΦ) and quantum yield (Φ). [a] relative Φ at 20 °C. [b] Sund *et al.*[273]

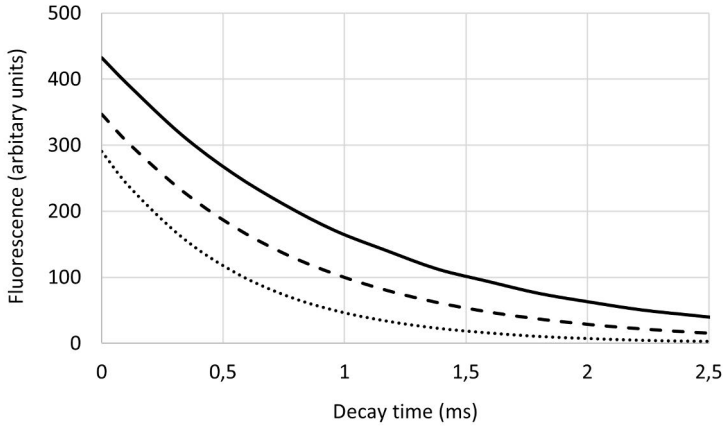

Figure 20. Fluorescence signal decay profile of glycine conjugated compound (19) at 20 °C (solid), 40 °C (long dash) and 60 °C (dot).

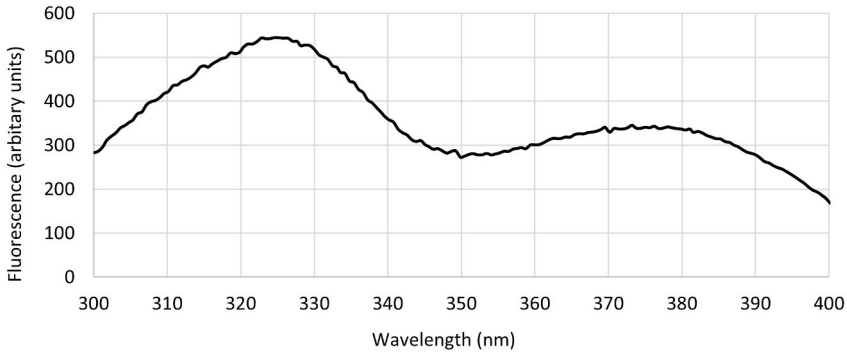

Figure 21. Fluorescence excitation spectrum of glycine conjugated compound (19). λem. 615 nm, time window 0.1–0.2 ms, ex. slit 5 nm, em. slit 10 nm. Matrix: TSA buffer. At 20 °C.

Based on the characterized luminescence properties, the newly synthesized labels (6) and (13) offered improved label brightness at 360 nm and equal or slightly lower brightness at 340 nm when compared to Eu-d9. The exceptional performance of these newly developed labels at 360 nm excitation, may enable the use of high-power LED excitation. The use of LED excitation sources could offer a cost-effective means for small measurement systems with improved excitation efficiency compared to conventional mercury arc lamps used in analytical instruments.[316] High-power LEDs with multi-watt output power tend to exist in wavelengths of 360 nm and above.[317] Therefore, these newly developed compounds could open interesting possibilities regarding the utilization of LED excitation sources.

The novel labels exhibited high temperature dependence affecting their photoluminescence decay times. This might be due to compounds (6), (13) and (19) having a low energy charge transfer state to which the energy can backflow from the excited triple state of the europium. In some applications this could cause issues as lower signal output is reached at higher temperatures and if the temperature varies between calibration and the measurement. However, this property could also be exploited in other applications, such as matrix embedded temperature sensors.[318,319] Compound (6) exhibited 17 µs/K change in photoluminescence decay times between +20 °C and +40 °C and 3.2-fold decrease when the temperature was increased from +6 °C to +60 °C. In comparison, in a previous study the most prominent europium and terbium compounds achieved 9.2 to 13.8 µs/K sensitivity.[320] Similarly in another study, several β-diketonate complexes achieve only around 2.6–2.7 decrease in luminescence decay times with larger temperature rise (+1 °C to +60 °C).[321] In addition, the use of multidente ligand, such as those synthesised in this thesis, usually produces more stable compounds against different environmental conditions.[9]

Overall, compound (6) had superior luminescence characteristics when compared to the reference chelate. The addition of methoxy group into the label

chromophore design of compound (6) caused compound (13) to have lower relative quantum yield and faster biphasic fluorescence signal decay, which resulted in lower label brightness compared to compound (6). Compound (19) exhibited excellent fluorescence lifetimes, but due to missing data, the label performance can only be estimated based on its results in cTnI immunoassay.

5.3.2 Performance of Synthesized Labels in cTnI Assay

Compounds (6) and (13) outperformed the reference chelate Eu-d9 in cTnI immunoassay both at 340 nm and 365 nm excitation wavelengths by achieving lower LoD estimates as presented in Table 10. Compound (19) was slightly inferior at 340 nm, but clearly outperformed the reference chelate at 365 nm.

Table 10. Estimated LoDs (ng/L) of cTnI assay with different labels and excitation wavelengths.

Excitation wavelength	Compound 6	Compound 13	Compound 19	Ref. chelate Eu-d9
340 nm	11.3	16.6	21.4	18.0
365 nm	11.8	18.0	27.0	122

The newly developed labels containing 2-(pyridin-4-ylethynyl)pyrazine chromophore offer new possibilities, especially when used in applications that utilize 365 nm excitation. However, it must be noted that factors such as labeling degree of the antibody and other batch-to-batch variations may cause slight shifts in the relative performance of the studied labels.

In immunoassay development, several aspects need to be considered when choosing the optimal label for a specific application. These factors include, but are not limited to, the luminescence characteristics dictated by the application platform, the performance and stability characteristics of the label under intended storage and application conditions, cost and ease of manufacture, end-product consistency and occupational safety during synthesis. Although many of these factors are outside the scope of this thesis, issues related to end-product consistency ultimately prevented compound (6) from being utilized in the long cTnT assay. New batch of compound (6) was synthesized and tested in combination with tracer mAb 329cc. This batch caused an increase in the immunoassay background signal, probably due to impurities in the synthesized end-product and was not therefore utilized.

6 Conclusions

Coronary artery disease and myocardial infarction are a major producer of DALYs (disability-adjusted life year), thus negatively affecting societies and the lives of many individuals and families.[2] Although strong emphasis should and is put to the prevention of CVDs, it is evident that not all cases of MI can be prevented.[322,323]

The extent of ischemic myocardial damage suffered during MI correlates with the outcome of the patient.[324] Fast intervention that restores blood flow to myocardial tissue is crucial in prevention of further damage. For proper treatment, correct diagnosis is needed. In case of STEMI, diagnosis is often straight forward based on ECG.[325] In case of NSTEMI, the correct diagnosis often relies on cTn measurements. Due to the fact that many non-MI conditions have chronically elevated cTn concentrations, diagnosis of MI must rely on algorithms that utilize repeated measurements, thus extending the time between the onset of MI and the treatment.[5,213,218] Therefore, it would be diagnostically highly advantageous if chronic cTnT elevations could be differentiated from acute cTnT elevations related to MI using a single, rapid measurement at presentation.

In this thesis, the first long cTnT immunoassay was successfully developed and evaluated according to CLSI guidelines. This assay measures only the intact or almost intact forms of cTnT (referred as long cTnT), whereas the Roche Elecsys hs-cTnT measures even the highly fragmented forms of cTnT. In this thesis, the clinical potential of long cTnT was evaluated and it was shown for the first time ever, that specific forms of cTnT (long cTnT) can differentiate between cTn elevations measured in chronic non-MI related conditions and acute cTnT elevations in NSTEMI. This work has already inspired further developments regarding intact forms of cTn and their possible future use in MI diagnostics.[242,289,298,315]

In addition, in this thesis three novel Eu(III)chelates with 2-(pyridin-4-ylethynyl)pyrazine chromophore were successfully synthesized and characterized for their luminescence properties. These novel chelates can be efficiently utilized as immunoassay labels at both 340 nm and 360 nm excitation wavelengths, thus enabling the use of high-power LED excitation sources, which can reduce instrument cost, decrease the need for analyzer maintenance and help in analyzer miniaturization.

The main conclusions based on the original publications are:

Study I: The first long cTnT assay that selectively targets intact and almost intact forms of cTnT was successfully developed and validated. The developed long cTnT immunoassay offers acceptable sensitivity and enables a fast and a convenient way to analyse long cTnT from LiH plasma. It is also demonstrated that long cTnT stability is not affected by freeze-thaw cycles and introducing the sample into assay buffer improves the stability of long cTnT. Elevated temperatures for prolonged periods affect the stability of long cTnT, thus fast analysis or freezing of samples after acquisition is recommended.

Study II: For the first time, it was demonstrated that an immunoassay measuring intact or almost intact cTnT (long cTnT) can differentiate between chronic cTnT elevations measured among ESRD patients and acute cTnT elevations related to type 1 MI (NSTEMI and STEMI); thus, offering substantial diagnostic improvement when compared to Roche Elecsys hs-cTnT assays. The capability of long cTnT assay to differentiate ESRD and NSTEMI patient cohorts was enhanced when utilized in combination with total cTnT as long/total cTnT ratio and especially during the first 24h hours after the onset of MI. Thus, antibody combinations targeting the cTnT cleavage area at aar 189–223, may improve the clinical specificity of cTnT immunoassays for MI.

Study III: Labels utilizing 2-(pyridin-4-ylethynyl)pyrazine chromophore can be efficiently excited at 360 nm, thus enabling the use of LED-light sources for excitation. These 2-(pyridin-4-ylethynyl)pyrazine Eu(III)chelate labels can also offer sensitivity improvement in applications such as immunoassays, even when utilized at conventional excitation wavelength of 340 nm. However, these labels may also be more susceptible to temperature changes and have low yielding CT -states, which could either enable their use as temperature sensors or lead to undesirable effects depending on the analytical application.

Acknowledgements

This research was carried out at the Department of Biotechnology at the University of Turku between 2018–2024 in collaboration with Turku University Hospital Heart Center. Financial support from Turku University Foundation, Finnish Society of Clinical Chemistry and Prof. Juhani Airaksinen are gratefully acknowledged.

I wish to thank Prof. Tero Soukka, Prof. Urpo Lamminmäki and Assoc. Prof. Saara Wittfooth for the opportunity to conduct my studies in the Department of Biotechnology, a globally renown academia.

To my supervisor Assoc. Prof. Saara Wittfooth I express my deepest gratitude. Without her encouragement, expertise and support, this journey would have not been possible. The most important aspect in supervisor is found in you, a kind spirit. Never did you tell me to bugger off, even though you had million other important things to do. You listened and answered to my silly questions with patience and understanding. I admire your passion and commitment for your work and I thank you for the time you invested to guide me.

I wish to present my special thanks to Teija Luotohaara and Docent Harri Takalo. Teija, you have been a saving grace more than ones, a person that I could turn to with all kind of practical problems, that would have otherwise ruined my day in the laboratory. Harri, without your guidance I would have not succeeded with the europium chelate synthesis. You had no obligation to me, but still due to the kindness of your heart you sacrificed your time to help me. Thank you.

This work would have not been possible without the contribution of my fellow researchers and co-authors. For this I wish to thank Akseli Lahtinen, Qi Wang, Jaana Rosenberg, Katriina Bamberg and Laura Koskimäki. I also want to thank Prof. Tero Soukka whos` knowledge beyond his own field of research I regard as extraordinary. I wish to extend my deepest gratitude to Prof. Juhani Airaksinen, MSc. Tuija Vasankari and PhD. Tapio Hellman for their collaboration and expertise in clinical research. Without their highly valued contribution, the work with long troponin would have not been possible.

During these years I had the privilege to meet people with diverse backgrounds and fields of research. It is not possible to mention you all here, but know this, I appreciate your input whatever it was; help, advise, answer, conversation or a simple

“hi” and smile. To mention a few: thank you Jari Vehmas and Jani Koskinen for keeping even the oldest equipment alive. Tuomas Karskela and Jani Rahkila for the help with the NMR and MS measurements. Anastasiia Kushnarova-Vakal for the conversations and special HPLC friendship. This list could go on and on, but I will end it with one collateral one. I would like to thank the Department of Clinical Chemistry at Tyks Laboratoriot and the wonderful people working there for providing me with a home for several years throughout the pandemic and this long PhD journey. You are the best <3 (and your friendship has meant a lot)

In my journey I would have not endured without the ones that matter the most.

My parents-in-law Sinikka and Timo, I am deeply grateful to you. Through every turn whenever needed you have shown unwavering support to our family and been superb grandparents to our little ones. Thank you.

Äidilleni ja Isälleni. Opetitte minua olemaan kiltti, kohtelias ja huomioimaan muita. Näytitte minulle esimerkkiä ahkeruudesta, rehellisyydestä ja sitkeydestä. Opetitte minulle lukuisia taitoja, jotka ovat kasvaneet ja kantaneet tähän päivään asti. Teitte aina kovasti töitä, eikä leipä tullut helpolla tai ollut aina leveä. Siitä huolimatta minulta ei koskaan puuttunut mitään. Olen saanut kokea lapsuuden ja nuoruuden, jollaista harvalla on mahdollisuus kokea; ajan, josta olen onnellinen ja Teille äärimmäisen kiitollinen. Kiitos. Rakastan Teitä.

Suvi, Ilari, Iisa and Iivo. When the path has been dark and full of despair, there has always been a guiding light that shines the way. Your smiles, your hugs. You are the most important thing in my life, my precious.

ps. Special thanks to Ilari for being my little lab assistant.

13.02.2026
Rami Aalto

List of References

[1] World Health Organization, *Fact Sheet - Cardiovascular diseases (CVDs)*. www.who.int/news-room/fact-sheets/detail/cardiovascular-diseases-(cvds) (accessed 2025-02-12).

[2] Vos, T., Lim, S. S., Abbafati, C., Abbas, K. M., Abbasi, M., Abbasifard, M., Abbasi-Kangevari, M., Abbastabar, H., Abd-Allah, F., Abdelalim, A., Abdollahi, M., Abdollahpour, I., Abolhassani, H., Aboyans, V., Abrams, E. M., et al., Global Burden of 369 Diseases and Injuries in 204 Countries and Territories, 1990–2019: A Systematic Analysis for the Global Burden of Disease Study 2019. *The Lancet* **2020**, *396* (10258), 1204–1222.

[3] Luengo-Fernandez, R., Walli-Attaei, M., Gray, A., Torbica, A., Maggioni, A., Huculeci, R., Bairami, F., Aboyans, V., Timmis, A., Vardas, P., Leal, J., Economic Burden of Cardiovascular Diseases in the European Union: A Population-Based Cost Study. *Eur. Heart J.* **2023**, *44* (45), 4752–4767.

[4] Birger, M., Kaldjian, A. S., Roth, G. A., Moran, A. E., Dieleman, J. L., Bellows, B. K., Spending on Cardiovascular Disease and Cardiovascular Risk Factors in the United States: 1996 to 2016. *Circulation* **2021**, *144* (4), 271–282.

[5] Thygesen, K., Alpert, J. S., Jaffe, A. S., Chaitman, B. R., Bax, J. J., Morrow, D. A., White, H. D., Infarction, T. E. G. on behalf of the J. E. S. of C. (ESC)/American C. of C. (ACC)/American H. A. (AHA)/World H. F. (WHF) T. F. for the U. D. of M., Fourth Universal Definition of Myocardial Infarction (2018). *Circulation* **2018**, *138* (20), e618–e651.

[6] Byrne, R. A., Rossello, X., Coughlan, J. J., Barbato, E., Berry, C., Chieffo, A., Claeys, M. J., Dan, G.-A., Dweck, M. R., Galbraith, M., Gilard, M., Hinterbuchner, L., Jankowska, E. A., Jüni, P., Kimura, T., et al., 2023 ESC Guidelines for the Management of Acute Coronary Syndromes: Developed by the Task Force on the Management of Acute Coronary Syndromes of the European Society of Cardiology (ESC). *Eur. Heart J.* **2023**, *44* (38), 3720–3826.

[7] Mingels, A. M. A., Cardinaels, E. P. M., Broers, N. J. H., Van Sleeuwen, A., Streng, A. S., Van Dieijen-Visser, M. P., Kooman, J. P., Bekers, O., Cardiac Troponin T: Smaller Molecules in Patients with End-Stage Renal Disease than after Onset of Acute Myocardial Infarction. *Clin. Chem.* **2017**, *63* (3), 683–690.

[8] Vylegzhanina, A. V., Kogan, A. E., Katrukha, I. A., Koshkina, E. V., Bereznikova, A. V., Filatov, V. L., Bloshchitsyna, M. N., Bogomolova, A. P., Katrukha, A. G., Full-Size and Partially Truncated Cardiac Troponin Complexes in the Blood of Patients with Acute Myocardial Infarction. *Clin. Chem.* **2019**, *65* (7), 882–892.

[9] Wang, Q., Nono, K. N., Syrjänpää, M., Charbonnière, L. J., Hovinen, J., Härmä, H., Stable and Highly Fluorescent Europium(III) Chelates for Time-Resolved Immunoassays. *Inorg. Chem.* **2013**, *52* (15), 8461–8466.

[10] Pernter, P., Pedrinolla, B., Gostner, P., Das Herz Des Mannes Aus Dem Eis. Ein Paleoradiologischer Fall. *RöFo* **2018**, *190* (1), 61–64.

[11] Allam, A. H., Thompson, R. C., Samuel Wann, L., Miyamoto, M. I., el-Halim Nur el-Din, A., Abd el-Maksoud, G., Al-Tohamy Soliman, M., Badr, I., Abd el-Rahman Amer, H., Linda Sutherland, M., Sutherland, J. D., Thomas, G. S., Atherosclerosis in Ancient Egyptian Mummies The Horus Study. *JACC Cardiovasc. Imaging* **2011**, *4* (4), 315–327.

[12] Wann, L. S., Narula, J., Blankstein, R., Thompson, R. C., Frohlich, B., Finch, C. E., Thomas, G. S., Atherosclerosis in 16th-Century Greenlandic Inuit Mummies. *JAMA Netw. Open* **2019**, *2* (12), E1918270.
[13] Slijkhuis, W., Mali, W., Appelman, Y., A Historical Perspective towards a Non-Invasive Treatment for Patients with Atherosclerosis. *Netherlands Heart Journal* **2009**, *17* (4), 140–144.
[14] Keele, K. D., Leonardo Da Vinci's Views on Arteriosclerosis. *Med. Hist.* **1973**, *17* (3), 304–308.
[15] Falloppio, G., *Lectiones de Partibus Similaribus Humani Corporis*, Theodorici Gerlachil: Norimberga, 1575.
[16] Fishbein, G. A., Fishbein, M. C., Arteriosclerosis: Rethinking the Current Classification. *Arch. Pathol. Lab. Med.* **2009**, *133* (8), 1309–1316.
[17] Ribatti, D., William Harvey and the Discovery of the Circulation of the Blood. *J. Angiogenes. Res.* **2009**, *1* (1), 3.
[18] Harvey, W., *Exercitatio Anatomica de Motu Cordis et Sanguinis in Animalibus* Sumptibus Guilielmi Fitzeri: Francofvrti, 1628.
[19] Lobstein, J. F., *Traité d'Anatomie Pathologique*, Levrault, F. G.: Paris, 1833, Vol. 2.
[20] André, É., Jean-Frédéric Lobstein: artériosclérose et ostéoporose. *Hist. Sci. Med.* **2018**, *52* (2), 197–208.
[21] Marchand F., Ueber Atherosclerosis. *Verhandlungen der Kongresse fuer Innere Medizin*. 1904.
[22] Rabson, S. M., Arteriosclerosis: Definitions. *Am. J. Clin. Pathol.* **1954**, *24* (4), 472–473.
[23] McMillan, G. C., Historical Review of Research on Atherosclerosis. In *Nutrition and Biotechnology in Heart Disease and Cancer*, Longenecker, J. B., Kritchevsky, D., Drezner, M. K., Eds., Springer US: Boston, MA, 1995, 1–6.
[24] Ghosh, S. K., Giovanni Battista Morgagni (1682–1771): Father of Pathologic Anatomy and Pioneer of Modern Medicine. *Anat. Sci. Int.* **2017**, *92* (3), 305–312.
[25] Morgagni, G., *De Sedibus, et Causis Morborum per Anatomen Indagatis Libri Quinque*, Ex Typographia Remondiniana: Venetiis, 1761.
[26] Jay, V., The Legacy of William Heberden. *Arch. Pathol. Lab. Med.* **2000**, *124* (12), 1750–1751.
[27] Proudfit, W. L., Views from the Past: John Fothergill and Angina Pectoris. *Br Heart J*. **1991**, 66 (4), 322-324.
[28] Parry, C. H., *An Inquiry into the Symptoms and Causes of the Syncope Anginosa, Commonly Called Angina Pectoris: Illustrated by Dissections*, Bath, Printed by R. Cruttwell and sold by Cadell and Davies: London, 1799.
[29] Hedley, F. O., Contributions of Edward Jenner to Modern Concepts of Heart Disease. *Am. J. Public Health* **1938**, *28*, 1165–1169.
[30] Evans, A., Views from the Past: Dr Black's Favourite Disease, *Br Heart J*. **1995**, 74 (6), 696-697.
[31] Black, S., *Clinical and Pathological Reports*, Newry, printed by Alexander Wilkinson, and sold by Longman, Hurst, Rees, Orme and Brown: London, 1819.
[32] Duncan, A. Sen., Duncan, A. Jun., *Annals of Medicine for the Year 1800*, Bell and Bradfute, and for G.G. and J. Robinson, London, by Adam Neill and Company: Edinburgh, 1801, Vol. 5.
[33] Morgan, A. D., Some Forms of Undiagnosed Coronary Disease in Nineteenth-Century England. *Med. Hist.* **1968**, *12* (4), 344–358.
[34] Williams, C. J. B., *The Pathology and Diagnosis of Diseases of the Chest*, 4th ed., Churchill: London, 1840.
[35] Quain, R., On Fatty Diseases of the Heart. *J. R. Soc. Med.* **1850**, *33* (190), 121–196.
[36] Mayerl, C., Lukasser, M., Sedivy, R., Niederegger, H., Seiler, R., Wick, G., Atherosclerosis Research from Past to Present - On the Track of Two Pathologists with Opposing Views, Carl von Rokitansky and Rudolf Virchow. *Virchows Archiv* **2006**, *449* (1), 96–103.
[37] Virchow, R., *Cellular Pathology*, 2nd ed., Chance, F., Ed., John Churchill: London, 1858.
[38] Bencard, E. J., *On the Cause of Thorvaldsen's Death*. The Thorvaldsens Museum Archives. https://arkivet.thorvaldsensmuseum.dk (accessed 2025-11-10).

[39] Cervellin, G., Lippi, G., Of MIs and Men—A Historical Perspective on the Diagnostics of Acute Myocardial Infarction. *Semin. Thromb. Hemost.* **2014**, *40* (05), 535–543.
[40] Herrick, J. B., Clinical Features of Sudden Obstruction of the Coronary Arteries. *JAMA* **1912**, 59 (23), 2015–2022.
[41] Cohneim, J., Schulthess-Rechberg, A., Ueber Die Folgen Der Kranzarterienverschliessung Für Das Herz. *Archiv f. pathol. Anat.* **1881**, *85*, 503–537.
[42] Waller, A. D., A Demonstration on Man of Electromotive Changes Accompanying the Heart's Beat. *J. Physiol.* **1887**, *8*, 229–233.
[43] Barold, S. S., Willem Einthoven and the Birth of Clinical Electrocardiography a Hundred Years Ago. *Card. Electrophysiol. Rev.* **2003**, *7* (1), 99–104.
[44] *Willem Einthoven - Biographical*. NobelPrize.org. Nobel Prize Outreach 2025. https://www.nobelprize.org/prizes/medicine/1924/einthoven/biographical/ (accessed 2025-02-12).
[45] Herrick, J. B., Thrombosis of the Coronary Arteries. *JAMA* **1919**, *72* (6), 387–390.
[46] Wilson, F. N., Kossmann, C. E., Burch, G. E., Goldberger, E., Graybiel, A., Hecht, H. H., Johnston, F. D., Lepeschkin, E., Myers, G. B., Recommendations for Standardization of Electrocardiographic and Vectorcardiographic Leads. *Circulation* **1954**, *10* (4), 564–573.
[47] Dessauer, F., A New Method of Instantaneous Radiography. *Archives of the Roentgen Ray* **1910**, *14* (8), 258–260.
[48] Dessauer, F., Apparat Zur Momentaufnahme Mit Roentgenstrahlen. DE254177C, 1909.
[49] *Werner Forssmann – Biographical*. NobelPrize.org. Nobel Prize Outreach 2026. https://www.nobelprize.org/prizes/medicine/1956/forssmann/biographical/ (accessed 2026-01-12).
[50] Ryan, T. J., The Coronary Angiogram and Its Seminal Contributions to Cardiovascular Medicine Over Five Decades. *Circulation* **2002**, *106* (6), 752–756.
[51] Richmond, C., Sir Godfrey Hounsfield. *BMJ* **2004**, *329* (7467), 687.
[52] Ritman, E. L., Cardiac Computed Tomography Imaging: A History and Some Future Possibilities. *Cardiol. Clin.* **2003**, *21* (4), 491–513.
[53] Blumgart, H. L., Yens, O. C., Studies on the Velocity of Blood Flow: I. The Method Utilized. *J Clin Invest* **1927**, *4*, 1–14.
[54] Blumgart, H. L., Weiss, S., Studies on the Velocity of Blood Flow IV. The Velocity of Blood Flow and Its Relation to Other Aspects of the Circulation m Patients with Arteriosclerosis and m Patients with Arterial Hypertension. *J Clin Invest* **1927**, *4*, 173–199.
[55] Zaret, B. L., William, S. H., Martin, N. D., Wells, H. P., Flamm, M. D., Noninvasive Regional Myocardial Perfusion with Radioactive Potassium. *New England Journal of Medicine* **1973**, *288* (16), 809–812.
[56] Zaret, B. L., Wackers, F. J. Th., *Nuclear Cardiac Imaging: Principles and Applications: 1. Nuclear Cardiology: History and Milestones*, 6th ed., Iskandrian, A. E., Hage, F. G., Eds., Oxford University Press, 2024.
[57] Nilsson, J., Westling, H., Ultrasound in Lund – Three World Premieres. *Clin. Physiol. Funct. Imaging* **2004**, *24* (3), 137–140.
[58] Edler, I., Hertz, C. H., The Use of Ultrasonic Reflectoscope for the Continuous Recording of the Movements of Heart Walls. *Kungl Fysiogr Sällskapets Förhandlingar* **1954**, *24* (3).
[59] LaDue, J. S., Wróblewski, F., Karmen, A., Serum Glutamic Oxaloacetic Transaminase Activity in Human Acute Transmural Myocardial Infarction. *Science (1979).* **1954**, *120* (3117), 497–499.
[60] Wróblewski, F., Ladue, J. S., Lactic Dehydrogenase Activity in Blood. *Proceedings of the Society for Experimental Biology and Medicine* **1955**, *90* (1), 210–213.
[61] Danese, E., Montagnana, M., An Historical Approach to the Diagnostic Biomarkers of Acute Coronary Syndrome. *Ann. Transl. Med.* **2016**, *4* (10).
[62] Dreyfus, J. Cl., Schapira, G., Resnais, J., Scebat, L., Serum Creatine Kinase in Diagnosis of Myocardial Infarction. *Revue Francaise d'Etudes Cliniques et Biologiques* **1960**, *5*, 386–387.

[63] Chan, D. W., Taylor, E., Frye, R., Blitzer, R. L., Immunoenzymetric Assay for Creatine Kinase MB with Subunit-Specific Monoclonal Antibodies Compared with an Immunochemical Method and Electrophoresis. *Clin. Chem.* **1985**, *31* (3), 465–469.

[64] Christenson, R. H., Newby, L. K., Ohman, E. M., Cardiac Markers in the Assessment of Acute Coronary Syndromes. *Md Med J* **1997**, (Suppl), 18–24.

[65] Stone, M. J., Willerson, J. T., Gomez-Sanchez, C. E., Waterman, M. R., Radioimmunoassay of Myoglobin in Human Serum. Results in Patients with Acute Myocardial Infarction. *J. Clin. Invest.* **1975**, *56* (5), 1334–1339.

[66] Ebashi, S., Kodama, A., A New Protein Factor Promoting Aggregation of Tropomyosin. *The Journal of Biochemistry* **1965**, *58* (1), 107–108.

[67] Greaser, M. L., Gergely, J., Reconstitution of Troponin Activity from Three Protein Components. *Journal of Biological Chemistry* **1971**, *246* (13), 4226–4233.

[68] Wilkinson, J. M., Troponin C from Rabbit Slow Skeletal and Cardiac Muscle Is the Product of a Single Gene. *Eur. J. Biochem.* **1980**, *103* (1), 179–188.

[69] Dhoot, G. K., Gell, P. G. H., Perry, S. V., The Localization of the Different Forms of Troponin I in Skeletal and Cardiac Muscle Cells. *Exp. Cell Res.* **1978**, *117* (2), 357–370.

[70] Dhoot, G. K., Frearson, N., Perry, S. V., Polymorphic Forms of Troponin T and Troponin C and Their Localization in Striated Muscle Cell Types. *Exp. Cell Res.* **1979**, *122* (2), 339–350.

[71] Wilkinson, J. M., Grand, R. J. A., Comparison of Amino Acid Sequence of Troponin I from Different Striated Muscles. *Nature* **1978**, *271* (5640), 31–35.

[72] Cummins, P., Auckland, M. L., *A New Cardiac Specific Radioimmunoassay for the Diagnosis of Myocardial Infarction and Evaluation of Cardiac Cell Injury*. Journal of Molecular and Cellular Cardiology. **1983**, 15(Suppl 1):129.

[73] Cummins, B., Auckland, M. L., Cummins, P., Cardiac-Specific Troponin-l Radioimmunoassay in the Diagnosis of Acute Myocardial Infarction. *Am. Heart J.* **1987**, *113* (6), 1333–1344.

[74] Katus, H. A., Remppis, A., Looser, S., Hallermeier, K., Scheffold, T., Kübler, W., Enzyme Linked Immuno Assay of Cardiac Troponin T for the Detection of Acute Myocardial Infarction in Patients. *J. Mol. Cell. Cardiol.* **1989**, *21* (12), 1349–1353.

[75] Katus, H. A., Looser, S., Hallermayer, K., Remppis, A., Scheffold, T., Borgya, A., Essig, U., Geuss, U., Development and In Vitro Characterization of a New Immunoassay of Cardiac Troponin T. *Clin. Chem.* **1992**, *38* (3), 386–393.

[76] Antman, E., Bassand, J. P., Klein, W., Ohman, M., Lopez Sendon, J. L., Rydén, L., Simoons, M., Tendera, M., Chaitman, B. R., Clemmensen, P., Falk, E., Fishbein, M. C., Galvani, M., Garson A., J., Grines, C., et al., Myocardial Infarction Redefined—a Consensus Document of The Joint European Society of Cardiology/American College of Cardiology Committee for the Redefinition of Myocardial Infarction: The Joint European Society of Cardiology/ American College of Cardiology Committee. *J. Am. Coll. Cardiol.* **2000**, *36* (3), 959–969.

[77] Mann, D. L., Zipes, D. P., Libby, P., Bonow, R. O., Atherosclerotic Cardiovascular Disease. In *Braunwald's Heart Disease E-Book: A Textbook of Cardiovascular Medicine*, Elsevier - Health Sciences Division: London, 2014.

[78] Windaus, A., Über Den Gehalt Normaler Und Atheromatöser Aorten an Cholesterin Und Cholesterinestern. *Biol. Chem.* **1910**, *67* (2), 174–176.

[79] Hansson, G. K., Atherosclerosis—An Immune Disease: The Anitschkov Lecture 2007. *Atherosclerosis* **2009**, *202* (1), 2–10.

[80] Steinberg, D., Thematic Review Series: The Pathogenesis of Atherosclerosis. An Interpretive History of the Cholesterol Controversy: Part I1. *J. Lipid Res.* **2004**, *45* (9), 1583–1593.

[81] Anitschkow, N. N., Chalatov, S. S., Über Experimentelle Cholesterinsteatose Und Ihre Bedeutung Für Die Entstehung Einiger Pathologischer Prozesse. *Zentralblatt für allgemeine Pathologie und pathologische Anatomie* **1913**, *24* (1), 1–9.

[82] Müller, C., Xanthomata, Hypercholesterolemia, Angina Pectoris. *Acta Med. Scand.* **1938**, *95* (89), 75–84.

[83] Goldstein, J. L., Brown, M. S., A Century of Cholesterol and Coronaries: From Plaques to Genes to Statins. *Cell*. Cell Press March 26, 2015, 161–172.
[84] Gofman, J. W., Lindgren, F. T., Elliott, H., Ultracentrifugal Studies of Lipoproteins of Human Serum. *Journal of biological chemistry.* **1949**, *179* (2), 973–979.
[85] Bolanle, I. O., de Liedekerke Beaufort, G. C., Weinberg, P. D., Transcytosis of LDL Across Arterial Endothelium: Mechanisms and Therapeutic Targets. *Arterioscler. Thromb. Vasc. Biol.* **2025**, *45* (4), 468–480.
[86] Gianazza, E., Zoanni, B., Mallia, A., Brioschi, M., Colombo, G. I., Banfi, C., Proteomic Studies on ApoB-Containing Lipoprotein in Cardiovascular Research: A Comprehensive Review. *Mass Spectrom. Rev.* **2023**, *42* (4), 1397–1423.
[87] Huang, L., Chambliss, K. L., Gao, X., Yuhanna, I. S., Behling-Kelly, E., Bergaya, S., Ahmed, M., Michaely, P., Luby-Phelps, K., Darehshouri, A., Xu, L., Fisher, E. A., Ge, W. P., Mineo, C., Shaul, P. W., SR-B1 Drives Endothelial Cell LDL Transcytosis via DOCK4 to Promote Atherosclerosis. *Nature* **2019**, *569* (7757), 565–569.
[88] Frank, P. G., Lee, H., Park, D. S., Tandon, N. N., Scherer, P. E., Lisanti, M. P., Genetic Ablation of Caveolin-1 Confers Protection Against Atherosclerosis. *Arterioscler. Thromb. Vasc. Biol.* **2004**, *24* (1), 98–105.
[89] Fernández-Hernando, C., Yu, J., Suárez, Y., Rahner, C., Dávalos, A., Lasunción, M. A., Sessa, W. C., Genetic Evidence Supporting a Critical Role of Endothelial Caveolin-1 during the Progression of Atherosclerosis. *Cell Metab.* **2009**, *10* (1), 48–54.
[90] Tao, B., Kraehling, J. R., Ghaffari, S., Ramirez, C. M., Lee, S., Fowler, J. W., Lee, W. L., Fernandez-Hernando, C., Eichmann, A., Sessa, W. C., BMP-9 and LDL Crosstalk Regulates ALK-1 Endocytosis and LDL Transcytosis in Endothelial Cells. *Journal of Biological Chemistry* **2020**, *295* (52), 18179–18188.
[91] Lee, S., Schleer, H., Park, H., Jang, E., Boyer, M., Tao, B., Gamez-Mendez, A., Singh, A., Folta-Stogniew, E., Zhang, X., Qin, L., Xiao, X., Xu, L., Zhang, J., Hu, X., et al., Genetic or Therapeutic Neutralization of ALK1 Reduces LDL Transcytosis and Atherosclerosis in Mice. *Nature Cardiovascular Research* **2023**, *2* (5), 438–448.
[92] Borén, J., Olin, K., Lee, I., Chait, A., Wight, T. N., Innerarity, T. L., Identification of the Principal Proteoglycan-Binding Site in LDL. A Single-Point Mutation in Apo-B100 Severely Affects Proteoglycan Interaction without Affecting LDL Receptor Binding. *J. Clin. Invest.* **1998**, *101* (12), 2658–2664.
[93] Flood, C., Gustafsson, M., Richardson, P. E., Harvey, S. C., Segrest, J. P., Borén, J., Identification of the Proteoglycan Binding Site in Apolipoprotein B48. *Journal of Biological Chemistry* **2002**, *277* (35), 32228–32233.
[94] Olin-Lewis, K., Krauss, R. M., La Belle, M., Blanche, P. J., Barrett, P. H. R., Wight, T. N., Chait, A., ApoC-III Content of ApoB-Containing Lipoproteins Is Associated with Binding to the Vascular Proteoglycan Biglycan. *J. Lipid Res.* **2002**, *43* (11), 1969–1977.
[95] Lundstam, U., Hurt-Camejo, E., Olsson, G., Sartipy, P., Camejo, G., Wiklund, O., Proteoglycans Contribution to Association of Lp(a) and LDL With Smooth Muscle Cell Extracellular Matrix. *Arterioscler. Thromb. Vasc. Biol.* **1999**, *19* (5), 1162–1167.
[96] Bancells, C., Benítez, S., Jauhiainen, M., Ordóñez-Llanos, J., Kovanen, P. T., Villegas, S., Sánchez-Quesada, J. L., Öörni, K., High Binding Affinity of Electronegative LDL to Human Aortic Proteoglycans Depends on Its Aggregation Level. *J. Lipid Res.* **2009**, *50* (3), 446–455.
[97] Camejo, G., Olofsson, S. O., Lopez, F., Carlsson, P., Bondjers, G., Identification of Apo B-100 Segments Mediating the Interaction of Low Density Lipoproteins with Arterial Proteoglycans. *Arteriosclerosis* **1988**, *8* (4), 368–377.
[98] Williams, K. J., Tabas, I., The Response-to-Retention Hypothesis of Early Atherogenesis. *Arteriosclerosis, Thrombosis, and Vascular Biology* **1995**, *15* (5), 551-561.

[99] Skålén, K., Gustafsson, M., Rydberg, E. K., Hultén, L. M., Wiklund, O., Innerarity, T. L., Borén, J., Subendothelial Retention of Atherogenic Lipoproteins in Early Atherosclerosis. *Nature* **2002**, *417* (6890), 750–754.

[100] Singh, N. K., Rao, G. N., Emerging Role of 12/15-Lipoxygenase (ALOX15) in Human Pathologies. *Prog. Lipid Res.* **2019**, *73*, 28–45.

[101] Sheehan, A. L., Carrell, S., Johnson, B., Stanic, B., Banfi, B., Miller Jr., F. J., Role for Nox1 NADPH Oxidase in Atherosclerosis. *Atherosclerosis* **2011**, *216* (2), 321–326.

[102] Förstermann, U., Xia, N., Li, H., Roles of Vascular Oxidative Stress and Nitric Oxide in the Pathogenesis of Atherosclerosis. *Circ. Res.* **2017**, *120* (4), 713–735.

[103] Ganji, M., Nardi, V., Prasad, M., Jordan, K. L., Bois, M. C., Franchi, F., Zhu, X. Y., Tang, H., Young, M. D., Lerman, L. O., Lerman, A., Carotid Plaques From Symptomatic Patients Are Characterized by Local Increase in Xanthine Oxidase Expression. *Stroke* **2021**, *52* (9), 2792–2801.

[104] Tangeten, C., Zouaoui Boudjeltia, K., Delporte, C., Van Antwerpen, P., Korpak, K., Unexpected Role of MPO-Oxidized LDLs in Atherosclerosis: In between Inflammation and Its Resolution. *Antioxidants* **2022**, *11* (5), 874.

[105] Nagy, E., Eaton, J. W., Jeney, V., Soares, M. P., Varga, Z., Galajda, Z., Szentmiklósi, J., Méhes, G., Csonka, T., Smith, A., Vercellotti, G. M., Balla, G., Balla, J., Red Cells, Hemoglobin, Heme, Iron, and Atherogenesis. *Arterioscler. Thromb. Vasc. Biol.* **2010**, *30* (7), 1347–1353.

[106] Ballinger, S. W., Patterson, C., Knight-Lozano, C. A., Burow, D. L., Conklin, C. A., Hu, Z., Reuf, J., Horaist, C., Lebovitz, R., Hunter, G. C., McIntyre, K., Runge, M. S., Mitochondrial Integrity and Function in Atherogenesis. *Circulation* **2002**, *106* (5), 544–549.

[107] Alanne-Kinnunen, M., Lappalainen, J., Öörni, K., Kovanen, P. T., Activated Human Mast Cells Induce LOX-1-Specific Scavenger Receptor Expression in Human Monocyte-Derived Macrophages. *PLoS One* **2014**, *9* (9), e108352-.

[108] Nozaki, S., Kashiwagi, H., Yamashita, S., Nakagawa, T., Kostner, B., Tomiyama, Y., Nakata, A., Ishigami, M., Miyagawa, J., Kameda-Takemura, K., Reduced Uptake of Oxidized Low Density Lipoproteins in Monocyte-Derived Macrophages from CD36-Deficient Subjects. *J. Clin. Invest.* **1995**, *96* (4), 1859–1865.

[109] Shao, B., Tang, C., Sinha, A., Mayer, P. S., Davenport, G. D., Brot, N., Oda, M. N., Zhao, X. Q., Heinecke, J. W., Humans with Atherosclerosis Have Impaired ABCA1 Cholesterol Efflux and Enhanced High-Density Lipoprotein Oxidation by Myeloperoxidase. *Circ. Res.* **2014**, *114* (11), 1733–1742.

[110] Thuahnai, S. T., Lund-Katz, S., Dhanasekaran, P., de la Llera-Moya, M., Connelly, M. A., Williams, D. L., Rothblat, G. H., Phillips, M. C., Scavenger Receptor Class B Type I-Mediated Cholesteryl Ester-Selective Uptake and Efflux of Unesterified Cholesterol: Influence of High Density Lipoprotein Size and Structure *. *Journal of Biological Chemistry* **2004**, *279* (13), 12448–12455.

[111] Shen, W.-J., Azhar, S., Kraemer, F. B., SR-B1: A Unique Multifunctional Receptor for Cholesterol Influx and Efflux. **2025**, *39*, 45.

[112] Chistiakov, D. A., Bobryshev, Y. V, Orekhov, A. N., Macrophage-Mediated Cholesterol Handling in Atherosclerosis. *J. Cell. Mol. Med.* **2016**, *20* (1), 17–28.

[113] Tabas, I., Free Cholesterol-Induced Cytotoxicity: A Possible Contributing Factor to Macrophage Foam Cell Necrosis in Advanced Atherosclerotic Lesions. *Trends Cardiovasc. Med.* **1997**, *7* (7), 256–263.

[114] Yin, Y.-W., Liao, S.-Q., Zhang, M.-J., Liu, Y., Li, B.-H., Zhou, Y., Chen, L., Gao, C.-Y., Li, J.-C., Zhang, L.-L., TLR4-Mediated Inflammation Promotes Foam Cell Formation of Vascular Smooth Muscle Cell by Upregulating ACAT1 Expression. *Cell Death Dis.* **2014**, *5* (12), e1574–e1574.

[115] Dove, D. E., Su, Y. R., Zhang, W., Jerome, W. G., Swift, L. L., Linton, M. F., Fazio, S., ACAT1 Deficiency Disrupts Cholesterol Efflux and Alters Cellular Morphology in Macrophages. *Arterioscler. Thromb. Vasc. Biol.* **2005**, *25* (1), 128–134.

[116] Bowden, K. L., Dubland, J. A., Chan, T., Xu, Y.-H., Grabowski, G. A., Du, H., Francis, G. A., LAL (Lysosomal Acid Lipase) Promotes Reverse Cholesterol Transport In Vitro and In Vivo. *Arterioscler. Thromb. Vasc. Biol.* **2018**, *38* (5), 1191–1201.

[117] Dubland, J. A., Allahverdian, S., Besler, K. J., Ortega, C., Wang, Y., Pryma, C. S., Boukais, K., Chan, T., Seidman, M. A., Francis, G. A., Low LAL (Lysosomal Acid Lipase) Expression by Smooth Muscle Cells Relative to Macrophages as a Mechanism for Arterial Foam Cell Formation. *Arterioscler. Thromb. Vasc. Biol.* **2021**, *41* (6), e354–e368.

[118] Sekiya, M., Osuga, J., Nagashima, S., Ohshiro, T., Igarashi, M., Okazaki, H., Takahashi, M., Tazoe, F., Wada, T., Ohta, K., Takanashi, M., Kumagai, M., Nishi, M., Takase, S., Yahagi, N., et al., Ablation of Neutral Cholesterol Ester Hydrolase 1 Accelerates Atherosclerosis. *Cell Metab.* **2009**, *10* (3), 219–228.

[119] Igarashi, M., Osuga, J., Uozaki, H., Sekiya, M., Nagashima, S., Takahashi, M., Takase, S., Takanashi, M., Li, Y., Ohta, K., Kumagai, M., Nishi, M., Hosokawa, M., Fledelius, C., Jacobsen, P., et al., The Critical Role of Neutral Cholesterol Ester Hydrolase 1 in Cholesterol Removal From Human Macrophages. *Circ. Res.* **2010**, *107* (11), 1387–1395.

[120] Wang, X., Collins, H. L., Ranalletta, M., Fuki, I. V, Billheimer, J. T., Rothblat, G. H., Tall, A. R., Rader, D. J., Macrophage ABCA1 and ABCG1, but Not SR-BI, Promote Macrophage Reverse Cholesterol Transport in Vivo. *J. Clin. Invest.* **2007**, *117* (8), 2216–2224.

[121] Tracy, R. E., Newman, W. P., Wattigney, W. A., Berenson, G. S., Risk Factors and Atherosclerosis in Youth Autopsy Findings of the Bogalusa Heart Study. *Am. J. Med. Sci.* **1995**, *310*, S37–S41.

[122] Strong, J. P., Malcom, G. T., Newman III, W. P., Oalmann, M. C., Early Lesions of Atherosclerosis in Childhood and Youth: Natural History and Risk Factors. *J. Am. Coll. Nutr.* **1992**, *11* (sup1), 51S-54S.

[123] Enos, W. F., Holmes, R. H., Beyer, J., Coronary Disease Among United States Soldiers Killed in Action in Korea: Preliminary Report. *J. Am. Med. Assoc.* **1953**, *152* (12), 1090–1093.

[124] McGill, H. C., Brown, B. W., Gore, I. R. A., McMillan, G. C., Paterson, J. C., Pollak, O. J., Roberts, J. C., Wissler, R. W., Report of Committee on Grading Lesions, Council on Arteriosclerosis, American Heart Association. *Circulation* **1968**, *37* (3), 455–459.

[125] Stary, H. C., Chandler, A. B., Glagov, S., Guyton, J. R., Insull, W., Rosenfeld, M. E., Schaffer, S. A., Schwartz, C. J., Wagner, W. D., Wissler, R. W., A Definition of Initial, Fatty Streak, and Intermediate Lesions of Atherosclerosis. A Report from the Committee on Vascular Lesions of the Council on Arteriosclerosis, American Heart Association. *Arterioscler. Thromb.* **1994**, *14* (5), 840–856.

[126] Stary, H. C., Chandler, A. B., Dinsmore, R. E., Fuster, V., Glagov, S., Insull, W., Rosenfeld, M. E., Schwartz, C. J., Wagner, W. D., Wissler, R. W., A Definition of Advanced Types of Atherosclerotic Lesions and a Histological Classification of Atherosclerosis. *Circulation* **1995**, *92* (5), 1355–1374.

[127] Stary, H. C., Natural History and Histological Classification of Atherosclerotic Lesions. *Arterioscler. Thromb. Vasc. Biol.* **2000**, *20* (5), 1177–1178.

[128] World Health Organization, Hypertension and Coronary Heart Disease: Classification and Criteria for Epidemiological Studies. *World Health Organ Tech Rep Ser.* **1959**, *58* (168), 1-28.

[129] Mendis, S., Thygesen, K., Kuulasmaa, K., Giampaoli, S., Mähönen, M., Ngu Blackett, K., Lisheng, L., infarction, W. group on behalf of the participating experts of the W. H. O. consultation for revision of W. H. O. definition of myocardial, World Health Organization Definition of Myocardial Infarction: 2008–09 Revision. *Int. J. Epidemiol.* **2011**, *40* (1), 139–146.

[130] Myocardial Infarction Redefined—A Consensus Document of The Joint European Society of Cardiology/American College of Cardiology Committee for the Redefinition of Myocardial Infarction. *Eur. Heart J.* **2000**, *21* (18), 1502–1513.
[131] Kraler, S., Mueller, C., Libby, P., Bhatt, D. L., Acute Coronary Syndromes: Mechanisms, Challenges, and New Opportunities. *Eur. Heart J.* **2025**, *46* (29), 2866–2889.
[132] Saaby, L., Poulsen, T. S., Hosbond, S., Larsen, T. B., Pyndt Diederichsen, A. C., Hallas, J., Thygesen, K., Mickley, H., Classification of Myocardial Infarction: Frequency and Features of Type 2 Myocardial Infarction. *Am. J. Med.* **2013**, *126* (9), 789–797.
[133] Rao, S. V, O'Donoghue, M. L., Ruel, M., Rab, T., Tamis-Holland, J. E., Alexander, J. H., Baber, U., Baker, H., Cohen, M. G., Cruz-Ruiz, M., Davis, L. L., de Lemos, J. A., DeWald, T. A., Elgendy, I. Y., Feldman, D. N., et al., 2025 ACC/AHA/ACEP/NAEMSP/SCAI Guideline for the Management of Patients With Acute Coronary Syndromes: A Report of the American College of Cardiology/American Heart Association Joint Committee on Clinical Practice Guidelines. *Circulation* **2025**, *151* (13), e771–e862.
[134] Suomalaisen Lääkäriseuran Duodecimin ja Suomen Kardiologisen Seuranasettama työryhmä, Sepelvaltimotautikohtaus. Käypä Hoito -Suositus. Suomalainen Lääkäriseura Duodecim: Helsinki 2022.
[135] Airaksinen, J., Aalto-Setälä, K., Hartikainen, J., Huikuri, H., Laine, M., Lommi, J., Raatikainen, P., Saraste, A., *Kardiologia*, 3rd ed., Duodecim, 2016.
[136] Kwok, C. S., Bennett, S., Holroyd, E., Satchithananda, D., Borovac, J. A., Will, M., Schwarz, K., Lip, G. Y. H., Characteristics and Outcomes of Patients with Acute Coronary Syndrome Who Present with Atypical Symptoms: A Systematic Review, Pooled Analysis and Meta-Analysis. *Coron. Artery Dis.* **2025**, *36* (3).
[137] Björck, L., Nielsen, S., Jernberg, T., Zverkova-Sandström, T., Giang, K. W., Rosengren, A., Absence of Chest Pain and Long-Term Mortality in Patients with Acute Myocardial Infarction. *Open Heart* **2018**, *5* (2), e000909.
[138] Canto, J. G., Shlipak, M. G., Rogers, W. J., Malmgren, J. A., Frederick, P. D., Lambrew, C. T., Ornato, J. P., Barron, H. V, Kiefe, C. I., Prevalence, Clinical Characteristics, and Mortality Among Patients With Myocardial Infarction Presenting Without Chest Pain. *JAMA* **2000**, *283* (24), 3223–3229.
[139] Schmitz, T., Harmel, E., Raake, P., Freuer, D., Kirchberger, I., Heier, M., Peters, A., Linseisen, J., Meisinger, C., Association Between Acute Myocardial Infarction Symptoms and Short- and Long-Term Mortality After the Event. *Canadian Journal of Cardiology* **2024**, *40* (7), 1355–1366.
[140] Nikus, K., Pahlm, O., Wagner, G., Birnbaum, Y., Cinca, J., Clemmensen, P., Eskola, M., Fiol, M., Goldwasser, D., Gorgels, A., Sclarovsky, S., Stern, S., Wellens, H., Zareba, W., de Luna, A. B., Electrocardiographic Classification of Acute Coronary Syndromes: A Review by a Committee of the International Society for Holter and Non-Invasive Electrocardiology. *J. Electrocardiol.* **2010**, *43* (2), 91–103.
[141] Verbeek, P. R., Ryan, D., Turner, L., Craig, A. M., Serial Prehospital 12-Lead Electrocardiograms Increase Identification of ST-Segment Elevation Myocardial Infarction. *Prehospital Emergency Care* **2012**, *16* (1), 109–114.
[142] Morris, F., Brady, W. J., ABC of Clinical Electrocardiography: Acute Myocardial Infarction—Part I. *BMJ* **2002**, *324* (7341), 831.
[143] Leivo, J., Anttonen, E., Jolly, S. S., Džavík, V., Koivumäki, J., Tahvanainen, M., Koivula, K., Nikus, K., Wang, J., Cairns, J. A., Niemelä, K., Eskola, M., The Prognostic Significance of Q Waves and T Wave Inversions in the ECG of Patients with STEMI: A Substudy of the TOTAL Trial. *J. Electrocardiol.* **2023**, *80*, 99–105.
[144] Chiang, C. H., Chiang, C. H., Pickering, J. W., Stoyanov, K. M., Chew, D. P., Neumann, J. T., Ojeda, F., Sörensen, N. A., Su, K. Y., Kavsak, P., Worster, A., Inoue, K., Johannessen, T. R., Atar, D., Amann, M., et al., Performance of the European Society of Cardiology 0/1-Hour, 0/2-

Hour, and 0/3-Hour Algorithms for Rapid Triage of Acute Myocardial Infarction An International Collaborative Meta-Analysis. *Ann. Intern. Med.* **2022**, *175* (1), 101–113.

[145] Wereski, R., Kimenai, D. M., Taggart, C., Doudesis, D., Lee, K. K., Lowry, M. T. H., Bularga, A., Lowe, D. J., Fujisawa, T., Apple, F. S., Collinson, P. O., Anand, A., Chapman, A. R., Mills, N. L., Cardiac Troponin Thresholds and Kinetics to Differentiate Myocardial Injury and Myocardial Infarction. *Circulation* **2021**, *144* (7), 528–538.

[146] Smyllie, J. H., Assmann, P. E., Sutherland, G. R., Fraser, A. G., Roelandt, J. R. T. C., The Role of Cardiac Ultrasound in the Diagnosis of the 'Surgical' Complications of Acute Myocardial Infarction. In *Ultrasound in Coronary Artery Disease: Present Role and Future Perspectives*, Iliceto, S., Rizzon, P., Roelandt, J. R. T. C., Eds., Springer Netherlands: Dordrecht, 1991, 183–196.

[147] Montalescot, G., Sechtem, U., Achenbach, S., Andreotti, F., Arden, C., Budaj, A., Bugiardini, R., Crea, F., Cuisset, T., Di Mario, C., Ferreira, J. R., Gersh, B. J., Gitt, A. K., Hulot, J.-S., Marx, N., et al., 2013 ESC Guidelines on the Management of Stable Coronary Artery Disease: The Task Force on the Management of Stable Coronary Artery Disease of the European Society of Cardiology. *Eur. Heart J.* **2013**, *34* (38), 2949–3003.

[148] Suomalaisen Lääkäriseuran Duodecimin ja Suomen Kardiologisen Seuran asettama työryhmä, Krooninen Sepelvaltimo-Oireyhtymä. Käypä Hoito -Suositus. Suomalainen Lääkäriseura Duodecim: Helsinki 2022.

[149] Falk, E., Shah, P. K., Fuster, V., Coronary Plaque Disruption. *Circulation* **1995**, *92* (3), 657–671.

[150] Marston, S. B., Redwood, C. S., Modulation of Thin Filament Activation by Breakdown or Isoform Switching of Thin Filament Proteins: Physiological and Pathological Implications. *Circulation Research*. **2003**, *93* (12), 1170–1178.

[151] Ohtsuki, I., Morimoto, S., Kitainda, V., *Encyclopedia of Biological Chemistry*, 3rd ed., Jez, J., Ed., Elsevir, 2021.

[152] Schreier, T., Kedes, L., Gahlmann, R., Cloning, Structural Analysis, and Expression of the Human Slow Twitch Skeletal Muscle/Cardiac Troponin C Gene. *Journal of Biological Chemistry* **1990**, *265* (34), 21247–21253.

[153] Marston, S., Zamora, J. E., Troponin Structure and Function: A View of Recent Progress. *J. Muscle Res. Cell Motil.* **2020**, *41* (1), 71–89.

[154] Rayani, K., Hantz, E. R., Haji-Ghassemi, O., Li, A. Y., Spuches, A. M., Van Petegem, F., Solaro, R. J., Lindert, S., Tibbits, G. F., The Effect of Mg2+ on Ca2+ Binding to Cardiac Troponin C in Hypertrophic Cardiomyopathy Associated TNNC1 Variants. *FEBS Journal* **2022**, *289* (23), 7446–7465.

[155] Rayani, K., Seffernick, J., Li, A. Y., Davis, J. P., Spuches, A. M., van Petegem, F., John Solaro, R., Lindert, S., Tibbits, G. F., Binding of Calcium and Magnesium to Human Cardiac Troponin C. *Journal of Biological Chemistry* **2021**, *296*.

[156] Bers, D. M., Calcium Fluxes Involved in Control of Cardiac Myocyte Contraction. *Circ. Res.* **2000**, *87*, 275–281.

[157] Wu, A. H. B., Release of Cardiac Troponin from Healthy and Damaged Myocardium. *Frontiers in Laboratory Medicine* **2017**, *1* (3), 144–150.

[158] Zhou, Z., Li, K.-L., Rieck, D., Ouyang, Y., Chandra, M., Dong, W.-J., Structural Dynamics of C-Domain of Cardiac Troponin I Protein in Reconstituted Thin Filament. *J Biol Chem* **2011**, *287* (10), 7661–7674.

[159] Giordano, S., Estes, R., Li, W., George, R., Gilford, T., Glasgow, K., Hallman, H., Josephat, F., Oliveira, A., Xavier, N., Chiasera, J. M., Troponin Structure and Function in Health and Disease. *Clin Lab Sci* **2018**, *31* (4), 192-199.

[160] Li, Y., Charles, P. Y. J., Nan, C., Pinto, J. R., Wang, Y., Liang, J., Wu, G., Tian, J., Feng, H. Z., Potter, J. D., Jin, J. P., Huang, X., Correcting Diastolic Dysfunction by Ca2+ Desensitizing Troponin in a Transgenic Mouse Model of Restrictive Cardiomyopathy. *J. Mol. Cell. Cardiol.* **2010**, *49* (3), 402–411.

[161] Stelzer, J. E., Patel, J. R., Walker, J. W., Moss, R. L., Differential Roles of Cardiac Myosin-Binding Protein C and Cardiac Troponin I in the Myofibrillar Force Responses to Protein Kinase A Phosphorylation. *Circ. Res.* **2007**, *101* (5), 503–511.

[162] Zhang, R., Zhao, J., Mandveno, A., Potter, J. D., Cardiac Troponin I Phosphorylation Increases the Rate of Cardiac Muscle Relaxation. *Circ. Res.* **1995**, *76* (6), 1028–1035.

[163] Zhang, J., Guy, M. J., Norman, H. S., Chen, Y.-C., Xu, Q., Dong, X., Guner, H., Wang, S., Kohmoto, T., Young, K. H., Moss, R. L., Ge, Y., Top-Down Quantitative Proteomics Identified Phosphorylation of Cardiac Troponin I as a Candidate Biomarker for Chronic Heart Failure. *J. Proteome Res.* **2011**, *10* (9), 4054–4065.

[164] Zhang, P., Kirk, J. A., Ji, W., dos Remedios, C. G., Kass, D. A., Van Eyk, J. E., Murphy, A. M., Multiple Reaction Monitoring to Identify Site-Specific Troponin I Phosphorylated Residues in the Failing Human Heart. *Circulation* **2012**, *126* (15), 1828–1837.

[165] Streng, A. S., de Boer, D., van der Velden, J., van Dieijen-Visser, M. P., Wodzig, W. K. W. H., Posttranslational Modifications of Cardiac Troponin T: An Overview. *J. Mol. Cell. Cardiol.* **2013**, *63*, 47–56.

[166] Bhavsar, P. K., Dhoot, G. K., Cumming, D. V. E., Butler-Browne, G. S., Yacoub, M. H., Barton, P. J. R., Developmental Expression of Troponin I Isoforms in Fetal Human Heart. *FEBS Lett.* **1991**, *292* (1–2), 5–8.

[167] Sheng, J. J., Jin, J. P., Gene Regulation, Alternative Splicing, and Posttranslational Modification of Troponin Subunits in Cardiac Development and Adaptation: A Focused Review. *Frontiers in Physiology*. **2014**, *5* (165).

[168] Wei, B., Jin, J. P., TNNT1, TNNT2, and TNNT3: Isoform Genes, Regulation, and Structure–Function Relationships. *Gene* **2016**, *582* (1), 1–13.

[169] *Human TNNT2 isoforms*. UniProt, P45379. https://www.uniprot.org/ (accessed 2025-04-29).

[170] Katrukha, I. A., Kogan, A. E., Vylegzhanina, A. V, Serebryakova, M. V, Koshkina, E. V, Bereznikova, A. V, Katrukha, A. G., Thrombin-Mediated Degradation of Human Cardiac Troponin T. *Clin. Chem.* **2017**, *63* (6), 1094–1100.

[171] Cardinaels, E. P. M., Mingels, A. M. A., Van Rooij, T., Collinson, P. O., Prinzen, F. W., Van Dieijen-Visser, M. P., Time-Dependent Degradation Pattern of Cardiac Troponin T Following Myocardial Infarction. *Clin. Chem.* **2013**, *59* (7), 1083–1090.

[172] Jin, J.-P., Chong, S. M., Localization of the Two Tropomyosin-Binding Sites of Troponin T. *Arch. Biochem. Biophys.* **2010**, *500* (2), 144–150.

[173] Zhang, J., Zhang, H., Ayaz-Guner, S., Chen, Y.-C., Dong, X., Xu, Q., Ge, Y., Phosphorylation, but Not Alternative Splicing or Proteolytic Degradation, Is Conserved in Human and Mouse Cardiac Troponin T. *Biochemistry* **2011**, *50* (27), 6081–6092.

[174] Anderson, P. A. W., Greig, A., Mark, T. M., Malouf, N. N., Oakeley, A. E., Ungerleider, R. M., Allen, P. D., Kay, B. K., Molecular Basis of Human Cardiac Troponin T Isoforms Expressed in the Developing, Adult, and Failing Heart. *Circ. Res.* **1995**, *76* (4), 681–686.

[175] Anderson, P. A., Malouf, N. N., Oakeley, A. E., Pagani, E. D., Allen, P. D., Troponin T Isoform Expression in Humans. A Comparison among Normal and Failing Adult Heart, Fetal Heart, and Adult and Fetal Skeletal Muscle. *Circ. Res.* **1991**, *69* (5), 1226–1233.

[176] Gomes, A. V., Venkatraman, G., Davis, J. P., Tikunova, S. B., Engel, P., Solaro, R. J., Potter, J. D., Cardiac Troponin T Isoforms Affect the Ca2+ Sensitivity of Force Development in the Presence of Slow Skeletal Troponin I: Insights into the Role of Troponin T Isoforms in the Fetal Heart. *Journal of Biological Chemistry* **2004**, *279* (48), 49579–49587.

[177] Du Fay De Lavallaz, J., Prepoudis, A., Wendebourg, M. J., Kesenheimer, E., Kyburz, D., Daikeler, T., Haaf, P., Wanschitz, J., Löscher, W. N., Schreiner, B., Katan, M., Jung, H. H., Maurer, B., Hammerer-Lercher, A., Mayr, A., et al., Skeletal Muscle Disorders: A Noncardiac Source of Cardiac Troponin T. *Circulation* **2022**, *145* (24), 1764–1779.

[178] Giordano, S., Estes, R., Li, W., George, R., Gilford, T., Glasgow, K., Hallman, H., Josephat, F., Oliveira, A., Xavier, N., Chiasera, J. M., Troponin Structure and Function in Health and Disease. *American Society for Clinical Laboratory Science* **2018**, *31* (4), 192–199.
[179] Marques, M. de A., de Oliveira, G. A. P., Cardiac Troponin and Tropomyosin: Structural and Cellular Perspectives to Unveil the Hypertrophic Cardiomyopathy Phenotype. *Front. Physiol.* **2016**, *7* (SEP), 222269.
[180] Jaffe, A. S., Another Unanswerable Question. *JACC Basic Transl. Sci.* **2017**, *2* (2), 115–117.
[181] Rudolph, F., Deutsch, M.-A., Friedrichs, K. P., Renner, A., Scholtz, W., Gerçek, M., Kirchner, J., Ayoub, M., Rudolph, T. K., Schramm, R., Gummert, J., Rudolph, V., Omran, H., Impact of Impaired Renal Function on Kinetics of High-Sensitive Cardiac Troponin Following Cardiac Surgery. *Clinical Research in Cardiology* **2025**.
[182] Henning, S., Evangelos, G., Simon, F., Constanze, M., Claus, J., A, K. H., Cardiac Troponin T at 96 Hours After Acute Myocardial Infarction Correlates With Infarct Size and Cardiac Function. *JACC* **2006**, *48* (11), 2192–2194.
[183] Diris, J. H. C., Hackeng, C. M., Kooman, J. P., Pinto, Y. M., Hermens, W. T., van Dieijen-Visser, M. P., Impaired Renal Clearance Explains Elevated Troponin T Fragments in Hemodialysis Patients. *Circulation* **2004**, *109* (1), 23–25.
[184] Katus, H. A., Remppis, A., Scheffold, T., Diederich, K. W., Kuebler, W., Intracellular Compartmentation of Cardiac Troponin T and Its Release Kinetics in Patients with Reperfused and Nonreperfused Myocardial Infarction. *Am. J. Cardiol.* **1991**, *67* (16), 1360–1367.
[185] Laugaudin, G., Kuster, N., Petiton, A., Leclercq, F., Gervasoni, R., Macia, J. C., Cung, T. T., Dupuy, A. M., Solecki, K., Lattuca, B., Cade, S., Cransac, F., Cristol, J. P., Roubille, F., Kinetics of High-Sensitivity Cardiac Troponin T and I Differ in Patients with ST-Segment Elevation Myocardial Infarction Treated by Primary Coronary Intervention. *Eur. Heart J. Acute Cardiovasc. Care* **2016**, *5* (4), 354–363.
[186] Bertinchant, J. P., Larue, C., Pernel, I., Ledermann, B., Fabbro-Peray, P., Beck, L., Calzolari, C., Trinquier, S., Nigond, J., Pau, B., Release Kinetics of Serum Cardiac Troponin i in Ischemic Myocardial Injury. *Clin. Biochem.* **1996**, *29* (6), 587–594.
[187] Kristensen, J. H., Koczulab, C. A. W., Frandsen, E. A., Hasselbalch, R. B., Strandkjær, N., Jørgensen, N. R., Østergaard, M., Møller-Sørensen, P. H., Nilsson, J. C., Afzal, S., Kamstrup, P. R., Dahl, M., Bor, M. V., Frikke-Schmidt, R., Jørgensen, N. R., et al., Kinetics of Cardiac Troponin and Other Biomarkers in Patients with ST Elevation Myocardial Infarction. *IJC Heart & Vasculature* **2023**, *48*, 101250.
[188] Mair, J., The Pathophysiology of Cardiac Troponin Release and the Various Circulating Cardiac Troponin Forms—Potential Clinical Implications. *J. Clin. Med.* **2025**, *14* (12), 4241.
[189] Adams, J. E., Abendschein, D. R., Jaffe, A. S., Biochemical Markers of Myocardial Injury: Is MB Creatine Kinase the Choice for the 1990s? *Circulation* **1993**, *88* (2), 750–763.
[190] Hammarsten, O., Mair, J., Möckel, M., Lindahl, B., Jaffe, A. S., Possible Mechanisms behind Cardiac Troponin Elevations. *Biomarkers* **2018**, *23* (8), 725–734.
[191] Salonen, S. M., Kristensen, J. H., Simonen, S., Hasselbalch, R. B., Strandkjær, N., Østergaard, M., Møller-Sørensen, H., Dahl, M., Bor, M. V., Frikke-Schmidt, R., Jørgensen, N. R., Rode, L., Holmvang, L., Kjærgaard, J., Bang, L. E., et al., Exploring the Role of Cardiac Troponin-Specific Autoantibodies: Prolonged Cardiac Troponin Elimination, Reduced Clearance, and Variable Interference across 5 Commercial Assays. *Clin. Chem.* **2025**, *71* (9), 970–979.
[192] Kristensen, J. H., Hasselbalch, R. B., Strandkjær, N., Jørgensen, N., Østergaard, M., Møller-Sørensen, P. H., Nilsson, J. C., Afzal, S., Kamstrup, P. R., Dahl, M., Bor, M. V., Frikke-Schmidt, R., Jørgensen, N. R., Rode, L., Holmvang, L., et al., Half-Life and Clearance of Cardiac Troponin I and Troponin T in Humans. *Circulation* **2024**, *150*, 1187–1198.
[193] IFCC, *High Sensitivity Cardiac Troponin I and T Assay Analytical Characteristics Designated by Manufacturer v062024*. Biomarkers Reference Tables. https://ifcc.org/ifcc-education-

division/emd-committees/committee-on-clinical-applications-of-cardiac-bio-markers-c-cb/biomarkers-reference-tables/ (accessed 2025-10-21).

[194] Hallermayer, K., Use of Recombinant Human Cardiac Troponin T for Standardization of Third Generation Troponin T Methods. *Scand J Clin Lab Invest* **1999**, *59* (Suppl230), 128–131.

[195] Jaffe, A. S., Vasile, V. C., Milone, M., Saenger, A. K., Olson, K. N., Apple, F. S., Diseased Skeletal Muscle: A Noncardiac Source of Increased Circulating Concentrations of Cardiac Troponin T. *J. Am. Coll. Cardiol.* **2011**, *58* (177), 1819–1824.

[196] Giannitsis, E., Mueller, C., Katus, H. A., Skeletal Myopathies as a Non-Cardiac Cause of Elevations of Cardiac Troponin Concentrations. *Diagnosis* **2019**, *6* (3), 189–201.

[197] Katrukha, A. G., Bereznikova, A. V, Esakova, T. V, Pettersson, K., Lövgren, T., Severina, M. E., Pulkki, K., Vuopio-Pulkki, L.-M., Gusev, N. B., Troponin I Is Released in Bloodstream of Patients with Acute Myocardial Infarction Not in Free Form but as Complex. *Clin. Chem.* **1997**, *43* (8), 1379–1385.

[198] Wu, A. H. B., Feng, Y.-J., Moore, R., Apple, F. S., McPherson, P. H., Buechler, K. F., Bodor, G., for, for the A. A., Standardization, C. C. S. on cTnI, Characterization of Cardiac Troponin Subunit Release into Serum after Acute Myocardial Infarction and Comparison of Assays for Troponin T and I. *Clin. Chem.* **1998**, *44* (6), 1198–1208.

[199] Katrukha, A. G., Bereznikova, A. V, Filatov, V. L., Esakova, T. V, Kolosova, O. V, Pettersson, K., Lövgren, T., Bulargina, T. V, Trifonov, I. R., Gratsiansky, N. A., Pulkki, K., Voipio-Pulkki, L.-M., Gusev, N. B., Degradation of Cardiac Troponin I: Implication for Reliable Immunodetection. *Clin. Chem.* **1998**, *44* (12), 2433–2440.

[200] Damen, S. A. J., Vroemen, W. H. M., Brouwer, M. A., Mezger, S. T. P., Suryapranata, H., van Royen, N., Bekers, O., Meex, S. J. R., Wodzig, W. K. W. H., Verheugt, F. W. A., de Boer, D., Cramer, G. E., Mingels, A. M. A., Multi-Site Coronary Vein Sampling Study on Cardiac Troponin T Degradation in Non–ST-Segment–Elevation Myocardial Infarction: Toward a More Specific Cardiac Troponin T Assay. *J. Am. Heart Assoc.* **2019**, *8* (14), e012602.

[201] Katrukha, I. A., Riabkova, N. S., Kogan, A. E., Vylegzhanina, A. V., Mukharyamova, K. S., Bogomolova, A. P., Zabolotskii, A. I., Koshkina, E. V., Bereznikova, A. V., Katrukha, A. G., Fragmentation of Human Cardiac Troponin T after Acute Myocardial Infarction. *Clinica Chimica Acta* **2023**, *542*.

[202] Denessen, E. J. S., Nass, S. I. J., Bekers, O., Vroemen, W. H. M., Mingels, A. M. A., Circulating Forms of Cardiac Troponin: A Review with Implications for Clinical Practice. *J. Lab. Precis. Med.* **2023**, *8*.

[203] Katrukha, I. A., Kogan, A. E., Vylegzhanina, A. V, Kharitonov, A. V, Tamm, N. N., Filatov, V. L., Bereznikova, A. V, Koshkina, E. V, Katrukha, A. G., Full-Size Cardiac Troponin I and Its Proteolytic Fragments in Blood of Patients with Acute Myocardial Infarction: Antibody Selection for Assay Development. *Clin. Chem.* **2018**, *64* (7), 1104–1112.

[204] Communal, C., Sumandea, M., de Tombe, P., Narula, J., Solaro, R. J., Hajjar, R. J., Functional Consequences of Caspase Activation in Cardiac Myocytes. *Proceedings of the National Academy of Sciences* **2002**, *99* (9), 6252–6256.

[205] Zhang, Z., Biesiadecki, B. J., Jin, J.-P., Selective Deletion of the NH2-Terminal Variable Region of Cardiac Troponin T in Ischemia Reperfusion by Myofibril-Associated μ-Calpain Cleavage. *Biochemistry* **2006**, *45* (38), 11681–11694.

[206] Streng, A. S., de Boer, D., van Doorn, W. P. T. M., Kocken, J. M. M., Bekers, O., Wodzig, W. K. W. H., Cardiac Troponin T Degradation in Serum Is Catalysed by Human Thrombin. *Biochem. Biophys. Res. Commun.* **2016**, *481* (1–2), 165–168.

[207] Vroemen, W. H. M., de Boer, D., Streng, A. S., Bekers, O., Wodzig, W. K. W. H., Thrombin Activation via Serum Preparation Is Not the Root Cause for Cardiac Troponin T Degradation. *Clin. Chem.* **2017**, *63* (11), 1768–1769.

[208] Vroemen, W. H. M., Denessen, E. J. S., van Doorn, W. P. T. M., Pelzer, K. E. J. M., Hackeng, T. M., Litjens, E. J. R., Henskens, Y. M. C., van der Sande, F. M., Wodzig, W. K. W. H., Kooman,

J. P., Bekers, O., de Boer, D., Mingels, A. M. A., Differences in Cardiac Troponin T Composition in Myocardial Infarction and End-Stage Renal Disease Patients: A Blood Tube Effect? *J. Appl. Lab. Med.* **2024**, *9* (5), 989–1000.

[209] Denessen, E. J. S., Vroemen, W. H. M., Litjens, E. J. R., Henskens, Y. M. C., van der Sande, F. M., Bekers, O., de Boer, D., Mingels, A. M. A., Cardiac Troponin T Degradation in End-Stage Renal Disease Patients Appears to Occur in Vivo. *J. Appl. Lab. Med.* **2023**, *8* (5), 1000–1002.

[210] Riabkova, N. S., Kogan, A. E., Katrukha, I. A., Vylegzhanina, A. V., Bogomolova, A. P., Alieva, A. K., Pevzner, D. V., Bereznikova, A. V., Katrukha, A. G., Influence of Anticoagulants on the Dissociation of Cardiac Troponin Complex in Blood Samples. *Int. J. Mol. Sci.* **2024**, *25* (16), 8919.

[211] Westermann, D., Neumann, J. T., Sörensen, N. A., Blankenberg, S., High-Sensitivity Assays for Troponin in Patients with Cardiac Disease. *Nat. Rev. Cardiol.* **2017**, *14* (8), 472–483.

[212] Roche Diagnostics, Elecsys Troponin T Hs Gen 6 [Package Insert, 09646922500V2.0]. *eLabDoc*. 2025.

[213] Badertscher, P., Boeddinghaus, J., Twerenbold, R., Nestelberger, T., Wildi, K., Wussler, D., Schwarz, J., Puelacher, C., Rubini Giménez, M., Kozhuharov, N., du Fay de Lavallaz, J., Cerminara, S. E., Potlukova, E., Rentsch, K., Miró, Ò., et al., Direct Comparison of the 0/1h and 0/3h Algorithms for Early Rule-Out of Acute Myocardial Infarction. *Circulation* **2018**, *137* (23), 2536–2538.

[214] Hammarsten, O., Warner, J. V, Lam, L., Kavsak, P., Lindahl, B., Aakre, K. M., Collinson, P., Jaffe, A. S., Saenger, A. K., Body, R., Mills, N. L., Omland, T., Ordonez-Llanos, J., Apple, F. S., Antibody-Mediated Interferences Affecting Cardiac Troponin Assays: Recommendations from the IFCC Committee on Clinical Applications of Cardiac Biomarkers. **2023**, *61* (8), 1411–1419.

[215] Schrapp, A., Fraissinet, F., Hervouet, C., Girot, H., Brunel, V., Biotin and High-Sensitivity Cardiac Troponin T Assay. *Biochem Med (Zagreb)* **2018**, *28* (3).

[216] IFCC, Cardiac Troponin Assay Interference Table Designated by Manufacturer: Hemolysis and Biotin V082025. *Biomarkers Reference Tables*.

[217] Wauthier, L., Plebani, M., Favresse, J., Interferences in Immunoassays: Review and Practical Algorithm. *Clin. Chem. Lab. Med.* **2022**, *60* (6), 808–820.

[218] Kelley, W. E., Januzzi, J. L., Christenson, R. H., Increases of Cardiac Troponin in Conditions Other than Acute Coronary Syndrome and Heart Failure. *Clin. Chem.* **2009**, *55* (12), 2098–2112.

[219] Knudsen, S. S., Hasselbalch, R. B., Strandkjaer, N., Hansen, M. H., Krag, T., Vissing, J., Hansen, H. P., Hougaard, A., Bundgaard H., Iversen, K. K., Cardiac Troponin Elevations across Non-Cardiac Diseases: A Comprehensive Analysis. *Eur. Heart J.* **2025**, *46* (Supplement_1), ehaf784.

[220] Tate, J. R., Bunk, D. M., Christenson, R. H., Barth, J. H., Katrukha, A., Noble, J. E., Schimmel, H., Wang, L., Panteghini, M., for the IFCC Working Group on Standardization of Cardiac Troponin I, Evaluation of Standardization Capability of Current Cardiac Troponin I Assays by a Correlation Study: Results of an IFCC Pilot Project. **2015**, *53* (5), 677–690.

[221] Christenson, R., Lowenthal, M., Newton, D., Phinney, K., Swart, C., A-004 Commutability Assessment for High-Sensitivity Cardiac Troponin I Reference Material 8121: A Human Plasma-Based Material Consisting of a Set of Four Relevant Hs-CTnI Concentrations. *Clin. Chem.* **2025**, *71* (Supplement_1), hvaf086.004.

[222] Radha, R., Shahzadi, S. K., Al-Sayah, M. H., Fluorescent Immunoassays for Detection and Quantification of Cardiac Troponin I: A Short Review. *Molecules* **2021**, *26* (16), 4812.

[223] Siemens Healthineers, Troponin I Ultra [Package Insert, 10995428_EN Rev. 02]. *Siemens Healthineers Document Library*. 2017.

[224] Balzer, A. H. A., Whitehurst, C. B., An Analysis of the Biotin–(Strept)Avidin System in Immunoassays: Interference and Mitigation Strategies. *Curr. Issues Mol. Biol.* **2023**, *45* (11), 8733–8754.

[225] Nascimento, E. D., de Almeida, S. V., dos Santos Araújo, S., da Silva, P. R. L., Santos, V. S., Faria, R. C., A Review of Magnetic Particles as Separation Tools in Electrochemical Detection of Biomarkers: Insights from COVID-19. *Anal. Chim. Acta* **2025**, *1372*, 344371.

[226] Apple, F. S., Sandoval, Y., Jaffe, A. S., Ordonez-Llanos, J., Cardiac Troponin Assays: Guide to Understanding Analytical Characteristics and Their Impact on Clinical Care. *Clin. Chem.* **2017**, *63* (1), 73–81.

[227] *Handbook of Immunoassay Technologies: Approaches, Performances, and Applications*, Vashist, S. K., Luong, J. H. t., Eds., Academic Press, 2018.

[228] Christenson, R. H., Frenk, L. D. S., de Graaf, H. J., van Domburg, T. S. Y., Wijnands, F. P. G., Foolen, H. W. J., Kemper, D. W. M., Bruinen, A. L., Meijering, B. D. M., Fonville, J. M., de Theije, F. K., Point-of-Care: Roadmap for Analytical Characterization and Validation of a High-Sensitivity Cardiac Troponin I Assay in Plasma and Whole Blood Matrices. *J. Appl. Lab. Med.* **2022**, *7* (4), 971–988.

[229] Apple, F. S., Jaffe, A. S., Collinson, P., Mockel, M., Ordonez-Llanos, J., Lindahl, B., Hollander, J., Plebani, M., Than, M., Chan, M. H. M., IFCC Educational Materials on Selected Analytical and Clinical Applications of High Sensitivity Cardiac Troponin Assays. *Clin. Biochem.* **2015**, *48* (4), 201–203.

[230] Wu, A. H. B., Christenson, R. H., Greene, D. N., Jaffe, A. S., Kavsak, P. A., Ordonez-Llanos, J., Apple, F. S., Clinical Laboratory Practice Recommendations for the Use of Cardiac Troponin in Acute Coronary Syndrome: Expert Opinion from the Academy of the American Association for Clinical Chemistry and the Task Force on Clinical Applications of Cardiac Bio-Markers of the International Federation of Clinical Chemistry and Laboratory Medicine. *Clin. Chem.* **2018**, *64* (4), 645–655.

[231] IFCC, Contemporary Cardiac Troponin I and T Assay Analytical Characteristics Designated by Manufacturer V082025. *Biomarkers Reference Tables*.

[232] IFCC, High-Sensitivity Cardiac Troponin I and T Assay Analytical Characteristics Designated by Manufacturer V092025. *Biomarkers Reference Tables*.

[233] Parwani, A. S., Boldt, L. H., Huemer, M., Wutzler, A., Blaschke, D., Rolf, S., Möckel, M., Haverkamp, W., Atrial Fibrillation-Induced Cardiac Troponin i Release. *Int. J. Cardiol.* **2013**, *168* (3), 2734–2737.

[234] Bond, M., Fagni, F., Moretti, M., Bello, F., Egan, A., Vaglio, A., Emmi, G., Dejaco, C., At the Heart of Eosinophilic Granulomatosis with Polyangiitis: Into Cardiac and Vascular Involvement. *Curr. Rheumatol. Rep.* **2022**, *24* (11), 337–351.

[235] Cyon, L., Kadesjö, E., Edgren, G., Roos, A., Acute Kidney Injury and High-Sensitivity Cardiac Troponin T Levels in the Emergency Department. *JAMA Netw. Open* **2024**, *7* (8), e2419602–e2419602.

[236] Kadoglou, N. P. E., Dimopoulou, A., Gkougkoudi, E., Parperis, K., Altered Arterial Stiffness, Ventricular–Arterial Coupling and Troponin Levels in Patients with Systemic Lupus Erythematosus. *Medicina 2024, Vol. 60, Page 821* **2024**, *60* (5), 821.

[237] Riley, E. D., Vittinghoff, E., Wu, A. H. B., Coffin, P. O., Hsue, P. Y., Kazi, D. S., Wade, A., Braun, C., Lynch, K. L., Impact of Polysubstance Use on High-Sensitivity Cardiac Troponin I over Time in Homeless and Unstably Housed Women. *Drug Alcohol Depend.* **2020**, *217*, 108252.

[238] Wallace, K. B., Hausner, E., Herman, E., Holt, G. D., MacGregor, J. T., Metz, A. L., Murphy, E., Rosenblum, I. Y., Sistare, F. D., York, M. J., Serum Troponins as Biomarkers of Drug-Induced Cardiac Toxicity. *Toxicol. Pathol.* **2004**, *32* (1), 106–121.

[239] Lowry, M. T. H., Doudesis, D., Wereski, R., Kimenai, D. M., Tuck, C., Ferry, A. V., Bularga, A., Taggart, C., Lee, K. K., Chapman, A. R., Shah, A. S. V., Newby, D. E., Mills, N. L., Anand, A., Influence of Age on the Diagnosis of Myocardial Infarction. *Circulation* **2022**, *146* (15), 1135–1148.

[240] Paana, T., Jaakkola, S., Bamberg, K., Saraste, A., Tuunainen, E., Wittfooth, S., Kallio, P., Heinonen, O. J., Knuuti, J., Pettersson, K., Airaksinen, K. E. J., Cardiac Troponin Elevations in

Marathon Runners. Role of Coronary Atherosclerosis and Skeletal Muscle Injury. The MaraCat Study. *Int. J. Cardiol.* **2019**, *295*, 25–28.
[241] Laura, D. M., Alberto, C., Sabino, I., Angela, D., S, J. A., Cardiac Troponin in Patients With Light Chain and Transthyretin Cardiac Amyloidosis. *JACC CardioOncol.* **2024**, *6* (1), 1–15.
[242] Li, L., Liu, Y., Katrukha, I. A., Zhang, L., Shu, X., Xu, A., Yang, J., Wu, Y., Jing, Y., Wang, H., Ni, T., Schulz, K., Bereznikova, A. V, Katrukha, A. G., Apple, F. S., et al., Characterization of Cardiac Troponin Fragment Composition Reveals Potential for Differentiating Etiologies of Myocardial Injury. *Clin. Chem.* **2025**, *71* (3), 396–405.
[243] Nseir, M., Mokhtari, A., Stanisic, M., Ekström U., Labaf A., Validation and correlation of high-sensitive troponin I and troponin T in the emergency department. *BMC Cardiovasc Disorders* **2024**, 24, 551.
[244] Vestergaard, K. R., Jespersen, C. B., Arnadottir, A., Sölétormos, G., Schou, M., Steffensen, R., Goetze, J. P., Kjøller, E., Iversen, K. K., Prevalence and Significance of Troponin Elevations in Patients without Acute Coronary Disease. *Int. J. Cardiol.* **2016**, *222*, 819–825.
[245] Wongcharoen, W., Chombandit, T., Phrommintikul, A., Noppakun, K., Variability of high-sensitivity cardiac troponin T and I in asymptomatic patients receiving hemodialysis. *Sci Rep* **2021**, 11, 17334.
[246] Panteghini, M., Gerhardt, W., Apple, F. S., Dati, F., Ravkilde, J., Wu, A. H., Quality Specifications for Cardiac Troponin Assays. *Clin Chem Lab Med* **2001**, *39* (2), 175–176.
[247] Apple, F. S., Collinson, P. O., Biomarkers, for the I. T. F. on C. A. of C., Analytical Characteristics of High-Sensitivity Cardiac Troponin Assays. *Clin. Chem.* **2012**, *58* (1), 54–61.
[248] Sauer, M., Hofkens, J., Enderlein, J., Handbook of Fluorescence Spectroscopy and Imaging: From Single Molecules to Ensembles. *Handbook of Fluorescence Spectroscopy and Imaging: From Single Molecules to Ensembles* **2011**.
[249] Valeur, B., Berberan-Santos, M. N., A Brief History of Fluorescence and Phosphorescence before the Emergence of Quantum Theory. *J. Chem. Educ.* **2011**, *88* (6), 731–738.
[250] del Valle, J. C., Catalán, J., Kasha's Rule: A Reappraisal. *Physical Chemistry Chemical Physics* **2019**, *21* (19), 10061–10069.
[251] *IUPAC - phosphorescence (P04569)*. IUPAC Gold Book. https://goldbook.iupac.org/terms/view/P04569 (accessed 2025-05-12).
[252] Salas Redondo, C., Kleine, P., Roszeitis, K., Achenbach, T., Kroll, M., Thomschke, M., Reineke, S., Interplay of Fluorescence and Phosphorescence in Organic Biluminescent Emitters. *The Journal of Physical Chemistry C* **2017**, *121* (27), 14946–14953.
[253] Bünzli, J. C. G., Lanthanide Luminescence for Biomedical Analyses and Imaging. *Chem. Rev.* **2010**, *110* (5), 2729–2755.
[254] Soini, E., Hemmilä, I., Fluoroimmunoassay: Present Status and Key Problems. *Clin.Chem.* **1979**, *25*, 353–361.
[255] Von Lode, P., Rosenberg, J., Pettersson, K., Takalo, H., A Europium Chelate for Quantitative Point-of-Care Immunoassays Using Direct Surface Measurement. *Anal. Chem.* **2003**, *75* (13), 3193–3201.
[256] Hemmilä, I., Laitala, V., Progress in Lanthanides as Luminescent Probes. *J. Fluoresc.* **2005**, *15* (4), 529–542.
[257] Cotton, S., *Lanthanide and Actinide Chemistry*, John Wiley & Sons Ltd., 2006.
[258] Parker, D., Fradgley, J. D., Wong, K.-L., The Design of Responsive Luminescent Lanthanide Probes and Sensors. *Chem. Soc. Rev.* **2021**, *50* (14), 8193–8213.
[259] Learmonth, R. P., Kable, S. H., Ghiggino, K. P., Basics of Fluorescence. In *Fluorescence applications in biotechnology and life sciences*, Wiley-Blackwell: Hoboken, 2009, 1–26.
[260] Dang, V. Q., Teets, T. S., A Practical Guide to Measuring and Reporting Photophysical Data. *Dalton Transactions* **2025**.
[261] Brouwer, A. M., Standards for Photoluminescence Quantum Yield Measurements in Solution (IUPAC Technical Report). *Pure and Applied Chemistry* **2011**, *83* (12), 2213–2228.

[262] *IUPAC - Kasha–Vavilov rule (K03371)*. IUPAC Gold Book. https://goldbook.iupac.org/terms/view/K03371 (accessed 2025-05-12).
[263] Ware, W. R., Baldwin, B. A., Effect of Temperature on Fluorescence Quantum Yields in Solution. *J. Chem. Phys.* **1965**, *43* (4), 1194–1197.
[264] Hoche, J., Schulz, A., Dietrich, L. M., Humeniuk, A., Stolte, M., Schmidt, D., Brixner, T., Würthner, F., Mitric, R., The Origin of the Solvent Dependence of Fluorescence Quantum Yields in Dipolar Merocyanine Dyes. *Chem. Sci.* **2019**, *10* (48), 11013–11022.
[265] Berezin, M. Y., Achilefu, S., Fluorescence Lifetime Measurements and Biological Imaging. *Chem. Rev.* **2010**, *110* (5), 2641.
[266] Baranowski, T., Dreier, T., Schulz, C., Endres, T., Excitation Wavelength Dependence of the Fluorescence Lifetime of Anisole. *Physical Chemistry Chemical Physics* **2019**, *21* (27), 14562–14570.
[267] Rae, B. R., Muir, K. R., Gong, Z., McKendry, J., Girkin, J. M., Gu, E., Renshaw, D., Dawson, M. D., Henderson, R. K., A CMOS Time-Resolved Fluorescence Lifetime Analysis Micro-System. *Sensors* **2009**, *9* (11), 9255–9274.
[268] Andolina, C. M., Mathews, R. A., Morrow, J. R., Solution Chemistry of Europium(III) Aqua Ion at Micromolar Concentrations as Probed by Direct Excitation Luminescence Spectroscopy. *Helv. Chim. Acta* **2009**, *92* (11), 2330–2348.
[269] *IUPAC - visible (VT07496)*. IUPAC Gold Book. https://goldbook.iupac.org/terms/view/VT07496 (accessed 2025-11-04).
[270] Housecroft, C. E., Sharpe, A. G., *Inorganic Chemistry*, 3rd ed., Pearson Educational Limited, 2008.
[271] Hagan, A. K., Zuchner, T., Lanthanide-Based Time-Resolved Luminescence Immunoassays. *Anal. Bioanal. Chem.* **2011**, *400* (9), 2847–2864.
[272] Beeby, A., M. Clarkson, I., S. Dickins, R., Faulkner, S., Parker, D., Royle, L., S. de Sousa, A., A. Gareth Williams, J., Woods, M., Non-Radiative Deactivation of the Excited States of Europium, Terbium and Ytterbium Complexes by Proximate Energy-Matched OH, NH and CH Oscillators: An Improved Luminescence Method for Establishing Solution Hydration States. *Journal of the Chemical Society, Perkin Transactions 2* **1999**, No. 3, 493–504.
[273] Sund, H., Blomberg, K., Meltola, N., Takalo, H., Design of Novel, Water Soluble and Highly Luminescent Europium Labels with Potential to Enhance Immunoassay Sensitivities. *Molecules* **2017**, *22* (10).
[274] Takalo, H., Mukkala, V.-M., Mikola, H., Liitti, P., Hemmila, I., Synthesis of Europium(III) Chelates Suitable for Labeling of Bioactive Molecules. *Bioconjug. Chem.* **1994**, *5* (3), 278–282.
[275] Hemmilä, I., Dakubu, S., Mukkala, V.-M., Siitari, H., Lövgren, T., Europium as a Label in Time-Resolved Immunofluorometric Assays. *Anal. Biochem.* **1984**, *137* (2), 335–343.
[276] Saito, K., Lee, R. T., Lee, Y. C., Quantification of Eu3+in Quantum-Dye-Labeled Materials by Ashing and Dissociation Enhancement. *Anal. Biochem.* **1998**, *258* (2), 311–314.
[277] Blomberg, K. R., Mukkala, V.-M., Hakala, H. H. O., Mäkinen, P. H., Suonpää, M. U., Hemmilä, I. A., A Dissociative Fluorescence Enhancement Technique for One-Step Time-Resolved Immunoassays. *Anal Bioanal Chem.* **2010**, *399* (4), 1677–1682.
[278] Holtkamp, U., Klein, J., Sander, J., Peter, M., Janzen, N., Steuerwald, U., Blankenstein, O., EDTA in Dried Blood Spots Leads to False Results in Neonatal Endocrinologic Screening. *Clin. Chem.* **2008**, *54* (3), 602–605.
[279] Smith, J. G., *Organic Chemistry*, 2nd ed., McGraw Hill, 2007.
[280] Ni, C.-K., Tseng, C.-M., Lin, M.-F., Dyakov, Y. A., Photodissociation Dynamics of Small Aromatic Molecules Studied by Multimass Ion Imaging. *J. Phys. Chem. B* **2007**, *111* (44), 12631–12642.
[281] Kushnarova-Vakal, A., Aalto, R., Huovinen, T., Wittfooth, S., Lamminmäki, U., Controlled Labelling of Tracer Antibodies for Time-Resolved Fluorescence-Based Immunoassays. *Sci. Rep.* **2024**, *14* (1), 18113.

[282] KDIGO 2012 Working Group Members, KDIGO 2012 Clinical Practice Guideline for the Evaluation and Management of Chronic Kidney Disease. *Kidney International Supplements*. 2013.
[283] CLSI, *Evaluation of Detection Capability for Clinical Laboratory Measurement Procedures, Approved Guideline-Second Edition. CLSI Document EP17-A2.*, 2012.
[284] Roche Diagnostics, Elecsys Troponin T Hs [Package Insert, 08469873500V5.0]. *eLabDoc*. 2021.
[285] Lam, S. H., Hung, H. Y., Kuo, P. C., Kuo, D. H., Chen, F. A., Wu, T. S., Application of Lanthanide Shift Reagent to the 1H-NMR Assignments of Acridone Alkaloids. *Molecules* **2020**, *25* (22).
[286] Lisowski, J., Enantiomeric Self-Recognition in Homo- and Heterodinuclear Macrocyclic Lanthanide(III) Complexes. *Inorg. Chem.* **2011**, *50* (12), 5567–5576.
[287] Savukoski, T., Jacobino, J., Laitinen, P., Lindahl, B., Venge, P., Ristiniemi, N., Wittfooth, S., Pettersson, K., Novel Sensitive Cardiac Troponin i Immunoassay Free from Troponin I-Specific Autoantibody Interference. *Clin. Chem. Lab. Med.* **2014**, *52* (7), 1041–1048.
[288] Katrukha, I., Vylegzhanina, A., Kogan, A., Mukharyamova, K., Bereznikova, A., Bogomolova, A., Koshkina, E., Katrukha, A., Full-Size Human Cardiac Troponin T and Its Fragments in the Plasma of Patients with Acute Myocardial Infarction. *AACC Annual Meeting, Poster A-030*. Hytest Ltd.: Anaheim August 2019.
[289] Salonen, S. M., Tuominen, T. J. K., Raiko, K. I. S., Vasankari, T., Aalto, R., Hellman, T. A., Lahtinen, S. E., Soukka, T., Airaksinen, K. E. J., Wittfooth, S. T., Highly Sensitive Immunoassay for Long Forms of Cardiac Troponin T Using Upconversion Luminescence. *Clin. Chem.* **2024**, *70* (8), 1037–1045.
[290] Mair, J., Hammarsten, O., Potential Analytical Interferences in Cardiac Troponin Immunoassays. *J. Lab. Precis. Med.* **2023**, *8*.
[291] Gaze, D. C., Collinson, P. O., Multiple Molecular Forms of Circulating Cardiac Troponin: Analytical and Clinical Significance. *Ann. Clin. Biochem.* **2008**, *45* (4), 349–355.
[292] Vylegzhanina, A. V, Kogan, A. E., Katrukha, I. A., Antipova, O. V, Kara, A. N., Bereznikova, A. V, Koshkina, E. V, Katrukha, A. G., Anti–Cardiac Troponin Autoantibodies Are Specific to the Conformational Epitopes Formed by Cardiac Troponin I and Troponin T in the Ternary Troponin Complex. *Clin. Chem.* **2017**, *63* (1), 343–350.
[293] Bolstad, N., Warren, D. J., Bjerner, J., Kravdal, G., Schwettmann, L., Olsen, K. H., Rustad, P., Nustad, K., Heterophilic Antibody Interference in Commercialimmunoassays, a Screening Study Using Paired Nativeand Pre-Blocked Sera. *Clin. Chem. Lab. Med.* **2011**, *49* (12), 2001–2006.
[294] Lippi, G., Aloe, R., Meschi, T., Borghi. Loris, Cervellin, G., Interference from Heterophilic Antibodies in Troponin Testing. Case Report and Systematic Review of the Literature. *Clinica Chimica Acta* **2013**, *426*, 79–84.
[295] Vilela, E. M., Bettencourt-Silva, R., da Costa, J. T., Barbosa, A. R., Silva, M. P., Teixeira, M., Primo, J., Gama Ribeiro, V., Nunes, J. P. L., Anti-Cardiac Troponin Antibodies in Clinical Human Disease: A Systematic Review. *Ann. Transl. Med.* **2017**, *5* (15).
[296] Adamczyk, M., Brashear, R. J., Mattingly, P. G., Prevalence of Autoantibodies to Cardiac Troponin T in Healthy Blood Donors. *Clin. Chem.* **2009**, *55* (8), 1592–1593.
[297] Savukoski, T., Twarda, A., Hellberg, S., Ristiniemi, N., Wittfooth, S., Sinisalo, J., Pettersson, K., Comparison of Cardiac Troponin I Immunoassays Variably Affected by Circulating Autoantibodies. *Clin. Chem.* **2013**, *59* (3), 512–518.
[298] Li, L., Liu, Y., Katrukha, I. A., Zhang, L., Shu, X., Xu, A., Yang, J., Wu, Y., Jing, Y., Wang, H., Ni, T., Schulz, K., Bereznikova, A. V, Katrukha, A. G., Apple, F. S., et al., Design and Analytical Evaluation of Novel Cardiac Troponin Assays Targeting Multiple Forms of the Cardiac Troponin I–Cardiac Troponin T–Troponin C Complex and Fragmentation Forms. *Clin. Chem.* **2025**, *71* (3), 387–395.
[299] Machovich, R., Mechanism of Action of Heparin through Thrombin on Blood Coagulation. *Biochim. Biophys. Acta* **1975**, *412* (1), 13–17.

[300] Jackson, C. M., Mechanism of Heparin Action. *Baillieres Clin. Haematol.* **1990**, *3* (3), 483–504.
[301] Li, A., Brattsand, G., Stability of Serum Samples and Hemolysis Interference on the High Sensitivity Troponin T Assay. *Clin. Chem. Lab. Med.* **2011**, *49* (2), 335–336.
[302] Michel, M., Mestari, F., Alkouri, R., Atlan, G., Dever, S., Devilliers, C., Imbert-Bismut, F., Bonnefont-Rousselot, D., Monneret, D., High-Sensitivity Cardiac Troponin T: A Preanalytical Evaluation. *Clin. Lab.* **2016**, *62* (4), 743–748.
[303] Mingels, A. M. A., Cobbaert, C. M., de Jong, N., van den Hof, W. F. P. M., van Dieijen-Visser, M. P., Time- and Temperature-Dependent Stability of Troponin Standard Reference Material 2921 in Serum and Plasma. *Clin. Chem. Lab. Med.* **2012**, *50* (9), 1681–1684.
[304] Gobeaux, C., Lefevre, G., Lehodey, B., Kuentz, M., Bourbonneux, V., Pecquet, M., Hausfater, P., Beauvieux, M.-C., Gil-Jardine, C., Choquet, C., Machie, V., Brunel, V., Guenezan, J., Charpentier, S., Claessens, Y.-E., Enquête Nationale Sur Les Délais de Réalisation Des Analyses de TROponine Prescrites Aux Urgences Adultes : État Des Lieux de La PRISE En Charge et Des Modalités d'interprétation - Protocole EN-TRO-PRISE. *Ann. Biol. Clin. (Paris).* **2025**, *83* (3), 293–302.
[305] Ervasti, M., Penttilä, K., Siltari, S., Delezuch, W., Punnonen, K., Diagnostic, Clinical and Laboratory Turnaround Times in Troponin T Testing. *Clin. Chem. Lab. Med.* **2008**, *46* (7), 1030–1032.
[306] Egger, M., Dieplinger, B., Mueller, T., One-Year in Vitro Stability of Cardiac Troponins and Galectin-3 in Different Sample Types. *Clinica Chimica Acta* **2018**, *476*, 117–122.
[307] Henricks, L. M., Romijn, F. P. H. T. M., Cobbaert, C. M., Evidence for Stability of Cardiac Troponin T Concentrations Measured with a High Sensitivity TnT Test in Serum and Lithium Heparin Plasma after Six-Year Storage at −80 °C and Multiple Freeze-Thaw Cycles. *Clin. Chem. Lab. Med.* **2024**, *63* (3), 645–652.
[308] Nowak, R., Mueller, C., Giannitsis, E., Christ, M., Ordonez-Llanos, J., DeFilippi, C., McCord, J., Body, R., Panteghini, M., Jernberg, T., Plebani, M., Verschuren, F., French, J. K., Christenson, R., Jacobsen, G., et al., High Sensitivity Cardiac Troponin T in Patients Not Having an Acute Coronary Syndrome: Results from the TRAPID-AMI Study. *Biomarkers* **2017**, *22* (8), 709–714.
[309] Giannitsis, E., Katus, H. A., Cardiac Troponin Level Elevations Not Related to Acute Coronary Syndromes. *Nat. Rev. Cardiol.* **2013**, *10*, 623–634.
[310] Ritzmann, P., Frey, R., Rüttimann, S., Acute Myocardial Infarction: Time Delay from Onset of Pain to Hospital Presentation and Thrombolysis. *Schweiz Med Wochenschr* **2000**, *130* (18), 657–663.
[311] Nilsson, G., Mooe, T., Söderström, L., Samuelsson, E., Pre-Hospital Delay in Patients with First Time Myocardial Infarction: An Observational Study in a Northern Swedish Population. *BMC Cardiovasc Disord* **2016**, *16* (93).
[312] Zhang, Y., Guo, S., Xu, J., Multifunctional Applications and Research Advances of Low-Molecular-Weight Heparin. *Front. Pharmacol.* **2025**, *16*.
[313] Airaksinen, K. E. J., Paana, T., Vasankari, T., Salonen, S., Tuominen, T., Linko-Parvinen, A., Pallari, H.-M., Hellman, T., Teppo, K., Heinonen, O. J., Jaakkola, S., Wittfooth, S., Composition of Cardiac Troponin Release Differs after Marathon Running and Myocardial Infarction. *Open Heart* **2024**, *11* (2), e002954.
[314] Airaksinen, J. K. E., Tuominen, T., Paana, T., Hellman, T., Vasankari, T., Salonen, S., Junes, H., Linko-Parvinen, A., Pallari, H.-M., Strandberg, M., Teppo, K., Jaakkola, S., Wittfooth, S., Novel Troponin Fragmentation Assay to Discriminate between Takotsubo Syndrome and Acute Myocardial Infarction. *Eur. Heart J. Acute Cardiovasc. Care* **2024**, *13* (11), 782–788.
[315] Teppo, K., Airaksinen, K. E. J., Vasankari, T., Linko-Parvinen, A., Pallari, H.-M., Paana, T., Jaakkola, S., Junes, H., Salonen, S., Tuominen, T., Simonen, S., Strandberg, M., Hellman, T., Wittfooth, S., Long Forms of Cardiac Troponin T for Myocardial Infarction Diagnosis: The SuperTROPO Study. *Eur. Heart J.* **2026**, *47* (4), 490–499.

[316] Hölz, K., Lietard, J., Somoza, M. M., High-Power 365 Nm UV LED Mercury Arc Lamp Replacement for Photochemistry and Chemical Photolithography. *ACS Sustain. Chem. Eng.* **2017**, *5* (1), 828–834.
[317] Mondal, R. K., Adhikari, S., Chatterjee, V., Pal, S., Recent Advances and Challenges in AlGaN-Based Ultra-Violet Light Emitting Diode Technologies. *Mater. Res. Bull.* **2021**, *140* (111258).
[318] Okabe, K., Sakaguchi, R., Shi, B., Kiyonaka, S., Intracellular Thermometry with Fluorescent Sensors for Thermal Biology. *Pflugers Arch.* **2018**, *470* (5), 717–731.
[319] Cheung, T. L., Ju, Z., Zhang, W., Parker, D., Deng, R., Mechanistic Investigation of Sensitized Europium Luminescence: Excited State Dynamics and Luminescence Lifetime Thermometry. *ACS Appl. Mater. Interfaces* **2024**, *16* (33), 43933–43941.
[320] Yu, J., Sun, L., Peng, H., Stich, M. I. J., Luminescent Terbium and Europiumprobes for Lifetime Based Sensing of Temperature between 0 and 70 °C. *J. Mater. Chem.* **2010**, *20*, 6975–6981.
[321] Borisov, S. M., Wolfbeis O. S., Temperature-Sensitive Europium(III) Probes and Their Use for Simultaneous Luminescent Sensing of Temperature and Oxygen. *Anal. Chem.* **2006**, *78* (14), 5094–5101.
[322] Vartiainen, E., Laatikainen, T., Jousilahti, P., Peltonen, M., Niiranen, T., Salomaa, V., Sepelvaltimotaudin Ja Aivohalvauksen Riskin Arviointi FINRISKI 2.0 -Laskurilla. *Suomen Lääkärilehti* **2020**, *75* (50), 2778–2782.
[323] Lloyd-Jones D.M., Huffman, M. D., Karmali, K. N., Sanghavi, D. m., Wright. J.S., Pelser, C., Gulati, M., Masoudi, F. A., Goff, D. C., Estimating Longitudinal Risks and Benefits From Cardiovascular Preventive Therapies Among Medicare Patients. *JACC* **2017**, *69* (12), 1617–1636.
[324] Stone, G. W., Selker, H. P., Thiele, H., Mehta, R. P., Jüni, E. U., Ørn, E. M., Motoki, A., Engström, I., Gibson, C. M., Price, J. L., Ndrepepa, M., Ben-Yehuda, O., Relationship Between Infarct Size and Outcomes Following Primary PCI. *JACC* **2016**, *67* (14), 1674–1683.
[325] Wellens, H. J. J., Gorgels, A. P. M., Doevendans, P. A., *The ECG in Acute Myocardial Infarction and Unstable Angina: Diagnosis and Risk Stratification*, Kluwer Academic Publishers: Dordrecht, 2003.

Appendix I. Structural data of compound 19 and its intermediates

Compound (14): 3-amino-6-bromopyrazine-2-carboxylic acid

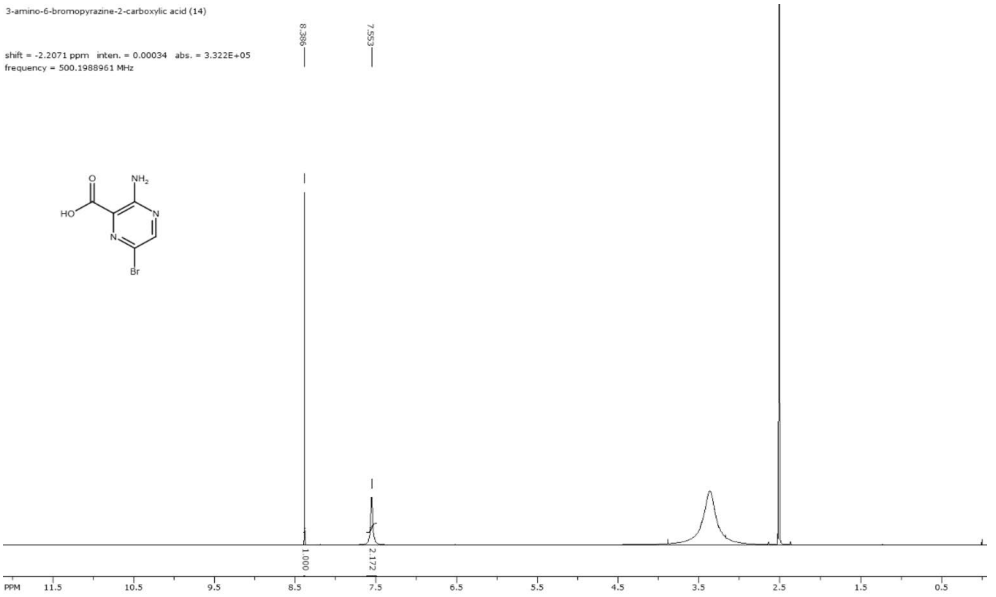

Figure A1 Compound (14) ^{1}H NMR (500 MHz, $(CD_3)_2SO$): δ [ppm]: 7.55 (s, 2H; NH_2); 8.39 (s, 1H; ArH); carboxylic acid proton not found.

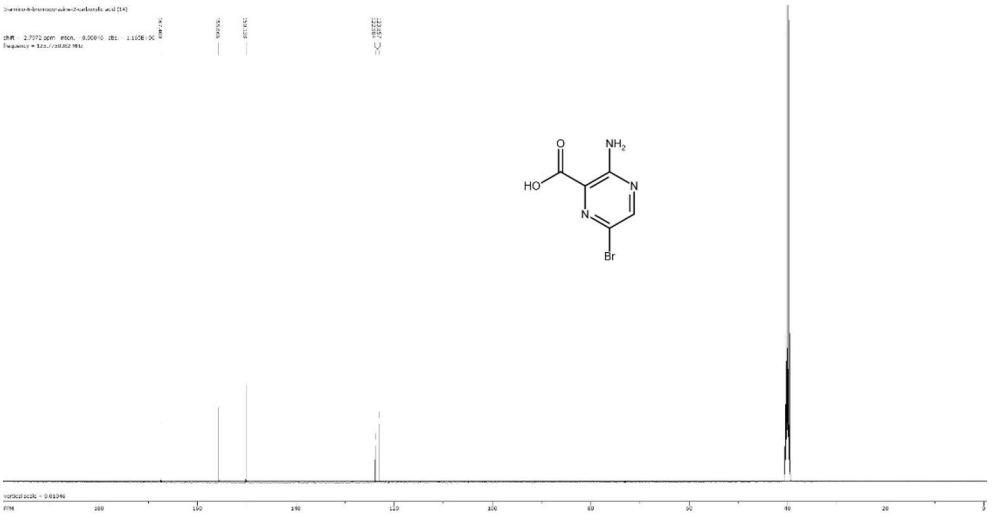

Figure A2 Compound (14) ^{13}C NMR (125 MHz, $(CD_3)_2SO$): δ [ppm]: 123.0 (ArC); 123.9 (ArC); 150.1 (ArC); 155.7 (ArC); 167.4 (COOH).

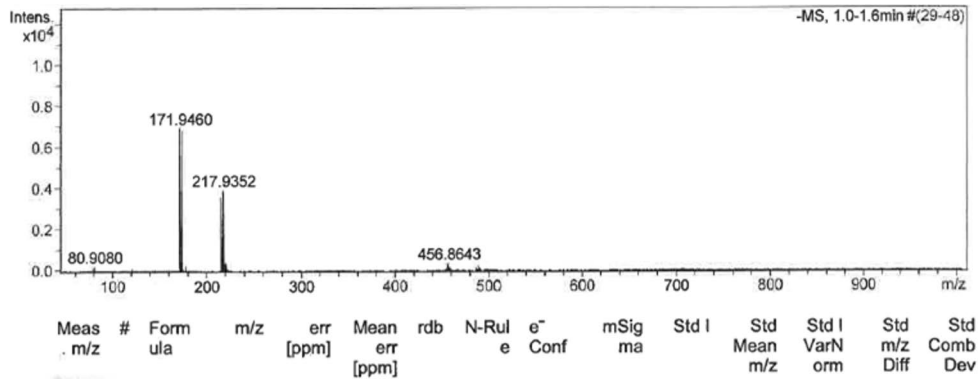

Figure A3 Compound (14). HRMS: m/z calc. for $[C_5H_4BrN_3O_2]$– 215.9414, 217.9393. Found [M-H]– 217,9352, 215.9374.

Compound (15): tert-butyl (4-((3-amino-6-bromopyrazine-2-carboxamido)methyl)-phenyl)carbamate

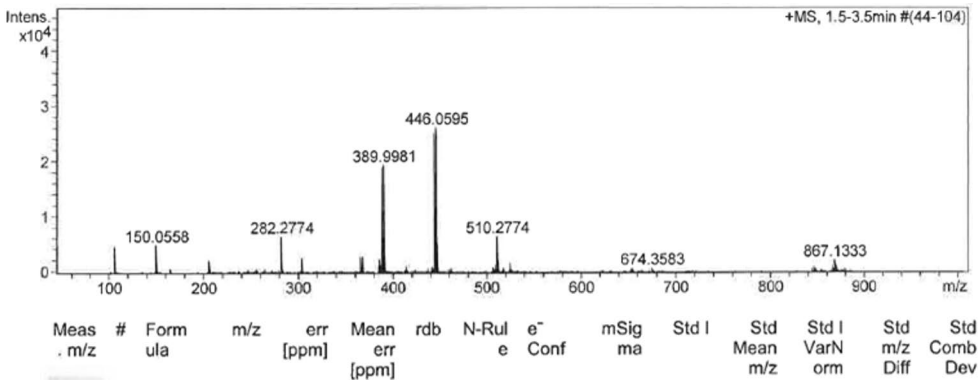

Figure A4 Compound (15). HRMS: m/z calc. for $[C_{17}H_{20}BrN_5NaO_3]$+ 444.0642, 446.0622. Found [M+Na]+ 446.0595, 444.0642.

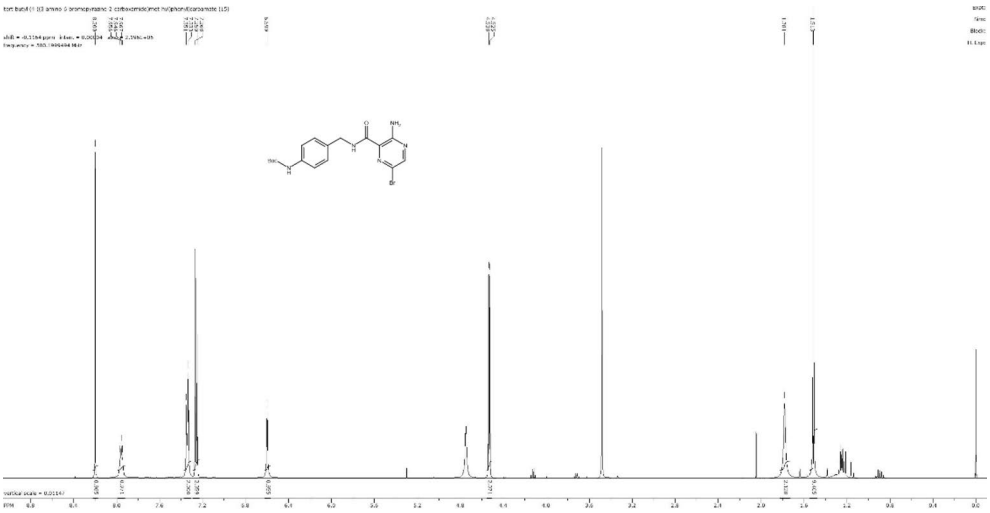

Figure A5 Compound (15) ^{1}H NMR (500 MHz, $CDCl_3$): δ [ppm]: 1.51 (s, 9H; $C(CH_3)_3$); 1.78 (s, 2H; NH_2); 4.53 (d, J = 6.5 Hz, 2H; CH_2); 6.60 (s, 1H; NH); 7.26 (d, J = 9 Hz, 2H; ArH); 7.34 (d, J = 9 Hz, 2H; ArH); 7.96 (t, J = 5.5 Hz, 1H; NH); 8.20 (s, 1H; ArH).

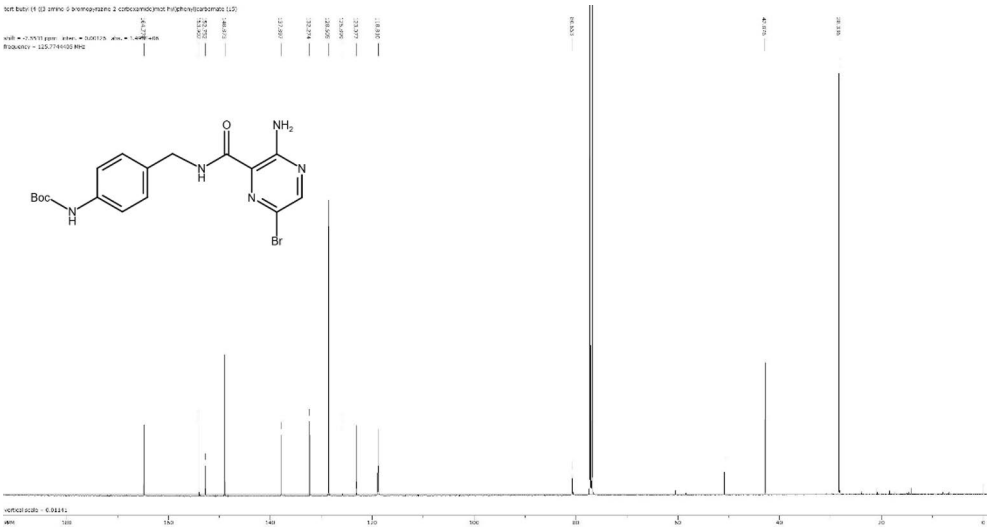

Figure A6 Compound (15) ^{13}C NMR (125 MHz, $CDCl_3$): δ [ppm]: 28.3 ($(CH_3)_3$); 42.9 (CH_2); 80.7 ($C(R)_3$); 118.8; 123.1; 125.9; 128.6; 132.3; 137.9; 148.9; 152.8; 153.9; 164.8.

Compound (16): tert-butyl (4-((3-amino-6-((trimethylsilyl)ethynyl)pyrazine-2-carboxamido)methyl)phenyl)carbamate

Figure A7 Compound (16) ^{1}H NMR (500 MHz, $CDCl_3$): δ [ppm]: 0.26 (s, 9H; $Si(CH_3)_3$); 1.52 (s, 9H; $C(CH_3)_3$); 1.57 (s, 2H; NH_2); 4.54 (d, J = 6 Hz, 2H; CH_2); 6.47 (s, 1H; NH); 7.27 (d, J = 8 Hz, 2H; ArH); 7.34 (d, J = 8 Hz, 2H; ArH); 8.14 (t, J = 6 Hz, 1H; NH); 8.27 (s, 1H; ArH).

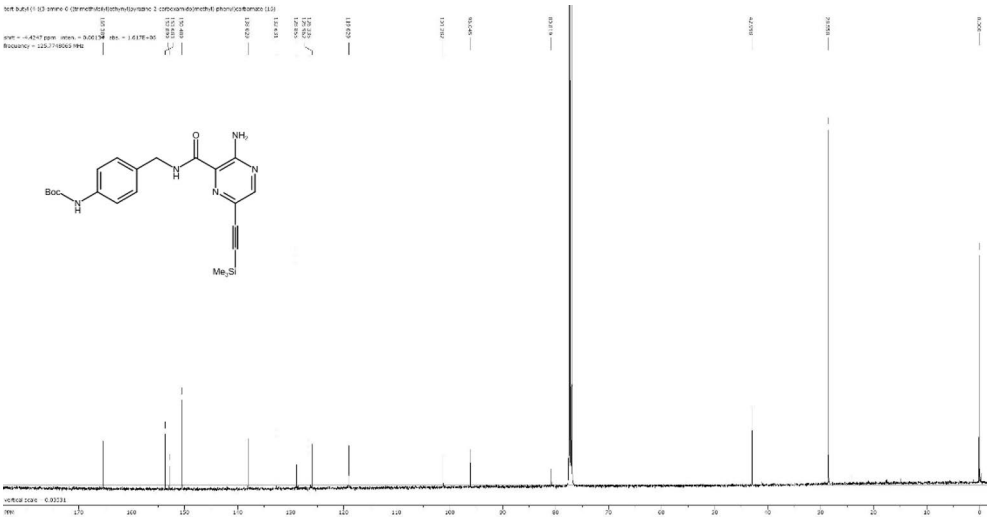

Figure A8 Compound (16) ^{13}C NMR (125 MHz, $CDCl_3$): δ [ppm]: 0.0 ($Si(CH)_3$); 28.6 ($(CH_3)_3$); 43.0 (CH_2); 80.8 ($C(R)_3$); 96.0; 101.3; 119.0; 126.0; 126.3; 128.9; 132.6; 138.0; 150.5; 152.9; 153.7; 165.4.

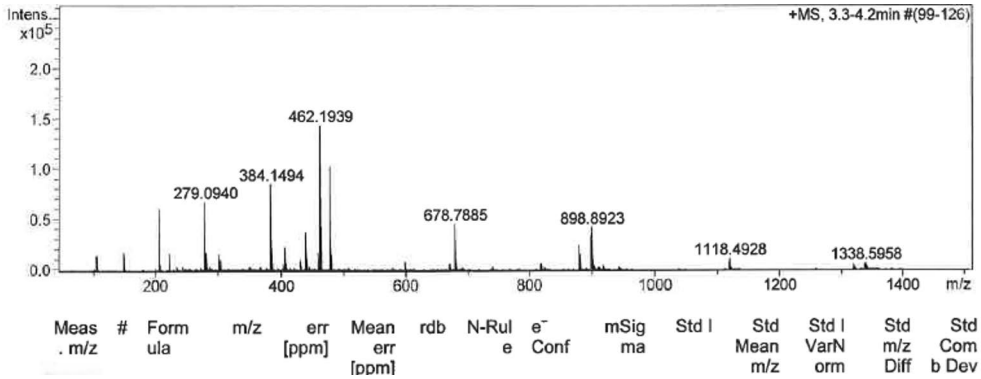

Figure A9 Compound (16). HRMS: m/z calc. for $[C_{22}H_{29}N_5NaO_3Si]+$ 462.1932. Found [M+Na]+ 462.1939.

Compound (17): tert-butyl (4-((3-amino-6-ethynylpyrazine-2-carboxamido)-methyl)phenyl)carbamate

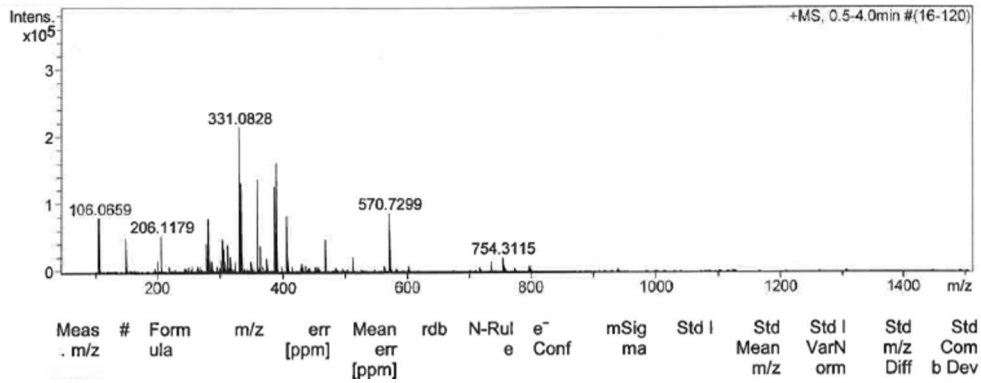

Figure A10 Compound (17). HRMS: m/z calc. for $[C_{19}H_{21}N_5NaO_3]+$ 390.1537. Found [M+Na]+ 390.1541.

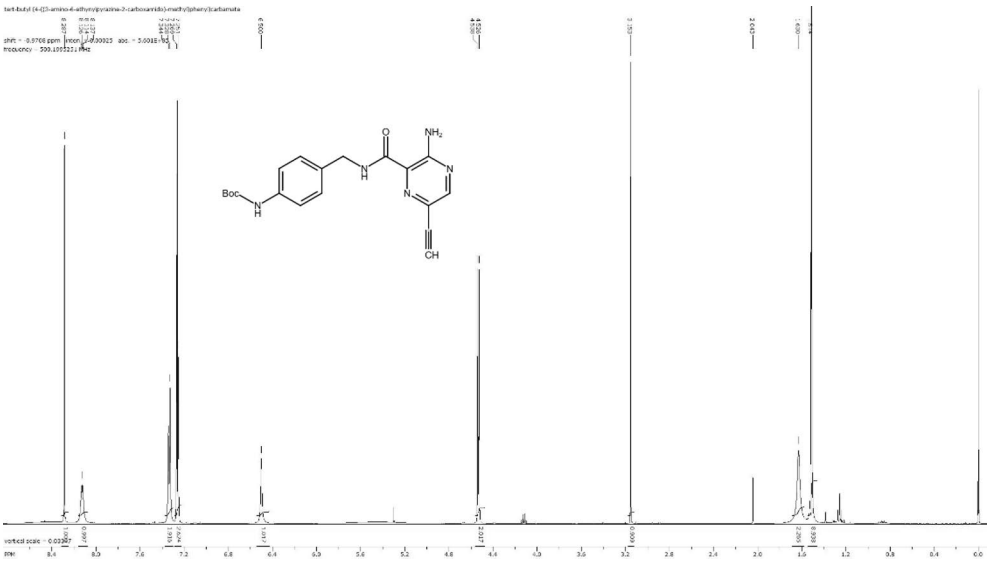

Figure A11 Compound (17) ^{1}H NMR (500 MHz, $CDCl_3$): δ [ppm]: 1.51 (s, 9H; $C(CH_3)_3$); 1.63 (s, 2H; NH_2); 3.15 (s, 1H; CH); 4.53 (d, J = 6 Hz, 2H; CH_2); 6.50 (s, 1H; NH); 7.26 (d, J = 8 Hz, 2H; ArH); 7.34 (d, J = 8 Hz, 2H; ArH); 8.13 (t, J = 6 Hz, 1H; NH); 8.29 (s, 1H; ArH).

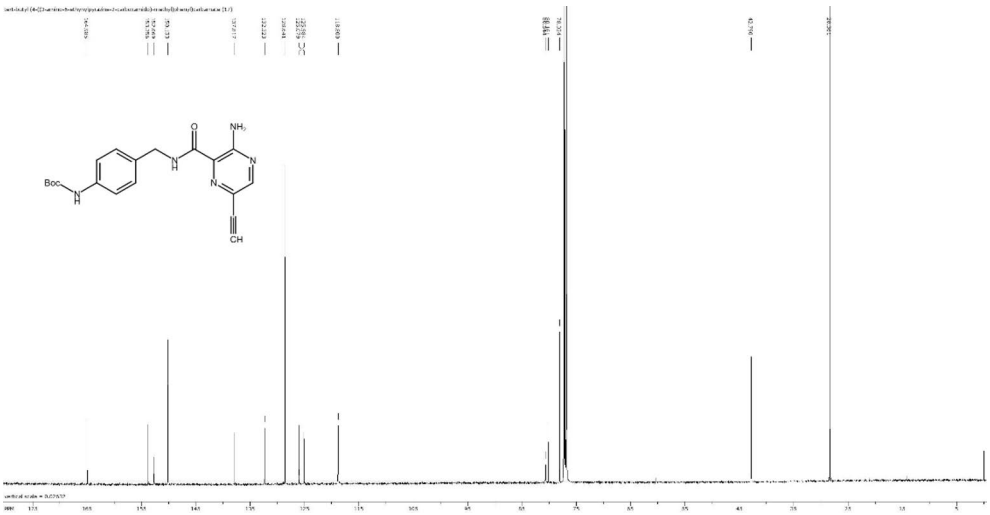

Figure A12 Compound (17) ^{13}C NMR (125 MHz, $CDCl_3$): 28.4 ($(CH_3)_3$); 42.8 (CH_2); 78.0; 80.2; 80.6; 118.8; 125.1; 126.0; 128.6; 132.3; 137.8; 150.1; 152.7; 153.8; 165.0.

Compound (18): di-tert-butyl 2,2'-(((4-((5-amino-6-((4-((tert-butoxycarbonyl)-amino)benzyl)carbamoyl)pyrazin-2-yl)ethynyl)-6-(((2-(bis(2-(tert-butoxy)-2-oxoethyl)amino)ethyl)(2-(tert-butoxy)-2-oxoethyl)amino)methyl)pyridin-2-yl)methyl)azanediyl)diacetate

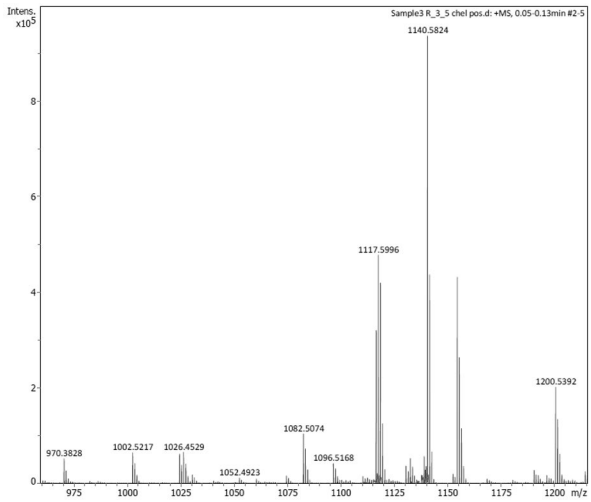

Figure A13 Compound (18). HRMS: m/z calc. for $[C_{58}H_{86}N_9O_{13}]$+ 1116,6340, 1117,6374. Found [M+H]+ 1117,5996.

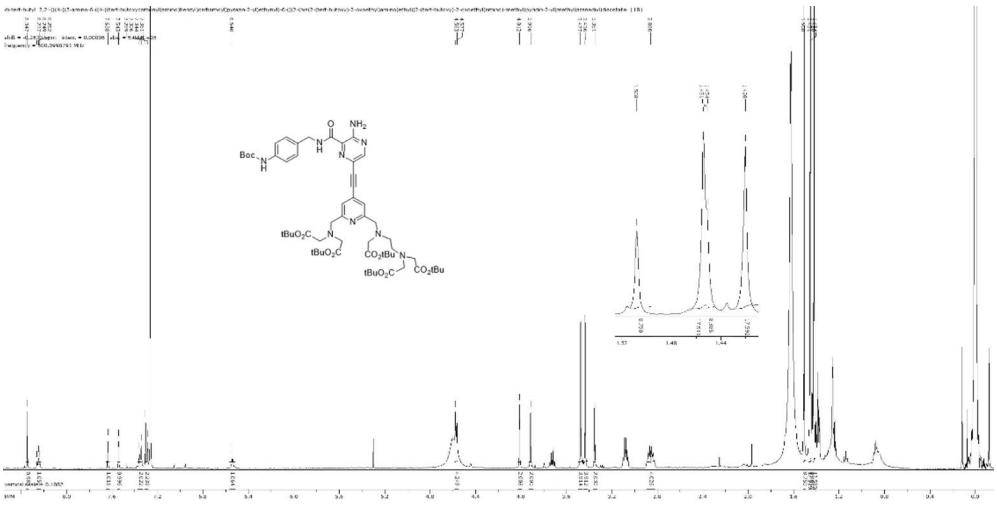

Figure A14 Compound (18) ^{1}H NMR (500 MHz, $CDCl_3$): δ [ppm]: 1.42 (s, 18H; $C(CH_3)_3$); 1.45 (s, 9H; $C(CH_3)_3$); 1.45 (s, 18H; $C(CH_3)_3$); 1.51 (s, 9H; $C(CH_3)_3$); 2.86 (m, 4H; CH2-CH2); 3.35 (s, 2H; CH_2); 3.44 (s, 4H; CH_2); 3.48 (s, 4H; CH_2); 3.92 (s, 2H; CH_2); 4.01 (s, 2H; CH_2); 4.57 (d, J = 7 Hz, 2H; CH_2); 6.54 (s, 1H; NH); 7.30 (d, J = 8,5 Hz, 2H; ArH); 7.35 (d, J = 8,5 Hz, 2H; ArH); 7.54 (s, 1H; ArH); 7.64 (s, 1H; ArH); 8.25 (t, J = 6,5 Hz, 1H; NH); 8.58 (s, 1H; ArH). Amine protons around 1.60 not found due to overlap.

2,2'-(((4-((5-amino-6-((4-aminobenzyl)carbamoyl)pyrazin-2-yl)ethynyl)-6-(((2-(bis(carboxylatomethyl)amino)ethyl)(carboxylatomethyl)amino)methyl)pyridin-2-yl)methyl)azanediyl)diacetate europium(III)

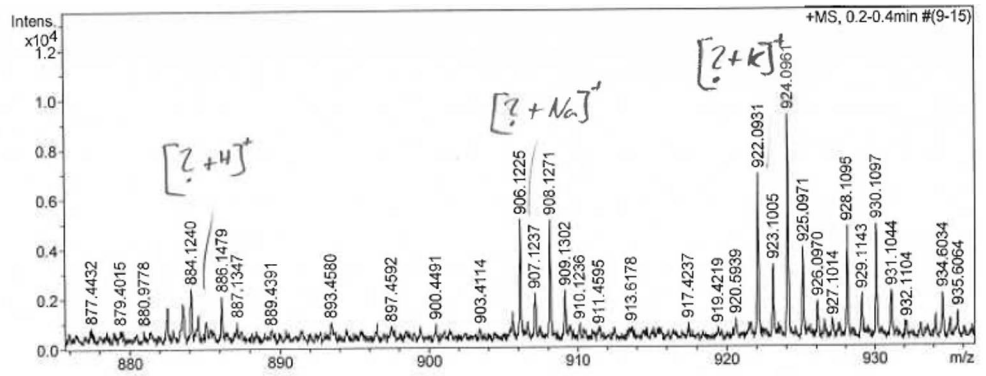

Figure A15 2,2'-(((4-((5-amino-6-((4-aminobenzyl)carbamoyl)pyrazin-2-yl)ethynyl)-6-(((2-(bis(carboxylatomethyl)amino)ethyl)(carboxylatomethyl)amino)methyl)pyridin-2-yl)methyl)azanediyl)diacetate europium(III). HRMS: m/z calc. for $[C_{33}H_{34}EuN_9NaO_{11}]+$ 908.1483, 906.1469. Found [M+Na]+ 906.1225, 908.1271.

Compound (19): 2,2'-(((4-((5-amino-6-((4-isothiocyanatobenzyl)carbamoyl)-pyrazin-2-yl)ethynyl)-6-(((2-(bis(carboxylatomethyl)amino)ethyl)(carboxylate-methyl)amino)methyl)pyridin-2-yl)methyl)azanediyl)diacetate europium(III)

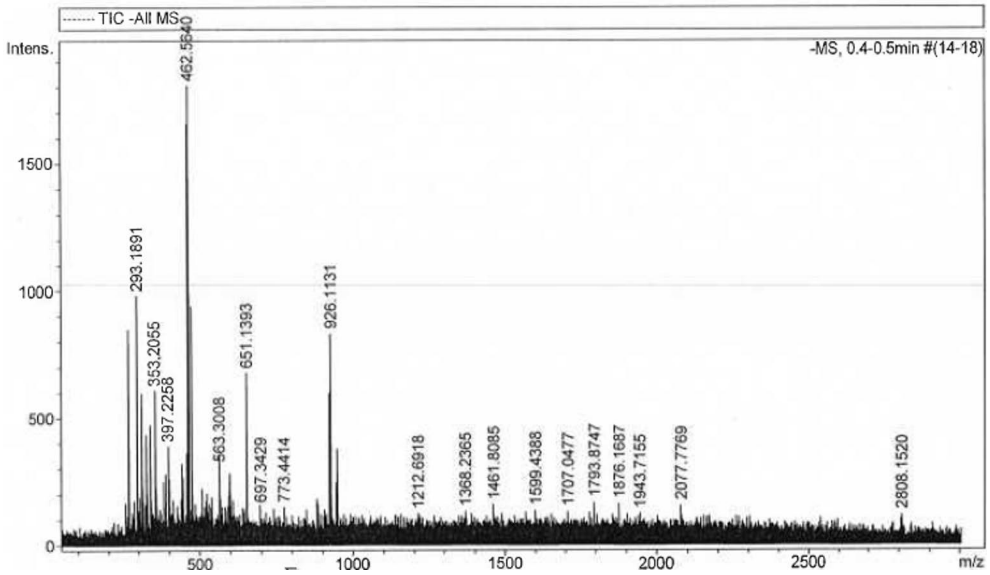

Figure A16 Compound (19) HRMS: m/z calc. for $[C_{34}H_{30}EuN_9O_{11}S]2-$ 462.5504. Found [M-H]2– 462.5640.

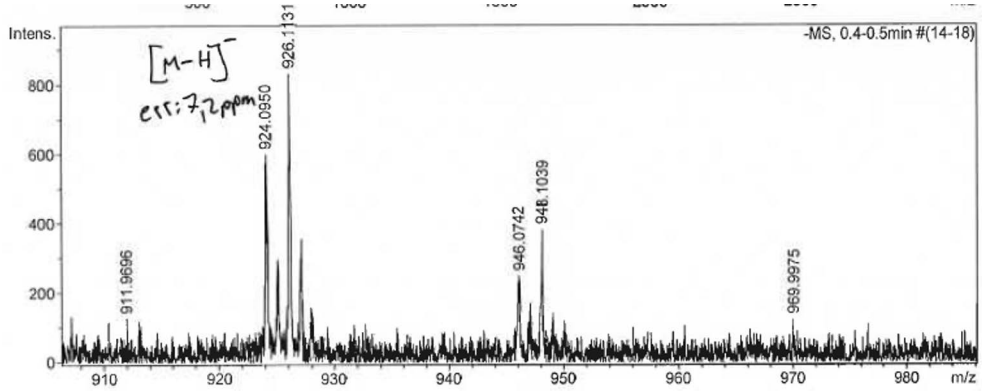

Figure A17 Compound (19) HRMS: m/z calc. for $[C_{34}H_{30}EuN_9O_{11}S]$– 926.1081, 924.1067. Found [M-H]– 926.1131, 924.0950.

TURUN
YLIOPISTO
UNIVERSITY
OF TURKU

Painosalama, Turku, Finland 2026

ISBN 978-952-02-0635-2 (PRINT)
ISBN 978-952-02-0636-9 (PDF)
ISSN 2736-9390 (Painettu/Print)
ISSN 2736-9684 (Sähköinen/Online)